Founded 1925

Incorporated
by Royal Charter 1961

To promote the advancement of radio electronics and kindred subjects by the exchange of information in these branches of engineering

Volume 44 No. 5

May 1974

The Radio and Electronic Engineer

The Journal of the Institution of Electronic and Radio Engineers

The British Electronics Industry and World Competition

AT this time of year, the main trade associations of the electronics industry, namely the Electronic Engineering Association (EEA), the British Radio Equipment Manufacturers' Association (BREMA) and the Radio and Electronic Component Manufacturers Federation (RECMF), hold their annual general meetings and present reports on their operations. It is instructive to read and compare these reports and to try and form an overall idea of the industry's views on future development.

Because it is so fresh in the mind and also because it achieved a measure of world press coverage that has grossly overstated its impact, one may look first at the reactions to the fuel crisis and the ensuing three-day working week that affected the whole of British industry at the end of 1973. There is a fairly generally held opinion that the challenge to management and production workers caused the effect of short-time working to be minimal—because the reports cover the calendar year, quantified details cannot be given but percentage falls in production for many firms were certainly far less than the reduction in the working week might have been expected to cause. The retiring President of the EEA, Mr. R. R. C. Rankin, made this point and deplored particularly the long-term damage to the reputation of British Industry through the resulting questioning of its ability to meet delivery dates. For its part, the RECMF viewed its greatest future problems as deriving from worldwide shortages of some materials and pieceparts.

BREMA's problems for the future are seen mainly to arise from the reduced purchasing power of the consumer. The industry produced well over two million colour television receivers in 1973—unsatisfied public demand was such as to absorb a further 700,000 imported sets—but reimposition of credit controls has caused 1974 market estimates to be drastically revised. A point to be noted is that the growth in demand for colour receivers in the UK was to some extent unexpected and has not been matched elsewhere; it is due mainly to three-quarters of all sets being rented.

The President of BREMA, Lord Thorneycroft referred to the industry's concern at the rapidity with which Japanese industry in particular has obtained a sizeable share of the home market, and further discussions are to be held with the Japanese to seek some restrictions of exports to the UK. RECMF naturally shares this concern to some extent and in addition are seeking an assurance of significant UK component content in equipment assembled here by overseas manufacturers.

The EEA takes a happier view of overseas competition and, with its sister associations and industry in general, welcomes the EEC, although its impact on the electronics industry so far has been relatively small. Important areas of discussion with the EEC countries have been quality assurance and harmonization of standards for components, and electrical safety aspects for domestic equipment have also been prominent. On the marketing side, trade with the EEC countries is generally higher than with other defined overseas markets (e.g. the Commonwealth, EFTA, USA, Japan, etc.): some 40% of the industry's production is exported and nearly half of this goes to the Common Market.

Just as an Institution must rely for its effectiveness on the time and effort of its members, so too with a trade association. The three industry reports for 1973 make this point either explicitly or implicitly, and co-operation in many fields, only a few of which have been mentioned here, is increasingly important. Whilst electronics may not be one of the country's largest exporting industries, the high labour content of its products means that its prosperity is a vital factor in the Nation's economy.

Contributors to this issue*

Dr. **T. J. Bennett** received a B.Sc. in electrical engineering at Southampton University in 1962, and this was followed by a Ph.D. in microwave spectroscopy and a year's post-doctoral fellowship work also at Southampton University.

Dr. Bennett joined the Plessey Company's Roke Manor research establishment in 1966 as a Senior Engineer and for the next three years worked on a simplified rubidium atomic frequency source.

Apart from his work on feedforward he has also, as a Principal Engineer, been responsible for work on high dielectric constant microstrip, active filters, co-sited aerial problems and injection locked oscillators. He has recently joined the Ministry of Defence.

Dr. P. G. Ladbrooke received the B.Tech. degree in electrical engineering from Loughborough University in 1967, and the Ph.D. degree from the University of Cambridge in 1971; his thesis subject was non-uniformities in Gunn and Schottky GaAs diodes. He spent eight years altogether with International Computers Limited where he worked on optical character recognition systems, and on methods for magneto-optic read-out from magnetic disk stores. From 1971 to 1973 he held a British Government Senior Research Fellowship at the Royal Military College of Science, Shrivenham, working on microwave integrated circuits and metal-semiconductor contacts, and he has published several papers on these subjects. Dr. Ladbrooke is now working as a Principal Engineer, involved in environmental studies, at the Plessey Radar Research Centre at Havant, Hampshire.

Mr. R. F. Clements received a B.Sc. honours degree in electrical engineering from the CNAA in 1968 following studies at the Borough Polytechnic. After completing a Graduate Apprenticeship with British Relay Electronics Limited, he remained as a Development Engineer in this Company's Research Laboratories engaged on circuit design for advanced cable television systems. In 1970 he moved to Plessey Avionics and Communications Laboratories at Roke Manor and is currently a Senior Engineer engaged in work on active aerials at h.f.

Dr. F. W. Stephenson is a Lecturer in the Department of Electronic Engineering at the University of Hull. He was educated at Rutherford College of Technology and King's College, Newcastle, from which he graduated in 1961 with first-class honours in electrical engineering. In 1965 he was awarded the degree of Ph.D. by the University of Newcastle for research on active filters. For the next two-and-a-half years Dr. Stephenson was employed by Electrosil Limited and held the post of Technical Manager in the Company's Microelectronics Division. In May 1967 he returned to the University of Newcastle as a Senior Research Associate in network theory under the sponsorship of the Ministry of Technology. He took up his present appointment in October 1968. Dr. Stephenson is co-author of a book on Linear Microelectronic Systems, published in 1973 and of several papers on R–C active networks and circuit theory published in this Journal.

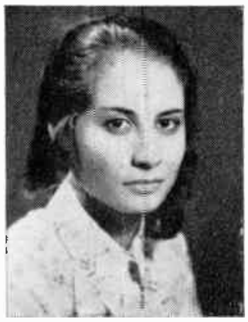

Miss Muna M. A. El Futuh joined the Faculty of Engineering, University of Khartoum, as an undergraduate student in 1970. In the summer of 1973 she spent two months in the Electrical Engineering Department of the University of Bradford where she helped in the preparation of the present paper. Miss Futuh is currently a final-year student in electrical engineering at the University of Khartoum.

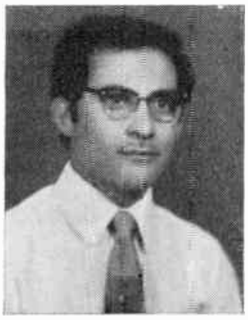

Dr. S. I. Ghobrial received his B.Sc. in electrical engineering from the University of Khartoum in 1969. After a period of post-graduate work he was awarded a British Council Scholarship to study in England for higher degrees. He received the M.Sc. and Ph.D. in 1971 and 1973, both from the University of Bradford; his doctoral thesis was on cross-polarization in reflector antennas. Dr. Ghobrial has now returned to the University of Khartoum as a Lecturer in the Department of Electrical Engineering.

*See also pages 249 and 285.

UDC 621.395.625.3: 621.397.6

Feasibility study for a new compatible quadruplex video recording standard

KOICHI SADASHIGE, B.S.E.E., M.S.M.E.*

Based on a paper presented at the IERE Conference on Video and Data Recording held in Birmingham from 10th to 12th July 1973

SUMMARY

All the parameters affecting the performance of a video recording system are critically considered and proposals are made for achieving the necessary quality of output with the tape speed reduced to 6 in/s for 2-in wide tape. The new standard calls for reducing head size, track widths and guard bands. Unwanted beat components in the f.m. system are reduced by adopting a super highband system with the black carrier frequency being about 10 MHz and the white carrier in the 12 to 13 MHz region. A pilot tone error correction system is described. Factors affecting audio recording quality are also discussed.

* *RCA Corporation, Electronic Recording Engineering, Camden, N.J. 08102, U.S.A.*

1 Introduction

The technology of magnetic video recording has been in continuous development during the last two decades, the mainstay of the high quality video recording having been the quadruplex system. Its rate of development especially in the past decade has been quite rapid, and today, it has reached a very high state of refinement.

Another technological development which also uses magnetic principles is the computer memory system, and as shown in Fig. 1, the information density of computer magnetic tape systems was a mere 10,000 bits per square inch in the late 1950s, about the time of the birth of quadruplex video recording. Now, in the early 1970s, computer systems are approaching the capability of packing information at the density rate of 1,000,000 bits per square inch. Thus during the fifteen-year period which brought quadruplex video recording to the present level of refinement, the computer industry has increased its packing density by nearly 100 fold.

Accelerated development of technologies related to video recording in the past several years have been based on progress in the areas of (1) magnetic tape, (2) magnetic head design, (3) magnetic head material, (4) electronic components and circuit technique, and (5) synthesis and realization of networks through the use of computers.[1] However, it has been a growing feeling among design engineers that the existence of rigid standards and recommended practices has tended to impede our efforts to incorporate new technical advancement. The industry-wide standards, accepted and used by both equipment manufacturers and users, have been the basic reason for the world-wide acceptance, and guaranteed interchangeability of recorded materials regardless of origin.[2] However, they tend to impede the application of new innovations whenever they interfere with the current standard.

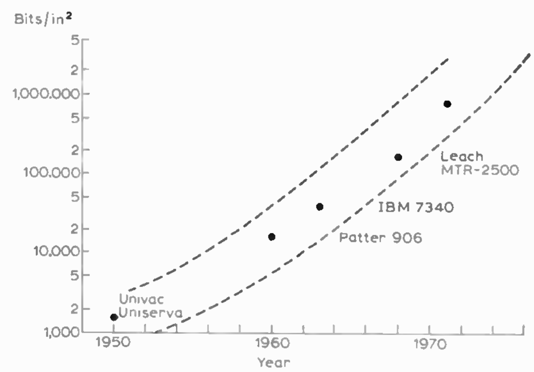

Fig. 1. The increase in information density of computer magnetic tape systems.

2 Previous Activities at RCA

Significant improvements in performance and operational characteristics and incorporation of new features, are possible once we are free to step outside of the current standards.

As early as in 1969, at RCA, we showed that 4-to-1 reduction in tape usage can be realized while maintaining the essential signal characteristics of the quadruplex recorder intact, by the application of new magnetic head material, and with the use of a special high performance tape. Custom-built equipment embodying some of these techniques has been built for nonbroadcast applications. Also during the 1969 to 1970 period, we conducted studies which provided information on how much video performance improvement could be realized if we move the f.m. deviation standard from the current third-shelf operation into the fourth or fifth shelf.

Pre-equalization of the f.m. signal prior to recording had been known to be of importance. Through analytical and empirical studies, we have learned that on the third shelf f.m. system, increased pre-equalization normally affects signal/noise and signal/moiré in opposite directions. We have further learned that certain characteristics make possible modest improvement of both figures. Currently practised equalization is not optimum from these viewpoints.

3 Advantages of Quadruplex System

A number of newly developed video tape recorders are now emerging in the market place. Most of them have chosen the tape format in which the vido track is laid in a slanted angle with respect to the longitudinal edge of the tape, or a helical scan format.

Since these recorders were conceived and designed within the last few years, they all have benefited greatly from the latest technological advances. Much of the equipment users' desire and requests, results of the long usage of quadruplex recorders in the field, have also been embodied into the basic design of these new systems. Most of all, the designers were free to establish both electrical and mechanical parameters of the system without regard to conformance with the established standard. Therefore, from the standpoint of comparisons of specifications and features, the new equipments appear to be of acceptable design. However, the basic shortcoming of the system lies in its tape format, the helical scan.

3.1 Dimensional Instability of Tape and Tracking Difficulty

A typical base material of magnetic tape is duPont Mylar, and its physical characteristics are well known. As shown in Table 1, the weakness is in the area of its dimensional instability by the change of environmental conditions.

Table 1. Dimensional instability of tape

Coefficient of elongation by temperature: $K_T = 1{\cdot}5 \times 10^{-5}$ per degF

Coefficient of elongation by hygroscopic variation:

$K_H = 1{\cdot}1 \times 10^{-5}$ per % r.h.

Mistracking due to tape elongation:

Tracking error as expressed by % of trackwidth

$$= 100\,\frac{S(TK_T + HK_M)\sin\alpha}{W_T}$$

where

S = longitudinal tape dimension covered by one track

T = temperature change.

H = humidity change

W_T = track width

α = tracking angle with respect to the longitudinal edge of tape

The dimensional instability will result in mistracking of the recorded track by the scanning head. The degree of mistracking is proportional to the ratio of the dimensional change of the tape length covered by one head track to the track width.

In a quadruplex system where the track is essentially perpendicular to the longitudinal axis of tape, the mistracking due to the tape dimensional instability is almost non-existent. However, if the track is laid out at a small angle with respect to the edge of tape as in the case of the helical scan recorders, a high degree of mistracking takes place even for a small dimensional change of the tape, as shown in Fig. 2.

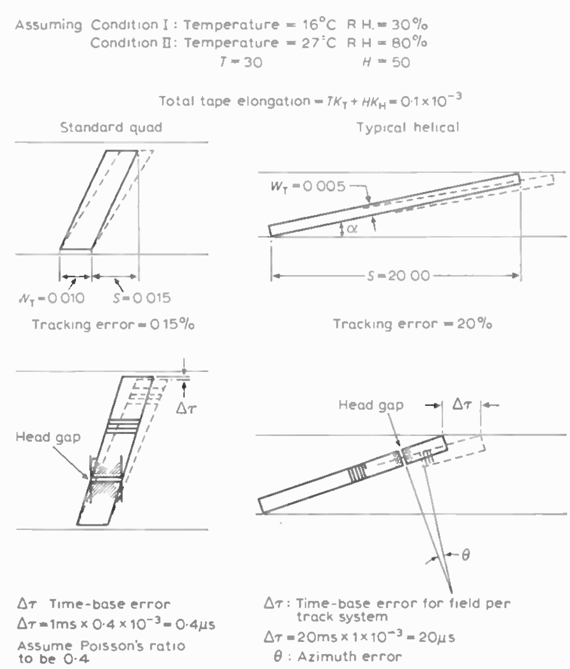

Fig. 2. Tracking error.

Dimensional instability of the tape also relates to one other detrimental factor of the playback system, i.e., the time-base error. Since one track of a helical scan recorder normally covers an entire television field, the accumulated time-base error within one track is substantial, and could be as much as 20 μs.[3]

In a quadruplex system, where the tracks are essentially perpendicular to the tape edges, an increase in tape length actually shortens the track length, or vice-versa. For a given percentage change in tape length, the track length change is reduced over that percentage by a factor—Poisson's ratio—which is normally 0·5 or less. This factor coupled with the fact that one quadruplex track covers only 1 ms, makes the time error in the system much smaller than a helical system. (Fig. 2(b)). These comparisons show dramatically the importance of maintaining the temperature and humidity of the tape within a narrow range if one expects to have a reasonable chance of having interchangeability among the tapes and machines.

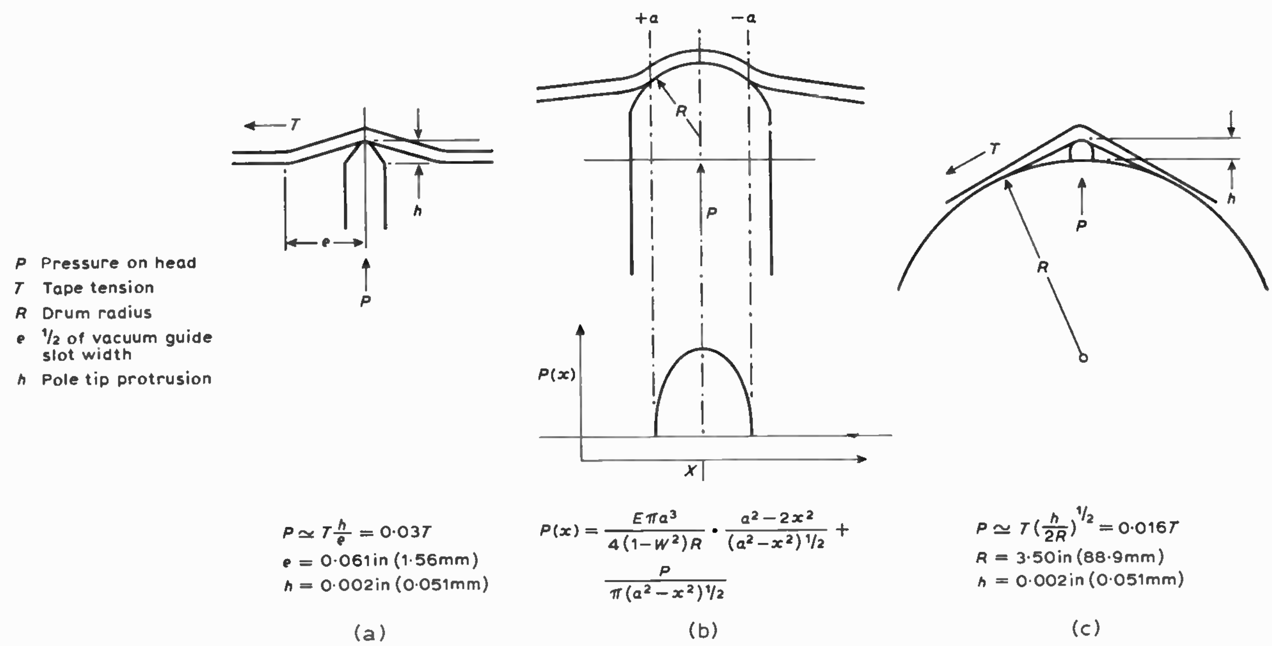

(a) Head-to-tape interface condition (b) Pressure distribution across the head (c) Typical helical.

Fig. 3

3.2 Head-to-Tape Interference Conditions

In a quadruplex system, a high degree of head-to-tape contact is maintained by penetrating the pole tip of the head into the tape which is held under tension by the use of a vacuum female tape guide.

A simplified analysis of the component of tape tension translated into pressure normal to the pole tip is as shown in Fig. 3(a). The overall pressure level applied to the general area of head then will follow a contour curve as shown in Fig. 3(b), with the peak value of the pressure approximately at, or slightly ahead, of the gap.

The physical strength of 2-in (5·08 cm) wide tape and the use of the vacuum female guide makes it possible to maintain a relatively high level of tape tension, and thus a high level of head-to-tape pressure. Adequate and consistent level of head-to-tape pressure is the reason for the repeatable and predictable performance of the f.m. playback system in quadruplex recorders.

Conditions for a typical helical scan geometry is shown in Fig. 3(c). For a given pole-tip protrusion and tape tension, the normal pressure applied to the head is only a half of the quadruplex system. However, in the quadruplex system, the tape tension is uniformly distributed across the tape width, so that the tension is consistent along the length of the video track. On the other hand, in a typical helical system, because of friction of the tape on the stationary surfaces of the scanning assembly, the tension varies along the length of the video track. It usually starts at a value substantially lower than quadruplex and increases as the tape wraps around the mandrel. The result is that the prevailing ratio of head-to-tape pressure between the quad system and the helical scan system is much greater than 2-to-1. This is directly translated into the wider fluctuation of f.m. system frequency response which in turn causes video performance variations and increased level of dropouts.

Table 2. Quad II development objectives

Operational economy	
Tape speed	approx. 6 in/s (15 cm/s)
Head life	300–500 hours
Audio characteristics (two channels)	
Signal/noise	55 dB min.
Video characteristics	
Signal/moiré (100% bars)	40 dB min.
Signal/noise	43 dB min.
Segmentation errors	not visible
High energy tape	can be used to achieve higher s/n
Compatibility with present Quad system	highly desirable

4 Objectives for Possible New Standards

Our objectives for a new standard have been determined from a careful study of user requirements and technical capabilities which we conducted on a worldwide basis early this year. Table 2 shows the objectives in detail and may be summarized by saying that we are trying to provide, at a tape speed considerably slower than present 15·6 in/s, such as 6 in/s with a standard 2 inch quadruplex tape, two high-quality sound channels, a code/cue channel, and video channel. The video characteristics should have improved signal/moiré figure, and lowest possible visibility of segmentation errors. The system should be capable of using high coercivity tape to achieve higher level of signal/noise ratio in both sound and video channels. These characteristics should be achieved in a recorder which would have the capability of being designed in a switchable standard version which would also operate on present quadruplex standards.

5 Technical Approaches

Details of the technical approaches which we plan to utilize to achieve these rather ambitious objectives will now be discussed.

5.1 Narrow Track Head and Reduced Guard Band

Video head track width is one of the parameters which govern the signal-to-noise ratio of the system. Although the output from the head decreases linearly with the track width, the signal/noise ratio does not degrade in the same proportion.[4,5]

Factors governing the signal output are:
Magnetic head track width
Efficiency of the head
F.m. carrier frequency range
Tape coercivity

Noise is generated in the following areas:
Modulator-demodulator electronics
F.m. preamplifier
Magnetic head
Tape

We are proposing to reduce the track width to 4·5 mils (0·114 mm) from the present 10·0 mils (0·254 mm). The corresponding reduction of signal level of 7 dB must be compensated in one form or another if we are to maintain an equal signal/noise ratio.

Techniques producing successful results are as follows:
Wider f.m. deviation to increase video signal level
Reduction of noise in f.m. preamplifier
Improved efficiency of the magnetic head and head-to-tape interface system

Reduction of guard band also yields meaningful improvement in tape usage. Present quadruplex standards specify that the total mechanical inaccuracy of the video headwheel assembly should be less than 0·4 mils (0·0102 mm) as shown in Table 3.

Table 3. Factors governing tracking accuracy

Headwheel mechanical accuracy	
Track width	
Pole tip positional error on carrier	
Carrier positional error on headwheel	
Co-planarity of headwheel with respect to the plane perpendicular to headwheel rotational axis	
Specified total accumulated error: 0·4 mil	
Capstan servo instability	
Peak-to-peak time base jitter: 75 μs	
Control track period: 4000 μs	
Control track spacing: 24 mils	
Tracking jitter: 0·45 mils	
D.c. instability equal to 1% of control track spacing: 0·24 mil	
Total possible tracking error	
Headwheel error (record)	0·4 mil
Headwheel error (play-back)	0·4 mil
Capstan jitter	0·45 mil
Capstan d.c. instability	0·24 mil
Total	1·49 mil

The recent introduction of the high data rate capstan servo system to quadruplex tape decks has reduced the prevailing level of longitudinal time-base jitter to be 75 μs or less. As shown in Table 3, these two factors indicate that a 1·5 mil (0·038 mm) guard band is adequate even under the worst conditions.

Therefore, the track pitch being proposed is 4·5 mils active track plus 1·5 mil guard band, or 6·0 mils (0·152 mm).

5.2 Realignment of Vertical Track Dimensions

In order to accommodate two full quality sound channels, and still maintain areas for cue/code track and control track, the tape area must be more efficiently used.

As is well known, the video tracks meander considerably within the presently designated area for the video track. By clearly defining the extent of meandering, one can establish the absolute minimum vertical track dimension required for the video track. The minimum track dimension is the distance between the start of the forward most track to the end of the rearmost track. As shown in Table 4, this distance can be computed by a rather straightforward mathematical expression.

Table 4. Minimum track length computation

H Horizontal scan rate = 15 625
V Vertical scan rate = 50 Hz
F Frame rate = 25 Hz
W_H Headwheel rev/s = 5 × V = 250
l_a Average track length expressed by number of horizontal lines
N Number of horizontal lines on longer tracks
x Number of longer tracks (with N horizontal lines)
y Number of shorter tracks (with $N-1$ horizontal lines)
l_{min} Minimum track length

$$x + y = (5 \times V/F) \times 4 = 40$$
$$l_a = 625/40 = 15{\cdot}625$$
$$625 = 16x + 15y, \quad x = 25, \quad y = 15$$
$$l_{min} = N + 2\frac{(x-y)}{x+y} = 16{\cdot}500$$

The absolute minimum dimension is equal to 16·500 horizontal lines, or 1·7117 in (4·3477 cm). Adding to this dimension will be the tolerance required for various time-base drifts normally associated with electronics. The dimension we have finally chosen as a safe, practical figure is 1·7603 in (4·4710 cm) for the video track, shown in Table 5, as compared to the present standard of 1·808 in (4·5923 mm).

The difference between two dimensions is almost enough to create an additional sound track with adequate

Table 5. Video track dimensions—length tolerances

Absolute minimum length	4·3477 cm	1·7117 in
Track width positional tolerance (10 μs)	0·0411 cm	0·0162 in
F.m. switching tolerance (20 μs)	0·0822 cm	0·0324 in
Practical minimum length	4·4710 cm	1·7603 in

track dimensions. Some reduction of the control track width was also made, to produce two sound channels with 60 mils (1·52 mm) track width each, and a limited performance channel of 20 mils (0·508 mm) track width, which is primarily intended for cue and code information. Details of the track dimensions are shown in Fig. 4. All of the longitudinal tracks except for the control track are now located at the top of tape.

5.3 Super Highband F.M. System

It has been known that the unwanted beat components, or moiré, observed at the output of a video tape recorder have two principal sources, namely (1) the second harmonic distortion of the f.m. record/playback electronics, and (2) the amplitude limiting process of the demodulation system.[6]

With improvements in the electronic circuit technique, the moiré caused by second harmonic distortion is typically 40 dB below the signal level, and this figure is considered to be acceptable.

However, the second source of moiré, is unavoidable even in an ideal system, and its level is strictly governed by the choice of the frequency spectrum of the f.m. system. A practical means to improve the moiré figure from the second source, which is typically 32 dB for 100% saturated colour bar signal for the current standard, is to move the f.m. spectrum to what is known as fourth shelf, or super highband.

The technique of selecting the frequency spectrum for optimum result is shown graphically in Fig. 5. In summary, we must follow the following steps:

Locate the carrier frequency so that the third lower sideband of the limited carrier falls outside of the frequency range of the first-order sidebands (4th shelf operation).

Use the widest possible carrier deviation for maximum signal/noise ratio.

Locate the carrier, and select the degree of video pre-emphasis so that signal inversion does not take place even for highly saturated colour.

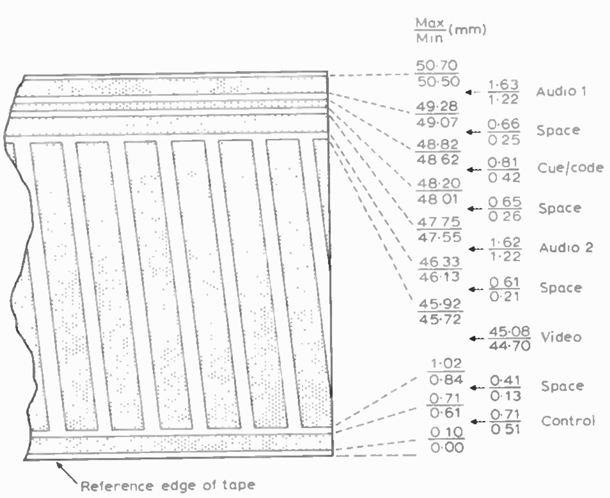

Fig. 4. Longitudinal track dimensions.

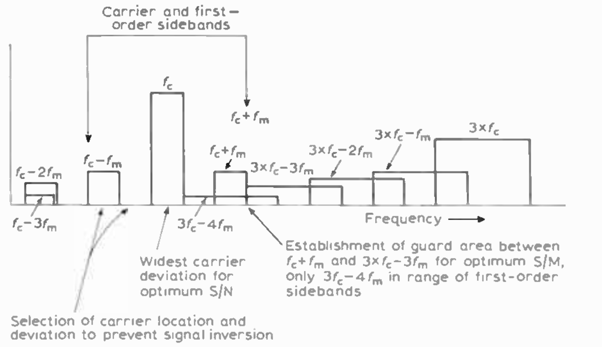

Fig. 5. Super high band f.m. system (4th shelf frequency spectrum).

Locate the carrier at as low a frequency as possible for maximum signal output with a given head-to-tape speed, and gap length.

In practice, these requirements violently conflict with each other, and a delicate compromise of the all governing parameters is necessary. We have tentatively chosen the black carrier frequency to be about 10 MHz, and the white carrier frequency to be in the 12 to 13 MHz region. This spectrum essentially meets our video signal objectives.

Various interference components falling within the baseband video are shown in Fig. 6.

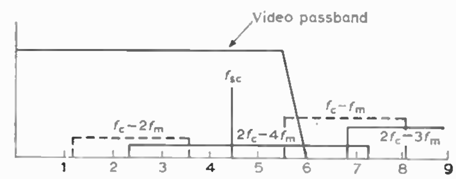

Fig. 6. Location of interference components for 625-line super high band (8·94–10·0–12·5 MHz).

Actual measurements of these components verify our analysis that the amplitude of the highest component, produced by 100% saturated colour bar signal, is approximately 40 dB below the signal.

5.4 Error Correction System with Pilot Tone

Figure 7 shows a block diagram of a pilot tone correction system from which it can be seen that a synchronous pilot signal f_p is generated at exactly 1·5 times the colour subcarrier frequency.

This signal, at low amplitude, is added to the video signal ahead of frequency modulation. The resultant f.m. spectrum after modulation passes through record and playback functions in the usual manner and is demodulated. At this point, the pilot tone is extracted by appropriate filters and it is processed against locally generated references to develop an error signal. This signal is supplied to the time-base compensator to assist in precise time-base compensation. The bandwidth of the pilot tone processor is great enough to provide essentially continuous correction not limited by the line-scanning frequency. Also included in the system is the use of an error signal developed in the pilot tone processor for correction of chroma amplitude errors in the system.

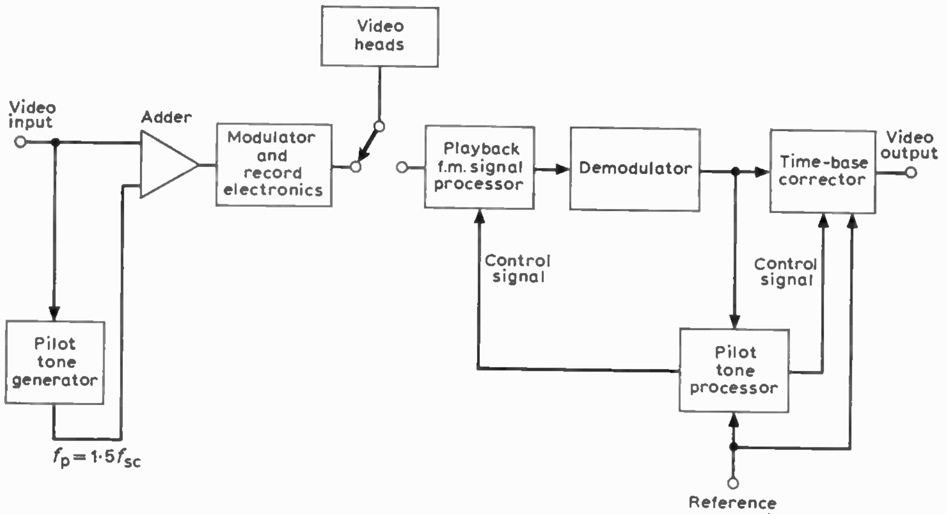

Fig. 7. Pilot tone error correction system.

5.5 Audio System

It has been known that the audio performance, especially the signal/noise ratio, of the quadruplex system is somewhat inferior to what a professional audio recorder is capable of achieving with the equal track width and the tape speed.

This is due to the fact that the tape used for the quadruplex system has its acicular particles oriented in a direction favoring its video tracks. The main disadvantage of using a tape with unfavoured particle orientation is that the signal output is significantly lower than the level which can be obtained from the same tape coercivity. This is shown in Fig. 8.

The difference in the output level between two tapes does not translate directly into the difference in the signal/noise ratio. However, this is one of the reasons that we are currently achieving only 55 dB unweighted signal/noise ratio at the standard tape speed of 15 in/s, and the nominal track width of 67 mils (1·702 mm).

We have established our objective of surpassing this level of signal/noise ratio at the tape speed of 6 in/s, and with a track width of 60 mils (1·524 mm).

As in the case for the f.m. signal playback system, the source of the noise in the audio system is also categorized into three major areas: i.e. electronics, magnetic head, and tape. A study of the degree of contribution from each of these noise sources plays an important part in whether we can achieve such an objective.

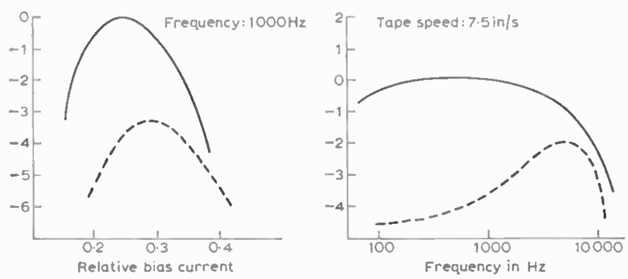

Fig. 8. Effects of particle orientation.
—— standard audio tape
---- quadruplex tape

A breakdown of noise sources can be made by measuring the system signal/noise ratio under the three conditions, i.e.. total system noise, which includes all three (electronics, head, and tape) noise sources, noise of the system under the condition of head not scanning the tape (electronics and head noise only), and the noise of the electronics only.

Results of such measurements made on standard 15 in/s quadruplex system are shown in Table 6. Spectrum distribution of these noise sources is shown in Fig. 9.

Table 6. Audio system signal/noise analysis

System	Signal/noise ratio	Noise sources
Total playback system	55 dB	Electronics Head Tape
Magnetic head connected to electronics but not in contact with tape	62 dB	Electronics Head
Electronics only with its input grounded through high-Q inductance	66 dB	Electronics

A study of these results show the following:

For the spectrum below 1000 Hz, the major noise source is the electronic circuit elements.

For the spectrum above 1000 Hz, the major noise source is the magnetic tape.

The noise contribution from the magnetic head is of significant value above 5000 Hz.

We have conducted a study of amplitude limiting and saturation characteristics of quadruplex tape in the audio region. It indicates that a more nearly optimum audio record equalization characteristic can be developed which will make a worthwhile reduction of tape noise in the frequency region above several kilohertz. This factor alone, we believe, will allow us to achieve our signal/noise ratio objective. Other system refinement possibilities, such as

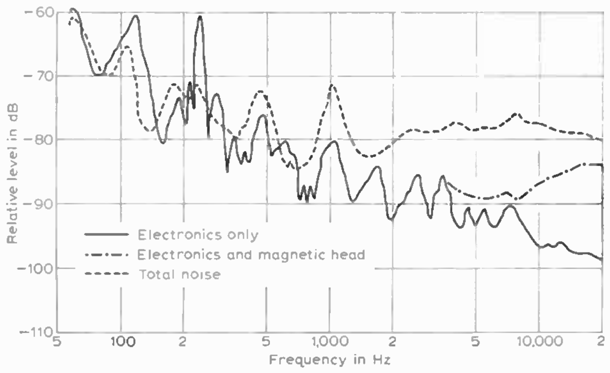

Fig. 9. Audio noise spectrum for standard 15 in/s quadruplex system.

improved electronics and optimization of head impedance are also being considered to further improve the system performance.

6 Conclusion

Progress we have made in our analytical study and empirical work towards a new quadruplex recording standard indicate that the objectives can be achieved with the presently known technology, electronic and electromechanical components, and system philosophy. We hope that, with the cooperation of industry committees, a new standard will be established which is acceptable to both equipment manufacturers and user groups.[7]

7 References

1. Sadashige, K. 'Selected topics on modern magnetic video recording technology.' Proceedings of Conference on Video and Data Recording, Birmingham 1973, p. 1 (IERE Conference Proceedings No. 26).
2. 'Specification for Transverse Track Video Tape Recording', British Standard 4967, 1973.
3. Wada, Y. 'Track straightness in helical scan vtr'. Proceedings of Conference on Video and Data Recording, Birmingham, 1973, p. 51 (IERE Conference Proceedings No. 26); *The Radio and Electronic Engineer*, 44, 1974 (To be published).
4. Coleman, C. H. 'The theory and design of f.m. systems for use in colour television tape-recorders: II. The choice of frequency parameters in colour television recorders', Internat. Conf. on Magnetic Recording, pp. 158–61 (IEE, London, 1964).
5. Felix, M. O. 'The theory and design of f.m. systems for use in colour television tape recorders: I. F.m. systems of exceptional bandwidth', Internat. Conference on Magnetic Recording, pp. 158–61, (IEE, London, 1964).
6. Tooms, M. S. 'Moiré effects in the reproduction of tv signals by vtr machines', *R. Television Soc. J.*, 13, No. 1, pp. 4–10, January/February 1970.

Manuscript received by the Institution on 28th August 1973 (Paper No. 1581/Com. 88).

The Author

Mr. Koichi Sadashige is leader of the Advanced Development Group on Electronic Recording Equipment Engineering with RCA Corporation, Camden, New Jersey. Since joining RCA in late 1953, he has been associated with the development of broadcast products, including colour television camera equipment. During 1965 and 1966 he was in charge of the Scientific Instruments Development group, where the EMU-4 electron microscope and EMTV-1 image intensifier system were designed. Since 1967, he has been engaged in the development of advanced video recording equipment.

Mr. Sadashige received his B.S.E.E. degree from the University of Chiba, Japan and his M.S.M.E. degree from California Institute of Technology, Pasadena, California. He has published over fifteen papers in the fields of television, electron microscopy and video recording technology and he holds a number of United States patents. His interests outside professional activities include acrobatic flying and the collection of antique aircraft and of rare Japanese and American coins.

UDC 621.372.57

Design tables for low-pass equal-valued capacitor active RC networks

F. W. STEPHENSON, B.Sc., Ph.D.*

SUMMARY

The design of low-pass equal-valued capacitor structures is discussed and applied to a number of approximating functions. Particular attention is paid to the suitability of the networks for realization in microelectronic form.

1 Introduction

The desirability of equal-valued-capacitor structures in the microelectronic realization of networks was first referred to by Huelsman.[1] Alternative networks have recently been presented by Dutta Roy and Malik[2] and their comparative performance was subsequently discussed by the writer.[3]

The general circuit arrangements are shown, together with their signal flow graphs in Figs. 1(a)–(d). The resulting transfer functions are:

$$\text{H1} \quad \frac{e_5}{e_1} = \frac{Y_2Y_4Y_6K_3}{(Y_4+Y_5+Y_6)(Y_2+Y_3+Y_4)(Y_1+Y_2)-Y_4^2(Y_1+Y_2)-Y_2^2(Y_4+Y_5+Y_6)-K_3Y_2Y_3(Y_4+Y_5+Y_6)} \tag{1a}$$

$$\text{H2} \quad \frac{e_5}{e_1} = \frac{K_2K_3Y_2Y_4Y_6}{(Y_4+Y_5+Y_6)Y_3(Y_1+Y_2[1-K_2K_3])+(Y_1+Y_2)Y_4(Y_5+Y_6)} \tag{1b}$$

$$\text{D1} \quad \frac{e_5}{e_1} = \frac{K_1K_3Y_2Y_4Y_6}{(Y_5+Y_6)\{(Y_3+Y_4)(Y_1+Y_2)+Y_2Y_1-K_3Y_2Y_3\}} \tag{1c}$$

$$\text{D2} \quad \frac{e_5}{e_1} = \frac{K_1K_2K_3Y_2Y_4Y_6}{(Y_5+Y_6)\{(Y_2+Y_1)(Y_3+Y_4)-Y_2Y_3K_2K_3\}} \tag{1d}$$

where the Y's represent admittances.

If these structures are used to exhibit a low-pass filter characteristic given by:

$$\frac{e_5}{e_1} = \frac{N}{a_3s^3+a_2s^2+a_1s+1} \tag{2}$$

then, in their equal-valued-capacitor form, they may be represented by the circuits in Figs. 2(a)–(d).

* *Department of Electronic Engineering, The University of Hull.*

It has been shown[3] that, if we let:

$$K = \begin{cases} (2-K_3) & \text{for H1 and D1} \\ (1-K_2K_3) & \text{for H2 and D2} \end{cases} \tag{3}$$

the following design equations result:

$$N = \begin{cases} K_3 & \text{for H1} \\ K_2K_3 & \text{for H2} \\ K_1K_3 & \text{for D1} \\ K_1K_2K_3 & \text{for D2} \end{cases} \tag{4}$$

$$a_3 = R_1R_2R_3 \quad \text{for H1, 2, D1, 2} \tag{5}$$

$$a_2 = \begin{cases} R_1R_2K+R_3(2R_1+R_2) & \text{for H1, 2} \quad (6a) \\ R_1R_2K+R_3(R_1+R_2) & \text{for D1, 2} \quad (6b) \end{cases}$$

$$a_1 = \begin{cases} (R_1+R_2)K+(R_1+R_3) & \text{for H1, 2} \quad (7a) \\ R_2K+R_1+R_3 & \text{for D1, 2} \quad (7b) \end{cases}$$

There are thus two sets of non-linear algebraic equations, one for H1, H2 and the other for D1, D2.

Solutions have been presented elsewhere for the special case when $K = 0$. This value of K not only simplifies the design equations but, more importantly, yields convenient values for K_1, K_2 and K_3. However, such realizations do not, in general, yield the minimum values for either the total resistor sum or the resistor spread. In the following Sections, the solution to the equations is considered, with particular reference to these latter parameters. The approximating functions consist of the Butterworth and a selection of Chebyshev polynomials, the coefficients of which are given in Appendix 1.

2 Network Realizations

2.1 Huelsman Forms H1, H2

Figure 3 shows the general form of solution for all functions considered, whilst Table 1 lists the limiting values of K for each case.

In addition to the practically desirable solution when $K = 0$, those interested in circuit fabrication would wish

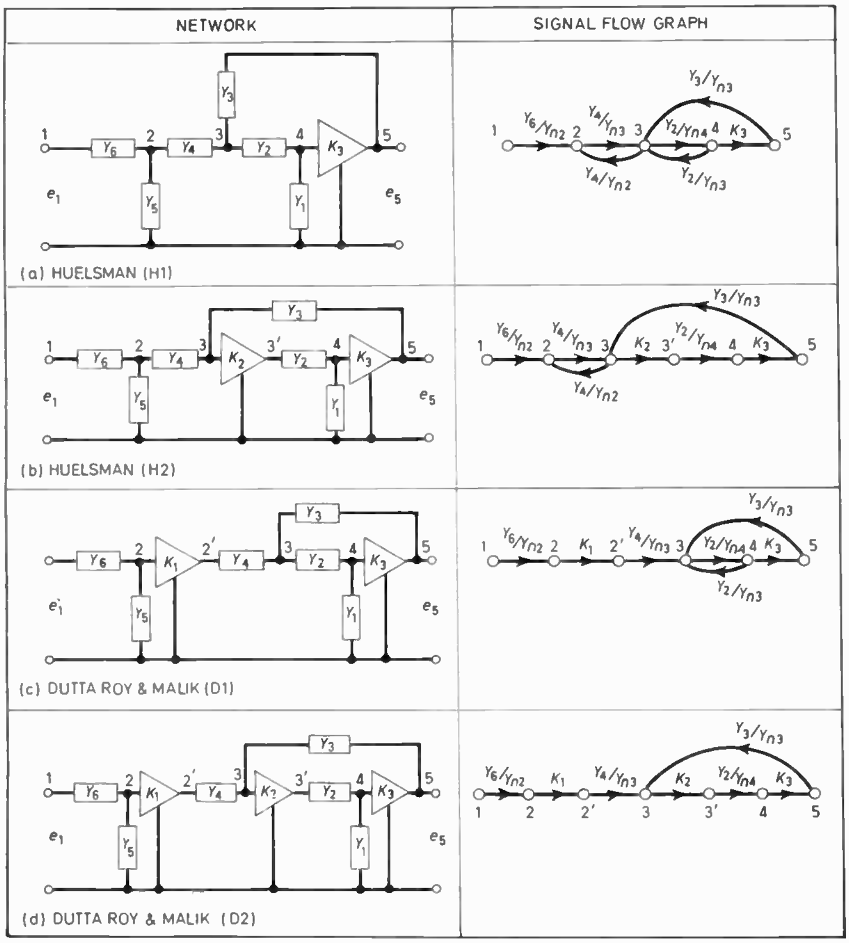

Fig. 1. General network configurations.
Note:
Y_{ni} = sum of admittances at node *i*.

Fig. 2. (*below*)
Equal-valued capacitor networks.
(a) Huelsman (H1)
(b) Huelsman (H2)
(c) Dutta Roy and Malik (D1)
(d) Dutta Roy and Malik (D2)

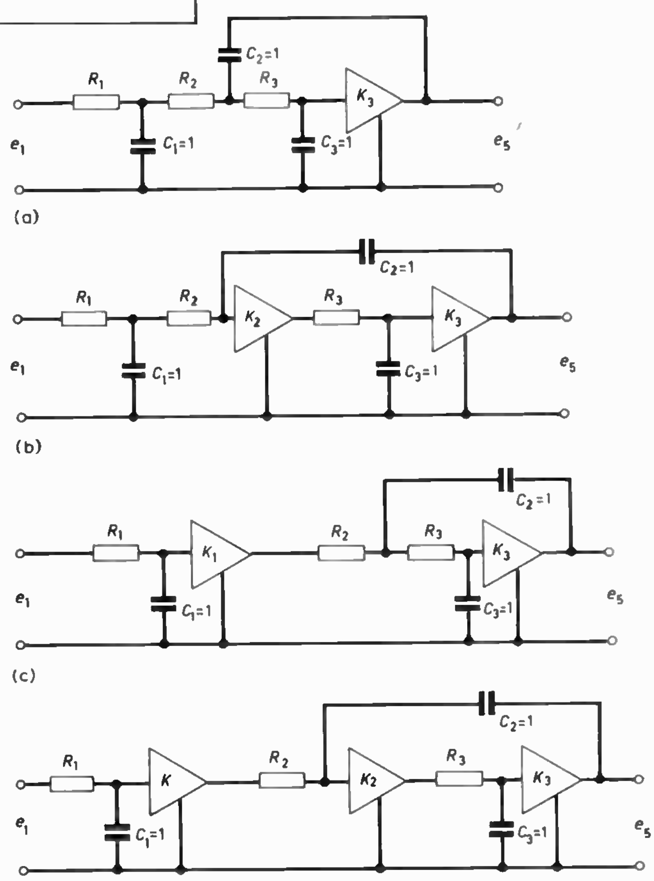

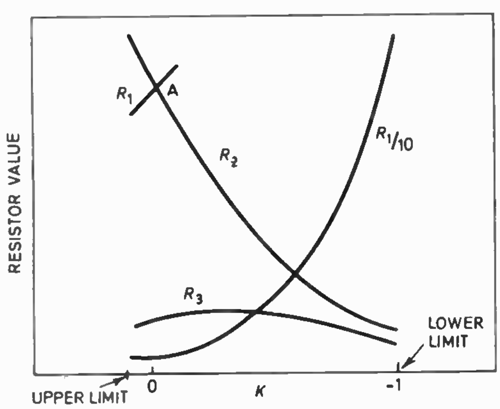

Fig. 3. General form of solution for H1, H2.

Table 1. Limit on K for realizable H1, H2 networks

Function	Limit on K	
	Upper	Lower
Butterworth	+0·11	
Chebyshev 0·5 dB	+0·06	
Chebyshev 1 dB	+0·04	−1
Chebyshev 2 dB	+0·03	in all cases
Chebyshev 3 dB	+0·03	

to determine the value of K:

(i) at the point A, where $R_1 = R_2$,

(ii) for which $(R_1+R_2+R_3)$ is a minimum,

(iii) for which the resistor spread is a minimum.

These realizations, together with that for $K = 0$, are shown in Tables 2(a)–(e), from which it will be seen that conditions (i) and (iii) are identical if practical accuracy is assumed.

The detailed solution of the equations in general, and for case (i) in particular, is given in Appendix 2.

2.2 Dutta Roy and Malik Forms D1, D2

Equations (5) (6b), and (7b) lead to a cubic in R_1 which is independent of K. R_1 is thus constant and depends only on the function being realized. The upper limit on K for realizable solutions is shown for each function in Table 3. No lower limit was sought due to the relatively large values of resistor spread and resistor

Table 3. Upper limit on K for realizable D1, D2 networks

Function	Upper limit on K
Butterworth	+0·13
Chebyshev 0·5 dB	+0·10
Chebyshev 1 dB	+0·08
Chebyshev 2 dB	+0·07
Chebyshev 3 dB	+0·06

Table 2. Network realizations for Huelsman forms, H1 and H2

(a) Butterworth function

Condition	Resistor value (Ω)			K	Resistor sum	Resistor spread
	R_1	R_2	R_3			
$K=0$	1·565	1·469	0·435	0	3·469	3·598
(i), (iii)	1·526	1·526	0·429	0·015	3·481	3·553
(ii)	1·655	1·360	0·444	−0·033	3·460	3·728

(b) Chebyshev 0·5 dB ripple

Condition	Resistor value (Ω)			K	Resistor sum	Resistor spread
	R_1	R_2	R_3			
$K=0$	1·339	2·537	0·411	0	4·287	6·173
(i), (iii)	1·677	1·677	0·497	−0·126	3·851	3·376
(ii)	1·792	1·536	0·508	−0·165	3·836	3·531

(c) Chebyshev 1 dB ripple

Condition	Resistor value (Ω)			K	Resistor sum	Resistor spread
	R_1	R_2	R_3			
$K=0$	1·621	3·217	0·390	0	5·228	8·249
(i), (iii)	2·016	2·016	0·501	−0·125	4·532	4·023
(ii)	2·206	1·770	0·521	−0·180	4·497	4·230

(d) Chebyshev 2 dB ripple

Condition	Resistor value (Ω)			K	Resistor sum	Resistor spread
	R_1	R_2	R_3			
$K=0$	1·859	4·131	0·398	0	6·388	10·357
(i), (iii)	2·357	2·357	0·551	−0·138	5·265	4·280
(ii)	2·586	2·054	0·576	−0·195	5·215	4·488

(e) Chebyshev 3 dB ripple

Condition	Resistor value (Ω)			K	Resistor sum	Resistor spread
	R_1	R_2	R_3			
$K=0$	1·958	4·790	0·426	0	7·174	11·244
(i), (iii)	2·548	2·548	0·615	−0·153	5·711	4·147
(ii)	2·774	2·251	0·639	−0·205	5·664	4·341

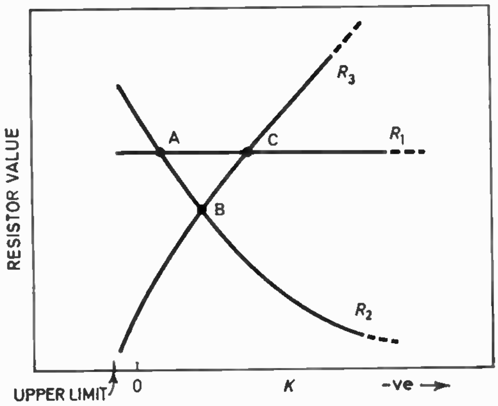

Fig. 4. General form of solution for D1, D2.

sum for decreasing K. Examples of these values are given in Table 4, where $K = -31$.

The general form of solution for the functions under consideration is illustrated in Fig. 4. The following cases are of interest:

(i) $K = 0$, easily realizable amplifier gains,
(ii) point A, at which $R_1 = R_2$,
(iii) point B, at which $R_2 = R_3$,
(iv) point C, at which $R_1 = R_3$,
(v) value of K for which $(R_1 + R_2 + R_3)$ is a minimum,
(vi) value of K for which the resistor spread is a minimum.

Since R_1 is constant, it is immediately clear that (iii) and (vi) are identical. It can also be shown that condition (v) coincides with (iii) and (iv).

Dutta Roy and Malik[2] have shown that, for the Butterworth characteristic, the points A, B and C are coincident when $K = 0$. Thus, the five cases reduce to a single realization in which all elements equal unity.

The results for the remaining functions are illustrated in Table 5.

The detailed solution of the equations is given in Appendix 3.

3 Sensitivity Considerations

Soderstrand and Mitra[4] have discussed the sensitivity of third-order functions. Expressions for S_x^Q and $S_x^{\omega_n}$ may thus be written as:

Table 4. Fabrication 'parameters' for D1, D2 networks when $K = -31$

Function	Total resistor sum (Ω)	Resistor spread
Butterworth	7·25	37·09
Chebyshev 0·5 dB	8·16	34·74
Chebyshev 1 dB	8·88	34·39
Chebyshev 2 dB	10·03	34·02
Chebyshev 3 dB	11·02	33·83

For the functions under consideration, these expressions may be re-written as:

$$S_x^Q = AS_x^{a_3} + BS_x^{a_2} + CS_x^{a_1} \tag{9a}$$

$$S_x^{\omega_n} = DS_x^{a_3} + ES_x^{a_2} + FS_x^{a_1} \tag{9b}$$

The coefficients A, B, C, D, E and F are listed in Table 6. The sensitivity functions $S_x^{a_1}$, $S_x^{a_2}$, $S_x^{a_3}$ for each of the four network structures are given in Table 7. Using this Table it is possible to obtain sensitivity expressions for any realization.

From an empirical study, D2 appears to be the least sensitive structure whilst H1 is the most sensitive. More precise statements on relative sensitivity cannot be made without further investigation.

4 Conclusions

The D1, D2 realizations of the Butterworth function are perfect answers to the fabrication engineer's requirements. Unfortunately, the coincidence of minimum spread, minimum sum, easily obtainable amplifier gain and unity passive element values does not extend to the realization of other functions. In view of this, the most suitable design will depend upon the relative importance placed on the various parameters, often including sensitivity.

The paper illustrates the various alternatives open to the designer and provides the necessary information for the realization of any third-order low-pass characteristic.

5 Acknowledgments

The author would like to acknowledge the advice and assistance of Dr. J. Dunning-Davies, Department of Applied Mathematics, and Mr. M. J. Norman, Centre for Computer Studies, both at the University of Hull.

$$S_x^Q = \frac{\frac{1}{a_3}(2\omega_n Q^2 + \gamma Q - \omega_n)(-S_x^{a_3}) + \frac{a_1}{a_3}(\omega_n^2 Q - 2\omega_n \gamma Q^2)[S_x^{a_1} - S_x^{a_3}] + \frac{a_2}{a_3}\omega_n^2(Q\gamma - 2\omega_n Q^2)(S_x^{a_2} - S_x^{a_3})}{2\omega_n^2[Q(\omega_n^2 + \gamma^2) - \omega_n]} \tag{8a}$$

$$S_x^{\omega_n} = \frac{\frac{(Q\gamma - \omega_n)}{a_3}(-S_x^{a_3}) + Q\omega_n^2 \frac{a_1}{a_3}(S_x^{a_1} - S_x^{a_3}) - Q\omega_n^2 \gamma \frac{a_2}{a_3}(S_x^{a_2} - S_x^{a_3})}{2\omega_n^2[Q(\omega_n^2 + \gamma^2) - \omega_n \gamma]} \tag{8b}$$

where γ, ω_n and Q are obtained from the factored form of the polynomial:

$$a_3 s^3 + a_2 s^2 + a_1 s + 1 = a_3(s + \gamma)\left(s^2 + \frac{\omega_n s}{Q} + 1\right)$$

Table 5. Network realizations for Dutta Roy and Malik forms, D1 and D2

(a) Chebyshev 0·5 dB ripple

Condition	Resistor value (Ω)			K	Resistor sum	Resistor spread
	R_1	R_2	R_3			
(i)	1·002	1·863	0·749	0	3·613	2·488
(ii)	in	1·002	1·392	−0·642	3·396	1·389
(iii), (v), (vi)	all	1·181	1·181	−0·366	3·364	1·179
(iv)	cases	1·392	1·002	−0·182	3·396	1·389

(b) Chebyshev 1 dB ripple

Condition	Resistor value (Ω)			K	Resistor sum	Resistor spread
	R_1	R_2	R_3			
(i)	1·283	2·178	0·728	0	4·189	2·990
(ii)	in	1·283	1·236	−0·395	3·803	1·038
(iii), (v), (vi)	all	1·259	1·259	−0·422	3·802	1·019
(iv)	cases	1·236	1·283	−0·449	3·803	1·038

(c) Chebyshev 2 dB ripple

Condition	Resistor value (Ω)			K	Resistor sum	Resistor spread
	R_1	R_2	R_3			
(i)	1·523	2·736	0·734	0	4·993	3·726
(ii)	in	1·523	1·319	−0·384	4·365	1·154
(iii), (v), (vi)	all	1·417	1·417	−0·482	4·358	1·074
(iv)	cases	1·319	1·523	−0·598	4·365	1·154

(d) Chebyshev 3 dB ripple

Condition	Resistor value (Ω)			K	Resistor sum	Resistor spread
	R_1	R_2	R_3			
(i)	1·618	3·223	0·765	0	5·606	4·211
(ii)	in	1·618	1·524	−0·469	4·760	1·061
(iii), (v), (vi)	all	1·570	1·570	−0·513	4·759	1·030
(iv)	cases	1·524	1·618	−0·559	4·760	1·061

Table 6. Sensitivity coefficients

Function	Sensitivity coefficient					
	A	B	C	D	E	F
Butterworth	1	−1	−1	0	−1	1
Chebyshev 0·5 dB	1·5776	−2·0293	−0·5483	−0·1275	−0·4208	0·5483
Chebyshev 1 dB	1·6953	−2·1983	−0·4971	−0·1893	−0·3078	0·4971
Chebyshev 2 dB	1·9744	−2·5581	−0·4163	−0·2035	−0·2128	0·4163
Chebyshev 3 dB	2·2995	−2·9436	−0·3559	−0·1907	−0·1652	0·3559

6 References

1. Huelsman, L. P., 'Equal-valued-capacitor active-RC-network realization of a third-order low-pass Butterworth characteristic', *Electronics Letters*, **7**, pp. 271–2, 20th May 1971.
2. Dutta Roy, S. C. and Malik, K. K., 'Active RC realization of a third-order low-pass Butterworth characteristic', *Electronics Letters*, **8**, pp. 630–1, 28th December 1972.
3. Stephenson, F. W., 'Comparative performance of equal-valued-capacitor active RC structures', *Electronics Letters*, **9**, No. 21, pp. 505–7, 18th October 1973.
4. Soderstrand, M. A. and Mitra, S. K., 'Sensitivity analysis of third-order filters', *Int. J. Electronics*, **30**, pp. 265–72, March 1971.

Table 7. Sensitivity coefficients

<table>
<tr><th rowspan="2">Sensitivity of</th><th rowspan="2">To</th><th colspan="4">Network</th></tr>
<tr><th>H1</th><th>H2</th><th>D1</th><th>D2</th></tr>
<tr><td rowspan="2">a_3</td><td>R_1, R_2, R_3
C_1, C_2, C_3</td><td colspan="4">1</td></tr>
<tr><td>K_1, K_2, K_3</td><td colspan="4">0</td></tr>
<tr><td rowspan="9">a_2</td><td>R_1</td><td colspan="2">$\frac{2R_1R_3}{a_2}$</td><td colspan="2">$\frac{R_1R_3}{a_2}$</td></tr>
<tr><td>R_2</td><td colspan="4">$\frac{R_3R_2}{a_2}$</td></tr>
<tr><td>R_3</td><td colspan="2">$\frac{R_3(2R_1+R_2)}{a_2}$</td><td colspan="2">$\frac{R_3(R_1+R_2)}{a_2}$</td></tr>
<tr><td>C_1</td><td colspan="4">$\frac{R_3R_1}{a_2}$</td></tr>
<tr><td>C_2</td><td>$\frac{\{R_3(R_1+R_2)-R_1R_2\}}{a_2}$</td><td>$\frac{R_3(R_1+R_2)}{a_2}$</td><td>$\frac{R_1(R_3-R_2)}{a_2}$</td><td>$\frac{R_3R_2}{a_2}$</td></tr>
<tr><td>C_3</td><td>$\frac{\{R_1R_2+R_3(2R_1+R_2)\}}{a_2}$</td><td>$\frac{R_3(2R_1+R_2)}{a_2}$</td><td>$\frac{(R_1R_2+R_3R_1+R_3R_2)}{a_2}$</td><td>$\frac{R_3(R_1+R_2)}{a_2}$</td></tr>
<tr><td>K_1</td><td colspan="2">—</td><td colspan="2">0</td></tr>
<tr><td>K_2</td><td>—</td><td>$\frac{-R_1R_2K_2K_3}{a_2}$</td><td>—</td><td>$\frac{-R_1R_2K_2K_3}{a_2}$</td></tr>
<tr><td>K_3</td><td>$\frac{-R_1R_2K_3}{a_2}$</td><td>$\frac{-R_1R_2K_2K_3}{a_2}$</td><td>$\frac{-R_1R_2K_3}{a_2}$</td><td>$\frac{-R_1R_2K_2K_3}{a_2}$</td></tr>
<tr><td rowspan="8">a_1</td><td>R_1, C_1</td><td colspan="4">$\frac{R_1}{a_1}$</td></tr>
<tr><td>R_2</td><td colspan="4">0</td></tr>
<tr><td>R_3</td><td colspan="4">$\frac{R_3}{a_1}$</td></tr>
<tr><td>C_2</td><td>$\frac{-(R_1+R_2)}{a_1}$</td><td>0</td><td>$\frac{-R_2}{a_1}$</td><td>0</td></tr>
<tr><td>C_3</td><td>$\frac{(R_1+R_2+R_3)}{a_1}$</td><td>$\frac{R_3}{a_1}$</td><td>$\frac{(R_2+R_3)}{a_1}$</td><td>$\frac{R_3}{a_1}$</td></tr>
<tr><td>K_1</td><td>—</td><td colspan="3">0</td></tr>
<tr><td>K_2</td><td>—</td><td>$\frac{-K_2K_3(R_1+R_2)}{a_1}$</td><td>—</td><td>$\frac{-R_2K_2K_3}{a_1}$</td></tr>
<tr><td>K_3</td><td>$\frac{-K_3(R_1+R_2)}{a_1}$</td><td>$\frac{-K_2K_3(R_1+R_2)}{a_1}$</td><td>$\frac{-R_2K_3}{a_1}$</td><td>$\frac{-R_2K_2K_3}{a_1}$</td></tr>
</table>

7 Appendix 1

The polynomial coefficients for the various functions under consideration are listed below:

Function	Coefficient		
	a_3	a_2	a_1
Butterworth	1	2	2
Chebyshev 0·5 dB	1·397246	2·144626	1·750627
Chebyshev 1 dB	2·035388	2·520644	2·011658
Chebyshev 2 dB	3·059132	3·127015	2·257094
Chebyshev 3 dB	3·990514	3·704585	2·383296

8 Appendix 2: H1, H2 Realizations

(i) *General.* Equations (5), (6a) and (7a) may be solved to yield the following polynomial in R_2:

$$R_2^6K^2\left(T^2-\frac{1}{4S^2}\right)+R_2^5\left(\frac{1}{2S^2}-2T^2\right)+$$
$$+R_2^4\left\{a_1^2\left(T^2-\frac{1}{4S^2}\right)+2a_2KT\right\}+$$
$$+R_2^3\left\{\frac{a_3}{S}-4a_3KT-2a_1a_2T\right\}+$$
$$+R_2^2\{a_2^2+4a_3a_1T\}-4a_3a_2R_2+4a_3^2=0 \quad (10)$$

where $S=(1+K)$

and $T=0{\cdot}5\left(\dfrac{K}{S}+1\right)$.

The remaining resistor values are given by:

$$R_1=\frac{(a_1-R_2K)}{2S}\pm\sqrt{\frac{(R_2K-a_1)^2}{4S^2}-\frac{a_3}{R_2S}} \quad (11)$$

and

$$R_3=a_1-R_2K-R_1S. \quad (12)$$

A computer was used to solve for R_2, one positive real root resulting for $0>K>-1$. In such cases, only one of the two values for R_1 yielded a realizable solution.

All solutions for $K>0$ yielded two sets of resistor values. However, one such set can be discarded due to the very high component spread.

(ii) $R_1=R_2=R$. To obtain the point A in Fig. 3, the following cubic in R must be solved:

$$R^3-a_1R^2+2Ra_2-5a_3=0 \quad (13)$$

K and R_3 are then given by:

$$K=\left(\frac{a_1}{2R}-0{\cdot}5-\frac{a_3}{2R^3}\right) \quad (14)$$

and

$$R_3=(a_1-R-2RK). \quad (15)$$

9 Appendix 3: D1, D2 Realizations

(i) *General.* Equations (5), (6b) and (7b) may be solved to yield:

$$R_1^3-a_1R_1^2+a_2R_1-a^3=0 \quad (16)$$

R_1 is thus dependent only upon the function being realized.

For values of $K<0$, only one realizable solution resulted. However, as with the Huelsman networks, dual solutions occurred for $K>0$.

(ii) $R_1=R_2=R$. To obtain point A in Fig. 4, the following cubic must be solved:

$$R^3-R^2a_1+Ra_2-a_3=0 \quad (17)$$

K and R_3 are then given by:

$$K=\frac{a_1}{R}-1-\frac{a_3}{R^3} \quad (18)$$

and

$$R_3=a_1-R-RK \quad (19)$$

(iii) $R_1=R_3=R$. To obtain point C in Fig. 4, the following equations must be solved:

$$a_3R_2^3+R_2^2(2a_1a_3-a_2^2)+R_2(a_1^2a_3-2a_3a_2)-a_3^2=0 \quad (20)$$

$$K=\frac{a_1}{R_2}\pm\sqrt{\frac{4a_3}{R_2^3}} \quad (21)$$

$$R_1=0{\cdot}5(a_1-R_2K) \quad (22)$$

(iv) $R_2=R_3=R$. To obtain point B in Fig. 4.

$$R^6-a_2R^4+a_1a_3R^2-a_3^2=0 \quad (23)$$

$$K=\frac{a_1}{R}-1-\frac{a_3}{R^3} \quad (24)$$

$$R_1=a_1-R-RK \quad (25)$$

Manuscript received by the Institution on 22nd November 1973 (Paper No. 1582/CC 197).

UDC 621.375.1

Feedforward—an alternative approach to amplifier linearization

T. J. BENNETT, B.Sc., Ph.D., C.Eng., M.I.E.E.*

and

R. F. CLEMENTS, B.Sc.(Eng.)†

Based on a paper presented at a meeting of the East Anglian Section of the Institution held in Chelmsford on 7th February 1973.

SUMMARY

Feedforward has largely been ignored as a circuit technique since feedback was introduced in the 1920s. Modern amplifiers can benefit from the application of feedforward as well as feedback and the principle can be applied to both h.f. and X-band amplifiers. The basic principles of feedforward are described and both equations and design curves are included. Two variants of the basic feedforward arrangement are also described. One is arranged for power conservation while the other uses two identical amplifiers at full power to give a more linear output than that available from either separately. The results of these different feedforward arrangements using a pair of proprietary 30 W h.f. amplifiers are included.

* *Formerly with Plessey Avionics and Communications; now with the Ministry of Defence.*

† *Plessey Avionics and Communications, Roke Manor, Romsey, Hampshire S05 02N.*

1 Introduction

In 1927 H.S. Black of the Bell Telephone Laboratories invented the idea of negative feedback as a useful circuit function. It is less generally known that three years earlier he similarly invented feedforward, and on the 9th October 1929, received the U.S. Patent No. 1,686,792 relating to it. Since then the use of negative feedback has predominated, and feedforward largely ignored until the late 1960s when Seidel and his co-workers,[1] again at Bell Laboratories, started to investigate the use of feedforward in amplifiers where inherent group delay precluded the use of feedback because of stability considerations. For instance a travelling-wave tube operating at 4 GHz with a transit time of 13 ns has 52 cycles phase difference between input and output. The phase shifts associated with amplifiers operating at lower frequencies are obviously smaller, but the delays can still be significant down to the h.f. band.

Feedback compares the output signal of an amplifier with its input, and uses the same amplifier to re-process the difference signal. Stability considerations dictate that the group delay of the amplifier (including the feedback path) must not introduce a significantly large phase shift at any frequency within its passband. (We are all familiar with the concept of gain and phase margin.) Feedforward compares, at the amplifier output, the input signal (delayed by a time equal to the amplifier group delay) with the amplifier output signal. A separate amplifier is used to provide a difference signal which is added in antiphase with the original output to give an undistorted output.

There are many potential advantages to feedforward:

- (i) It does not substantially reduce gain.
- (ii) Gain-bandwidth is conserved within the band of interest.
- (iii) It is independent of magnitude or shape of amplifier delay.
- (iv) It recognizes time flow and provides appropriately adapted control circuitry.
- (v) An arbitrarily low error may be achieved by a suitable number of stages.
- (vi) It is an unconditionally stable circuit arrangement.
- (vii) There is no direct relationship between gain and error correction.
- (viii) The second amplifier need only handle the error signals, and so is of lower-power and lower-noise; this results in a better noise figure overall.

So why has the technique been ignored for so long? There are three main reasons:

- (i) The circuit is open-loop so changes in device characteristics with time are not compensated.
- (ii) The circuit element transfer characteristics must be defined to a fraction of a dB over the frequency band.
- (iii) A second amplifier is used.

Traditionally, negative feedback has been used to define gain independently of spread in device characteristics, so it is not surprising that a technique which insists on closely defined device characteristics should be shunned.

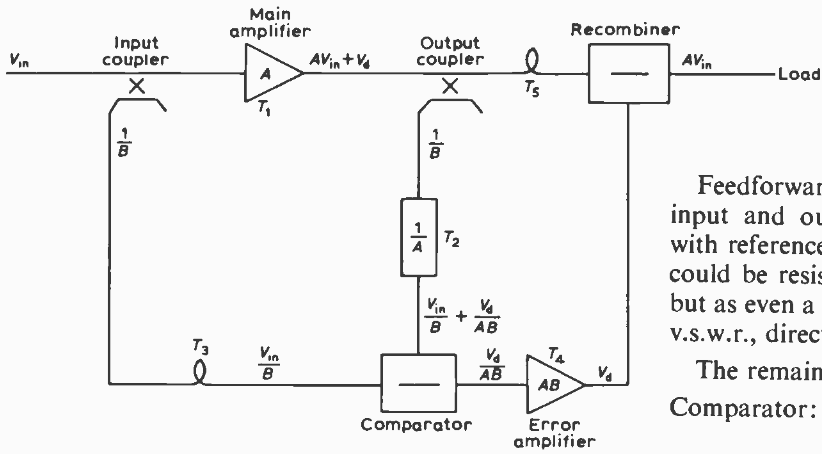

Fig. 1. Simplified principle of feedforward amplifier

However, the work reported by Seidel and his co-workers[1-3] has shown that very impressive results may be obtained when working with very linear amplifiers. The objective of this paper is not to restate these results but to present the concept of feedforward together with a set of design criteria and some practical examples.

2 Principles of Operation

As mentioned above, perhaps the most important feature in the operation of feedforward is that the amplified signal is compared with the reference signal at the output of the amplifier, after the reference signal has experienced a delay equal to the group delay of the amplifier. This is shown in Fig. 1 which depicts a complete feedforward amplifier.

In the diagram the input and output couplers have a voltage coupling ratio of B:1 where for simplicity B is assumed to be large enough to have no significant effect on the main signal path. The actual signal attenuation in these couplers can easily be allowed for. The main amplifier has a gain A, a group delay of T_1 and introduces an unwanted signal V_d. The output power is sampled using the output coupler and the sample passed through an attenuator with a voltage transfer ratio of $1/A$, which allows the comparator or difference hybrid to compare the output with the input at the same power level, while delay T_3 is arranged to equal T_1+T_2 so the two signals coincide in time. The output from the comparator is seen to be V_d/AB. The 3 dB loss expected from a practical difference hybrid can be assumed to be included in the $1/A$ attenuator in this case.

The input to the error amplifier is V_d/AB and may be considered to be composed of noise and distortion as well as signals due to variations from the main amplifier nominal gain and phase characteristic. The error amplifier gain is AB and the group delay is T_4.

Thus as long as T_5, the main signal delay, is arranged to equal T_2+T_4, the unwanted signal V_d will be cancelled in the recombiner difference hybrid. It will be seen that there is a continuous forward signal flow along separate paths with no stability problems being introduced by re-circulation.

The basic elements of a feedforward amplifier have now been described but as there are no standard terms, those used in this paper will be defined:

Feedforward amplifier, main amplifier, error amplifier, input and output couplers have already been defined with reference to Fig. 1. The input and output couplers could be resistive dividers in an ideally matched circuit but as even a small mismatch gives rise to an appreciable v.s.w.r., directional couplers are used in practice.

The remaining terms are:

Comparator: Difference hybrid or differential amplifier used to determine error signal V_d/AB.

Recombiner: A circuit element which allows the main amplifier and error amplifier outputs to be combined in such a way that the unwanted signals cancel.

Time delays: T_1, T_2 and T_4 are time delays inherent in the circuitry while T_3 and T_5 are delay lines inserted to compensate for the circuit delays.

It is already possible to determine at least qualitatively some characteristics of feedforward operation:

(i) The circuit corrects for both distortion and gain variation in the main amplifier.

(ii) The recombiner is likely to introduce attenuation into the main amplifier output.

(iii) The noise performance is likely to be dominated by the error amplifier.

In order to obtain design information and to provide quantitive performance information, it is necessary first of all to consider the two points where the signal paths interact: the comparator and recombiner.

2.1 Comparator

The comparator is most easily considered as a 3 dB lossless hybrid coupler with two input ports (ports 1 and 2) and two output ports (ports 3 and 4). For the case where the two input voltages are equal, $V_1 = V_2 = V\cos\omega t$; there will be an output of $(\surd 2)V\cos\omega t$ from port 3 and no output from port 4. In a balanced feedforward circuit the error amplifier would be connected to port 4 and no signal power would be fed to the error amplifier. If in addition an error signal is now introduced into one of the input ports from the main amplifier then this will split equally between ports 3 and 4 and thus give the necessary error signal to the error amplifier.

If the main amplifier gain varies from nominal then the signal inputs to the comparator are $V_1 = V\cos\omega t$ and $V_2 = kV\cos\omega t$. The signal output from port 4 is now not zero but $(1-k)(\surd 2)V\cos\omega t$ where $(1-k)$ is the fractional change in main amplifier gain. If, as well as change in gain there is a change in phase as shown in Fig. 2 then the comparator inputs may be written as $V_1 = V\cos\omega t$, $V_2 = kV\cos(\omega t+\phi)$ and now the amplitude of the voltage from port 4 becomes:

$$|V_4| = V(2+2k^2-4k\cos\phi)^{\frac{1}{2}}$$

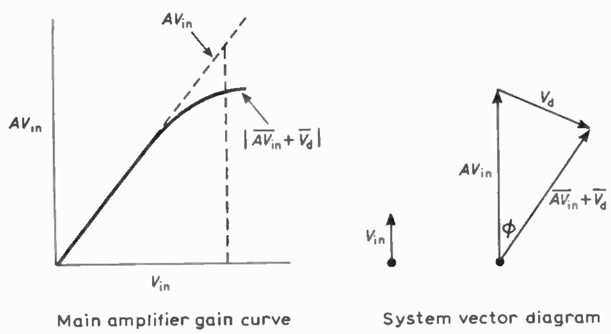

Fig. 2. Example of distortion V_d arising only from main amplifier gain and phase variation.

This expression gives rise to Fig. 3 which shows the power handled by the error amplifier as a function of gain and phase variations in the main amplifier. A similar set of curves may be obtained for increase in main amplifier gain, but as this results in overall power loss it will not be considered here for reasons which will be explained later. It will be noticed that when the main amplifier gain drops by 6 dB to half voltage, the two amplifiers provide equal power (assuming the error amplifier will operate linearly under these conditions). This apparent anomaly must be explained with reference to Section 2.2 where it is explained that the recombiner is assumed to be a 3-dB hybrid. So with no main amplifier gain variation there is a loss of 3 dB between the main amplifier output and the feedforward amplifier output. The error amplifier handles no signal. When the main amplifier gain has fallen by 6 dB each amplifier is providing half the total output power which is still 3 dB down on the main amplifier nominal power output.

Figure 3 allows us to define the requirements for the error amplifier with a knowledge of the gain and phase variations, and distortion products of the main amplifier. For example if the main amplifier gain decreases by 2 dB from nominal in the frequency range of interest and the phase varies by $\pm 9°$ then the error amplifier must deliver -12 dB of the main amplifier power to the output (any attenuation in the recombiner must be added). If the distortion in the form of intermodulation products etc.

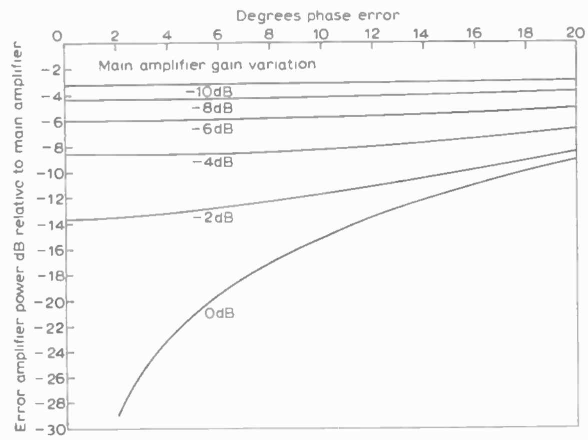

Fig. 3. Error amplifier power requirement as a function of main amplifier gain and phase variations.

is -20 dB relative to the wanted signal then the error amplifier power requirement is dominated by the main amplifier gain variation.

2.2 Recombiner

Let us now consider the recombiner. For convenience this will also be assumed to be a 3-dB hybrid coupler. Other alternatives will be considered later when the principles have been outlined. The arrangement is similar to that described for the comparator but this time the equivalence to port 3 is used as the output port, as the unwanted signals are now being cancelled. To determine the degree of cancellation obtained with variations in error amplifier gain and phase, the considerations and equations are similar to those for the comparator, and result in the curves of Fig. 4. Once again a further set of curves corresponding to gain increase may

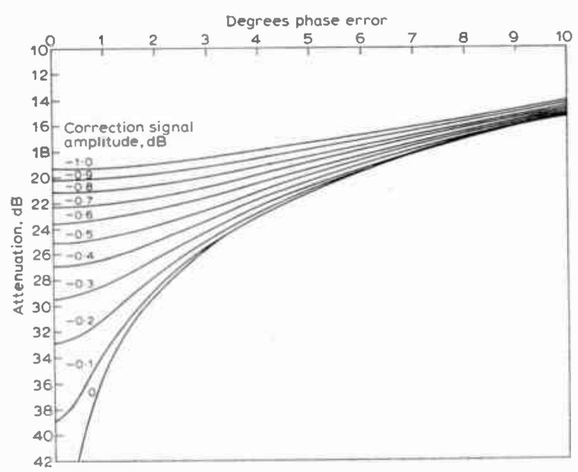

Fig. 4. Attenuation of error signal as a function of error amplifier gain and phase variations.

be obtained but the differences between the two sets of curves for up to 1 dB gain variation are very slight (-1 dB gain variation gives a curve approximately equivalent to that for a $+0{\cdot}9$ dB variation.) The figure shows the extent of the cancellation of unwanted signals for gain and phase variations in the error amplifier. Two very important characteristics of feedforward may be obtained from these figures.

Firstly, during the setting-up procedure the comparator balance determines the error amplifier power while the recombiner balance determines the quality of the distortion correction. Secondly, in order to obtain significant, consistent distortion cancellation the error amplifier gain and phase characteristics must be controlled very closely. The corollary to this, of course, is that the better the equipment you start with the greater the improvements obtained. A further point worth mentioning at this stage is that there is a practical limit to the degree of cancellation to be aimed at, and this is determined by the distortion in the error amplifier. If the error amplifier is handling only intermodulation distortion signals, for instance, and has an intermodulation product (i.p.) performance of -30 dB for two input tones, then 30 dB is the maximum distortion attenuation it is worth aiming at unless a second feedforward loop is used. This level

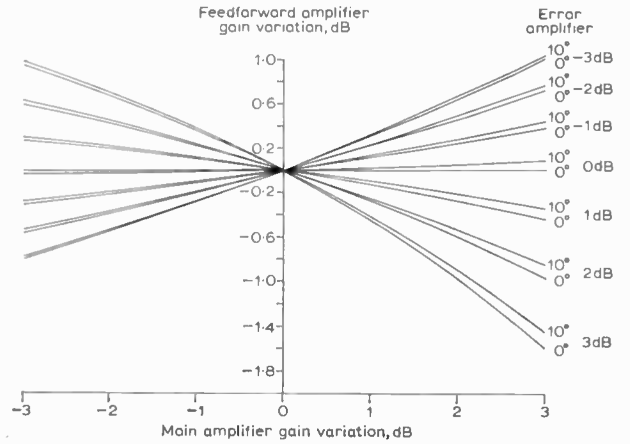

Fig. 5. Feedforward amplifier gain as a function of main and error amplifier gain and phase variations.

will be reduced if the error amplifier also has to handle some signal power.

2.3 Gain Control

As mentioned earlier the feedforward circuit corrects for gain variations in the main amplifier. Figure 5 shows the variation in feedforward amplifier gain as both main and error amplifier gains are varied. Small variations in phase are shown to be unimportant for this application.

2.4 Error Amplifier Gain

The error amplifier gain was shown to be AB in Fig. 1. This assumed that the input and output couplers were equal and that there was no loss in the recombiner. In practice the recombiner might be a 10 dB coupler to reduce the attenuation of the wanted signal power. The output coupler will probably be a 20-dB coupler and then the input coupler and the attenuator will most likely be chosen to match a suitable available error amplifier gain A wide range of amplifier gains can easily be accommodated.

3 Performance Considerations

Having described the basic mode of operation, performance characteristics and the relevant design criteria associated with them are now considered.

3.1 Noise Performance

The noise figure of the feedforward amplifier is the noise figure of the error amplifier in dB plus the attenuation in dB of the signal between the input to the input coupler and the input to the error amplifier. This means that in the practical case where the overall noise figure must be close to that of the error amplifier, the input coupler and comparator must be connected to give no attenuation to the reference signal. The result of this is that main amplifier gain is reduced by the coupling factor of the input coupler. However the overall result is a feedforward amplifier which has the noise figure of the error amplifier but the power handling capability of the main amplifier.

3.2 Amplifier Gain and Power Handling

It is probably fair to say that, in general, the output power level is more important than the amplifier gain so overall gain loss due to the choice of the input coupler is less important than loss of power due to output coupler and recombiner. If the output coupler ratio is 20 dB and the recombiner 10 dB, then the signal attenuation will be very small while the error amplifier power handling might still be significantly smaller than the main amplifier, provided the gain variations are very small and the initial distortion −20 dB or less.

3.3 Frequency Response and Bandwidth

In contrast to negative feedback, for feedforward the performance of the amplifiers and other components need only be specified over the frequency range of interest. The concepts of gain and phase margin for stability do not enter into the considerations since the feedforward arrangement is unconditionally stable, independent of the gains, phases and time delays used.

4 Power Conservation

The decision to use a directional coupler as the recombiner appears to result in the loss of some of the power handling capability available. For example, if a large coupling ratio is used then the main signal is imperceptibly attenuated, but as a result the error amplifier has to deliver a correspondingly higher level of power than is utilized. Conversely if a 3-dB coupler is used, the error amplifier needs only to handle the exact level of distortion existing in the signal path but half the output power is lost. If economics will not allow this power loss even in the pursuit of linear amplifiers, then it is possible to counter it by allowing the error amplifier to handle a controlled amount of the wanted signal power. This resulting arrangement is a system which, for convenience, is called feedforward type 2.

To determine the amount of power to be handled by the error amplifier, define a figure of merit F as the ratio of total output signal power to total amplifier power capability. Figure 6 shows figure-of-merit plotted as a function of recombiner coupler ratio and main amplifier gain variations. This figure takes no account of distortion power handled by the error amplifier; as this varies according to the particular amplifiers used it must be added separately.

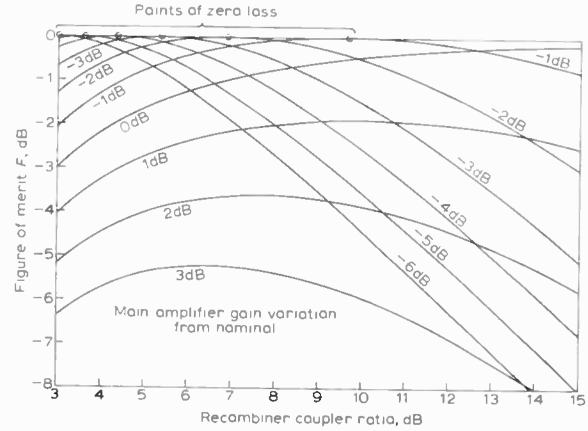

Fig. 6. Feedforward amplifier power loss with recombiner coupler ratio variation assuming no phase error.

The type 1, or basic arrangement, corresponds with the 0 dB curve where the figure of merit is just the forward loss through the coupler. If the main amplifier gain is reduced by 1 dB then from Fig. 6 there will be no overall power loss if a 9·5 dB coupler is used. Similarly, −2 dB corresponds to a 7 dB coupler. In these cases the gain variations are simulated by varying the attenuator prior to the comparator.

If Fig. 6 is used to set up the feedforward circuit then two design features must be taken into account. Firstly, the lower the recombiner ratio, the more power is handled by the error amplifier and consequently less distortion correction is possible. Secondly, the figure of merit is relatively insensitive to gain variations in the main amplifier.

5 Practical Examples

In practice it has been found that all the design criteria are accurate, and that all that is necessary to predict the performance of a particular arrangement is an accurate set of performance figures for all the components. This has been found to be the case for applications from audio frequencies to X-band.

5.1 Feedforward at X-Band

By suitable feedforward circuit arrangements using two t.w.t.s operating at 9 GHz, it was found possible to reduce i.p.s by more than 20 dB for a test with two tones separated in frequency by up to 100 MHz. These two t.w.t.s were operating at different power levels.

As any such feedforward arrangement requires two t.w.t.s, it is of interest to determine whether better performance can be achieved in this way than by the alternative method of operating the two tubes in parallel.

Two identical t.w.t.s were not available and so the comparison had to be calculated, based on the measurements made on a single tube. The maximum distortion allowable was assumed to be −30 dB i.p.s; 18 dBm output per tone was found to give this performance for a single tube.

Predictions were made, based on allowing the main amplifier t.w.t. to operate into saturation with −10 dB i.p.s, and assuming that the original feedforward arrangement could be used to give 20 dB improvement (i.e. −30 dB i.p.s). These predictions showed that the feedforward arrangement would give 4 dB more power output than the corresponding parallel arrangement. There are, of course, limitations to this, one of which is the reduction in gain. However, potential power improvements of this magnitude are worth considering, when it is at the expense of circuit complexity rather than capital cost.

5.2 Broadband H.F. Amplifier

Following demonstrations that the general design criteria were valid, it was decided to investigate the particular problems involved in applying feedforward to a broadband h.f. amplifier. Currently available h.f. power transistors impose a limit to the linearity of h.f. power amplifiers even when considerable negative feedback is applied. As one method of improving performance is to reduce the power level in the amplifier, a small amount of power loss using feedforward seemed acceptable.

The amplifier used for both main and error amplifiers was a proprietary transmitter amplifier which has a design performance of −25 dB i.p.s for two tones separated by 300 Hz to 3 kHz at 30 W p.e.p. into 50 Ω.

The gain of the amplifiers varied less than +1 dB from nominal over the 3–30 MHz h.f. band, while the phase response varied ±10° from that due to a nominal 54 ns group delay over most of the band increasing to about +30° at the 3 MHz band edge and −15° at the 30 MHz band edge due to the interstage coupling arrangements used.

5.3 Circuit Components

The practical circuit arrangement is shown in Fig. 7. The input and output couplers both had 20 dB coupling ratios while the recombiner has a 12 dB coupling ratio. All three of these were made from ferrite transformer pairs. The 20-dB couplers had a 0·25 dB insertion loss and ±0·1 dB coupling ratio variation between 2 and 30 MHz and a directivity of better than 31 dB. The comparator was a 180° 3-dB hybrid transformer and the delay lines were combinations of low-loss cable and variable air line sections. The attenuators used included variable attenuators with 0·1 dB steps so that amplitude match within 0·1 dB was possible.

5.4 Circuit Performance

As mentioned above the phase response of the group delay compensated amplifiers showed distinct variations at the band edges of the frequency band 3–30 MHz. Normally this has no effect on the performance of the amplifier but in the present case it is an important

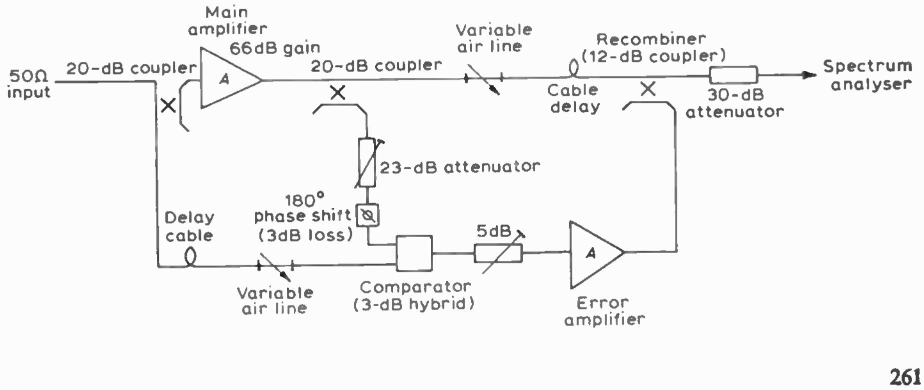

Fig. 7.
Experimental feedforward circuit.

feature. It was decided that it was sufficient for initial measurements to be made on the system with simple time-delay compensation, in order to confirm predictions. For a system the amplifier phase characteristic could be linearized and phase compensation used if necessary.

5.5 Results

Figure 8 shows the intermodulation product performance of the feedforward amplifier together with the performance of the basic amplifier, both at 30 W p.e.p. As expected the correction obtained at the band edges was considerably less than at the centre. An improvement of 20dB across the band could be obtained at spot frequencies by suitable adjustments of the variable delay line and wideband performance was predicted with the use of suitable phase shift networks.

In order to assess the feedforward circuit arrangement at this stage it is instructive to compare its performance with that of the two amplifiers connected in parallel as for the t.w.t.s. For the sake of comparison it is assumed that the output power required is that of a single amplifier operated at full power while the linearity of the single amplifier is inadequate. Both methods improve the linearity by introducing a second amplifier. In the feedforward case the improvement is obtained by using the second amplifier to handle the correction signal, while in the parallel case each amplifier handles half its rated power and is therefore operating more linearly. In neither case is the total power capability realized. Figure 8 also shows the performance of the under-run amplifiers. In this case it is interesting to note that there is no overall significant difference in the performance compared with the feedforward case, while the feedforward is potentially capable of improvement.

6 Feedforward Type 3

The considerations of power conservation and linearity improvement lead to consideration of a system which may be referred to as feedforward type 3. In this case two identical amplifiers are used and both are operated at full power. In this arrangement two types of linearization are applied simultaneously. The comparator circuit is arranged to give the error amplifier a predistortion signal, derived from the main amplifier transfer characteristic, together with a feedforward signal and half the

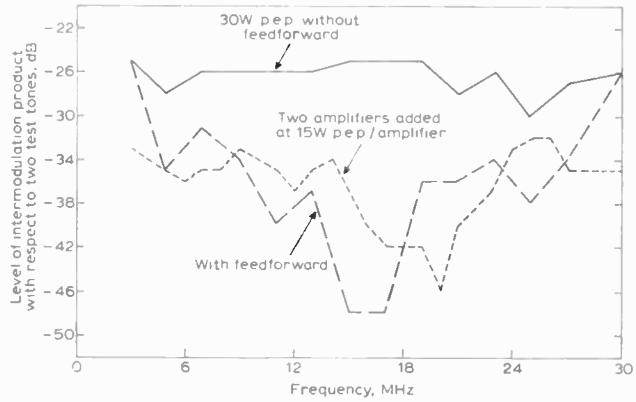

Fig. 8. Intermodulation performance of 30W amplifier with and without feedforward.

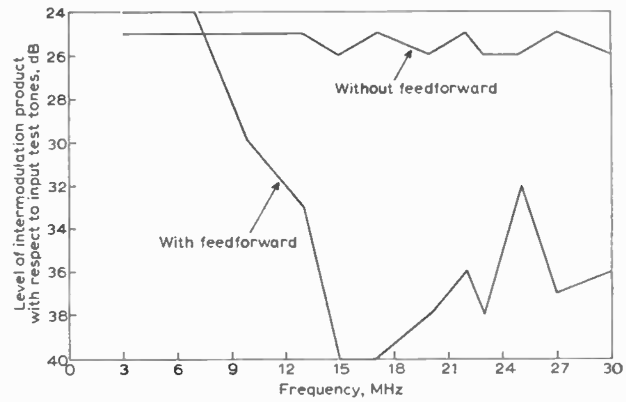

Fig. 9. Intermodulation performance of improved system.

wanted signal power. This means that the predistortion signal linearizes the error amplifier and this linear amplifier is then used to handle half the total output power together with the feedforward signal to linearize the main amplifier output. Figure 9 shows the results obtained using this system.

The amplifiers are again the 30 W p.e.p. transmitters but this time both are operating at 30 W p.e.p. and the combined output is 50 W p.e.p. The losses are due to output couplers and the 11 metres of delay line. The individual amplifiers are operating at around -25 dB i.p.s while the combination is significantly improved. Once again only the simple time delay compensation is used, which implies a system which may be more tolerant of phase differences.

7 Conclusions

The basic concept of feedforward has been described and various terms and design criteria introduced. Examples of the application of feedforward to X-band t.w.t.s and a wide band h.f. amplifier were given. Two variants of the basic feedforward circuit were described: one offered advantages in terms of power conservation, while the other allowed two identical amplifiers to be used at full power and for each amplifier to be used to linearize the other, with the result that the final output was more linear than that available from either amplifier. The results obtained with the latter arrangement lend an air of respectability to feedforward and promise to elevate it from the position of a long forgotten curio to that of a very useful technique in tomorrow's amplifiers.

8 References

1. Seidel, H., Beurrier, H. R. and Friedman, A. N., 'Error-controlled high-power linear amplifiers at v.h.f.', *Bell Syst. Tech. J.*, 47, pp. 651–722, May–June 1968.
2. Seidel, H., 'A feedforward experiment applied to an L-4 carrier system amplifier', *IEEE Trans. on Communications*, **COM-19**, pp. 320–5, June 1971.
3. Seidel, H., 'A microwave feedforward experiment', *Bell Syst. Tech. J.*, **50**, pp. 2879–2916, November 1971.
4. Jurgen, R. K., 'Feedforward correction: a late-blooming design', *IEEE Spectrum*, **9**, pp. 41–3, April 1972.

Manuscript first received by the Institution on 21st September 1973 and in revised form on 14th January 1974 (Paper No. 1583/CC198).

UDC 621.319-1:621.396.677.75: 621.396.965

Scanning ferroelectric apertures

S. N. DAS, M.Sc.*

SUMMARY

To reduce the loss of an array due to the fixed element pattern and to reduce the grating-lobe problem for large steering angles, the use of scanning ferroelectric apertures is proposed. The phase front and, as a result, the beam direction of a scanning ferroelectric element are determined by its permittivity controlled by the biasing voltage applied to it. The calculated angle of steering of a scanning element, made of polycrystalline $BaTiO_3$, is more than $\pm 75°$ at 10 GHz. A quality factor is defined for the purpose of comparing the efficiency of different ferroelectric materials for application in a scanning element.

* Consultant, P.O. Box 19142, Washington D.C. 20036, USA.

List of Symbols

A	area of the antenna aperture
d	distance between the centres of the adjacent elements of the array
D	aperture length
E	bias electric field, kV/cm
f	frequency in GHz
F	receiver noise figure
F_1	noise figure of the first low-noise amplifier
F_2	noise figure of the second low-noise amplifier (not shown in the text)
G	gain of the aperture
G_1	gain of the first low-noise amplifier
i	angle of the incident beam
l	width of the aperture
L_a	total aperture losses
L_r	receiver losses between the first and the second amplifiers
M	$\sin i_1$
n	refractive index
N	total number of individual antenna elements in the array
P	radiation pattern of the array
P_p	peak power
Q_F	quality factor
r	angle of the refracted beam
V_b	breakdown voltage
Z	impedance of the device
α	total losses of the ferroelectric device
α_c	copper losses in the conductive coating, dB/unit length
α_d	attenuation constant due to the dielectric losses, dB/unit length
ε	relative permittivity of the ferroelectric material
λ	free-space wavelength
σ	ratio of the refractive indices at zero bias and at a bias field E
θ	scan angle
μ	relative permeability of the ferroelectric, usually unity
$\tan \delta$	dielectric loss tangent
1, 2, 3	subscripts referring to the three media (Fig. 2)

1 Introduction

By scanning the element pattern synchronously with the array, the reduction of the array gain at large scan angles, due to the fixed element pattern and the grating-lobe problem can be minimized. Such element scanning, using ferromagnetic materials, has been reported.[1–7] Scanning of horn apertures using multi-mode excitation has also been proposed.[8] Angelakos and Korman[1] produced 40° electronic scanning in one plane with fields of 6×10^4 A/m with a completely filled open waveguide aperture at X-band. Palais[2] realized scan angles of $\pm 30°$ in one plane with maximum fields of 0·03 T. Wheeler[3] described a cylindrical waveguide aperture loaded with a ferrite sphere to produce conical scanning.

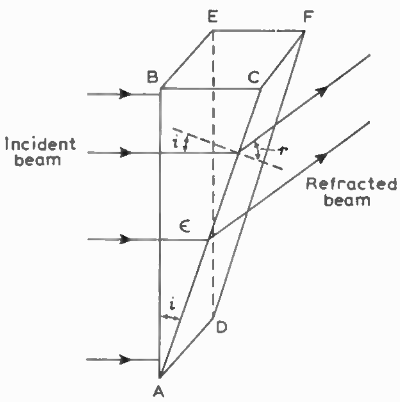

Fig. 1. Scanning of a beam by a ferroelectric aperture, horizontal scanning.

Engelbrecht[4] considered a post biased to ferromagnetic resonance and placed just outside the waveguide aperture at the focus of a parabolic reflector. The performance of an electronically-steerable array of ferrite scanner elements at millimetre wavelengths has been demonstrated.[7] An array of five elements was shown to be capable of scanning a beam $\pm 25°$ at a rate of $1°$/ms. The ferrites have a relatively slow scan speed, 50 ms (ref. 7). Increasing and decreasing fields of same magnitude produce different scan angles due to the hysteresis effect.[6] Ferroelectrics, on the other hand, can be switched[9] at a comparatively faster rate (microseconds or faster). Above the Curie temperature, where the ferroelectrics are generally used for microwave applications, they do not display hysteresis.[9] Ferroelectric materials inherently have a high peak-power handling capability. Their properties, however, are generally dependent on the operating temperature.[9]

2 Theory

A beam can be steered by altering the linear phase front of the wave by passing the incident beam through a dielectric whose properties can be electronically controlled. The refractive indices of a number of dielectric materials can be changed by the application of suitable biasing voltages. Consider the case of the TEM-mode propagation, such as in a balanced strip-line configuration, in a ferroelectric material fabricated in the form of a wedge (Fig. 1). Surfaces ABC and DEF are covered with conductive coatings. The normally incident wave traverses through the wedge (Fig. 1) obeying Snell's law:

$$\sin r/\sin i = n = \sqrt{\mu\varepsilon} \tag{1}$$

and

$$\theta = r - i \tag{2}$$

With a fixed incident beam, its direction is electronically controlled by changing the permittivity of the aperture. The maximum value of the wedge angle that can be used, to prevent internal reflexion, is given by

$$n \sin i = 1 \tag{3}$$

Figure 1 provides scanning in the horizontal plane alone. Scanning in the vertical plane is obtained by a similar wedge. Figure 1 provides scanning on one side of the boresight. Steering on both sides of the boresight can be achieved with two adjacent wedges. In practice, the two wedges are built from one piece of material (Fig. 2). Surfaces DEFG, ABC and A'B'C' are covered with conductive coatings leaving an insulating layer ACA'C' between the latter. As a result, bias voltages can be applied independently to the surfaces ABC and A'B'C'. For simplicity, the presence of the insulating layer ACA'C' is neglected in the following analysis. The path of a ray, in this case, is given by

$$n_1 \sin i_1 = n_2 \sin r_2 \tag{4}$$

$$n_2 \sin i_2 = n_3 \sin \theta \tag{5}$$

and

$$r_2 = i_1 + i_2 \tag{6}$$

The incident angle i_1 is equal to the wedge angle. Let

$$\sin i_1 = M \tag{7}$$

Combining equations (4)–(7), one obtains

$$\sin \theta = M(n_1\sqrt{1-M^2} - \sqrt{n_2^2 - n_1^2 M^2})/n_3 \tag{8}$$

For $M \ll 1$, an appropriate value of M is

$$M \simeq n_3/(n_1 - n_2) \tag{9}$$

When $n_2 > n_1$, the beam is deflected towards the reader. When $n_2 < n_1$, the beam is deflected away from the reader. As a result, by biasing the segment ABC or A'B'C', the beam can be scanned on both sides of the boresight. In practice, the aperture is designed to be trapezoidal, rather than rectangular, to prevent outer rays being reflected, during scanning, from the sides of the aperture element. The radiation pattern of the array is given by[7]

$$P = \left[\frac{\sin \dfrac{\pi D \sin \theta}{\lambda}}{\dfrac{\pi D \sin \theta}{\lambda}}\right]^2 \left[\frac{\sin \dfrac{N\pi d \sin \theta}{\lambda}}{N \sin \dfrac{\pi d \sin \theta}{\lambda}}\right]^2 \tag{10}$$

The first factor in the r.h.s. of equation (10) is contributed by the element and the second factor by the array.

2.1 Aperture Efficiency

2.1.1 *Ferroelectric aperture*

The radiation efficiency of the aperture depends on the losses of the ferroelectric medium. The dielectric loss tangent is the predominant source of loss in a ferroelectric material. For TEM-mode propagation through

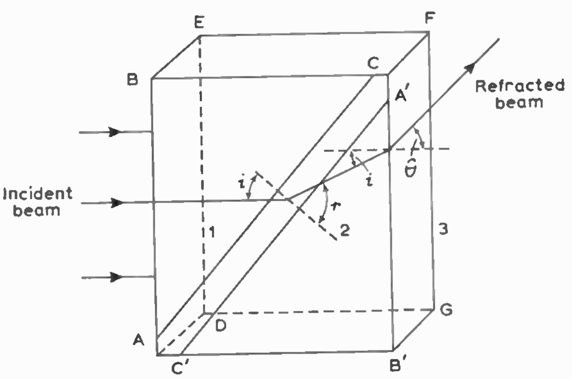

Fig. 2. Steering on both sides of the boresight by a single piece of material with two wedges.

materials with very large permittivity, the fringing field is extremely small and, as such, is neglected. Suitable transformers, of the same ferroelectric material or of low-loss rutile (TiO_2), are used[9] for matching purposes. The attenuation of a TEM-mode propagation due to losses in the dielectric material is given[10] by

$$\alpha_d = 27{\cdot}3\sqrt{\varepsilon}\tan\delta/\lambda \qquad (11)$$

For a 0·047 cm wide $BaTiO_3$ with a loss tangent[11] of 0·01 at 10 GHz, the insertion loss of the broadside beam is 0·33 dB. Because of the increase of the loss tangent with the applied bias, the insertion loss through 0·047 cm $BaTiO_3$ is 0·8 dB at a bias field of 6 kV/cm. Lower loss-tangent materials, such as KH_2PO_4 (ref. 12) and $SrTiO_3$ (ref. 13) are available. With a loss tangent of 0·0014 for a single crystal $SrTiO_3$ (40 K) for operation at 22 GHz, the loss is extremely small. Assuming uniform current distribution, for a balanced strip-line having an impedance of 1·08 Ω and a permittivity of 5475 (ref. 9), the copper loss is given, from Fig. 4,[14] by

$$\alpha_c = 0{\cdot}0008\sqrt{(\varepsilon f)}/l \qquad (12)$$

The total loss of the device is given by

$$\alpha = \alpha_c + \alpha_d \qquad (13)$$

2.1.2 *Ferromagnetic aperture*

The dielectric loss tangent of the ferromagnetic material [6,7] is 0·0005. As such, the dielectric loss of the ferromagnetic material is considerably smaller than that of the ferroelectric material. The saturation moment of the ferromagnetic material of 0·5 T (5000 gauss) limited the scan angle of the array.[7] A five-element ferrite-scanned millimetre array had a 2 dB loss at broadside and the measured gain of the array at a scan angle of 25° was reduced by a factor of 0·6 of the broadside gain.[7]

2.2 Transmitting Aperture

A transmitting aperture may be required to handle a large amount of power. The peak power handling capability of the aperture is given by

$$P_p = \frac{V_b^2}{Z} \qquad (14)$$

A conservative estimate for the breakdown voltage for $Pb_{0{\cdot}315}Sr_{0{\cdot}685}TiO_3$ (PS68·5) is 200 V for a 0·025 cm high 1·08 Ω device[9] giving a peak power handling capability of 37 kW. As the average power is increased, the performance of the device is degraded resulting from the rise in temperature of the ferroelectric due to the heating caused by the losses in the device. The rise in temperature of the device is a function of the loss tangent, the mass, the specific heat, the heat conductivity of the material, the ambient temperature and the method of removing the heat generated. A theoretical analysis of the temperature rise has been reported.[15] A time delay device made of PS68·5 handled 0·2 W average power at 3 GHz.[9] A ferroelectric limiter made of PS68·5 operated[16] with an input of 0·8 kW at 1 GHz at 23°C with a duty factor of $0{\cdot}027\times10^{-3}$. A third harmonic generator made of 73% $BaTiO_3$–27% $SrTiO_3$ operated[17] at 49°C with an input of 2 kW peak power at 3·01 GHz with a duty cycle of $2{\cdot}3\times10^{-5}$. A v.h.f. limiter handled 26·5 kW peak power.[15]

2.2.1 *Effect of increased average power*

A time-delay device made of $Pb_{0{\cdot}315}Sr_{0{\cdot}685}TiO_3$ handled 0·2 W average power.[9] With input average power levels greater than 0·2 W and with ferroelectric $Pb_{0{\cdot}315}Sr_{0{\cdot}685}TiO_3$, the temperature of the material will increase with increasing average power level and will move further away from the Curie temperature. This will result in (i) a decrease in the value of the permittivity of the ferroelectric material, (ii) a reduction of the non-linearity of the material and (iii) generally a reduction of the loss tangent of the material. The reduction in the value of the permittivity of the material will increase the v.s.w.r. of the aperture. The decrease in the non-linearity will result in a lower scanning angle for the same applied field or will require a greater biasing field to obtain the same scan angle as was obtained with lower power levels reducing the efficiency of the scanning aperture. The degradation of the scanning aperture is dependent on the average power level used, the material properties particularly the loss tangent, the heat sink and the type of cooling employed and will generally be different for different ferroelectric materials. At sufficiently high average power levels the scanning aperture will cease to function because of the resulting large v.s.w.r. and the small scan angle that can be practically obtained.

2.3 Receiving Aperture

The technological trend for the design of a phased array antenna is to use solid-state integrated circuits.[18,19] Typically each antenna element is connected through a circulator or a switch to the receive–transmit systems. On the transmit side (Fig. 3), the circulator is connected to a high-power transistor amplifier/frequency multiplier, IMPATT,[20] TRAPATT, or Gunn-[21] amplifier followed by a phase shifter and then to the

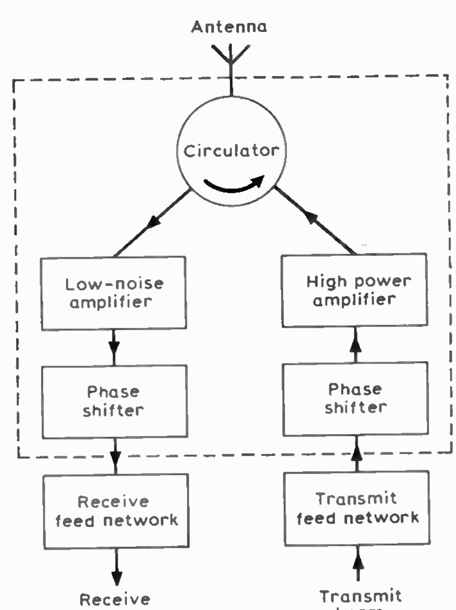

Fig. 3. A transmit–receive microwave integrated circuit module for a phased array element.

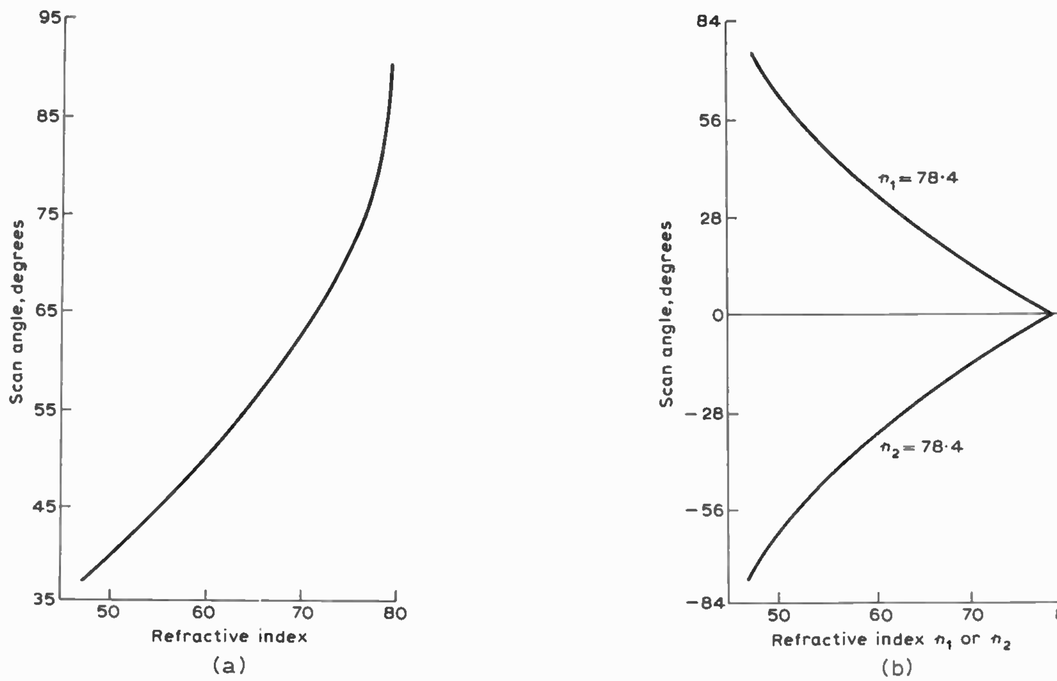

Fig. 4. Calculated (a) beam position for a single wedge of Fig. 1 with $i = \sin^{-1} 1/78{\cdot}4$ and (b) scan angle for a double wedge of Fig. 2 with $i_1 = \sin^{-1} 1/32$, as a function of the refractive index of the ferroelectric aperture.

transmit feed network. On the receive side, the circulator is connected to a low-noise amplifier[22–24] or a mixer followed by a phase shifter and then to the receive feed network. The components inside the dotted line are contained in an integrated circuit module. The noise factor of the receiver is given by

$$F = F_1 + \frac{F_2 - 1 + L_r}{G_1} \tag{15}$$

The gain of the aperture element is given by

$$G = \frac{4\pi A}{\lambda^2} - L_a \tag{16}$$

The aperture losses include the loss in the antenna element discussed in Section 2.1.1 and the circulator loss. The ferroelectric aperture introduces dielectric losses and the copper losses in the conductor. The dielectric loss tangent for PS68·5 (ref. 25) and $Ba_{0\cdot60}Sr_{0\cdot40}TiO_3$ (ref. 26) decreases and for $SrTiO_3$ (ref. 27) and for polycrystalline $BaTiO_3$ (ref. 11) increases with the applied electric field. The mechanism of electric field dependence of the dielectric loss tangent of $Ba_{0\cdot60}Sr_{0\cdot40}TiO_3$ at 3 GHz and at 26°C (ref. 26) and the temperature dependence of microwave loss in $SrTiO_3$ (refs. 13, 28) have been investigated.

3 Expected Results

At microwave frequencies, the permittivity and the refractive index of a polycrystalline $BaTiO_3$ are 6140 and 78·4 respectively.[11] The maximum value of the wedge angle (Fig. 1), with $BaTiO_3$, is restricted to $\sin^{-1}(1/78{\cdot}4)$. The calculated beam position, as a function of the refractive index, is plotted in Fig. 4(a) for a wedge of Fig. 1. With a variation[11] of 6140 to 2140 for the permittivity, the beam position is changed from 90° to 36·2° with a steering of 53·8°. With an aperture configuration of Fig. 2 and a wedge angle of $\sin^{-1}(1/32)$, the calculated scan angle of the beam (Fig. 4(b)) varies over $\pm 75{\cdot}7°$. Using the published non-linearity[11] of $BaTiO_3$, the expected biasing field to produce a scan angle of $\pm 75{\cdot}7°$ is 9·6 kV/cm. For a 0·025 cm high aperture, 240 V is required to obtain a bias field of 9·6 kV/cm. Use of $SrTiO_3$ would require a smaller operating bias voltage. The impedance of the aperture is dependent on its height resulting in a trade-off between the impedance of the device and the bias voltage.

4 Quality Factor

Electrical properties, affecting scanning apertures, vary from one ferroelectric material to another. Some have a large non-linearity,[29] some require a lower biasing field[30] and some have a comparatively lower loss tangent.[13] To set a yardstick for the comparison of different ferroelectric materials for application in scanning apertures an electrical quality factor (Q_F) is defined by

$$Q_F = N/lE\alpha_d \tag{17}$$

For an aperture length of $\lambda/2$, we have from equation (9), for $n_3 = 1$,

$$2l/\lambda = M \simeq 1/(n_1 - n_2) \tag{18}$$

Combining equations (11), (17)–(18), one obtains

$$Q_F \simeq 2(\sigma - 1)/(27{\cdot}3\,E\tan\delta) \tag{19}$$

The larger the numerical value of the quality factor, generally, the better is the material. A large non-linearity results in worsening the v.s.w.r. with increasing bias field and in a larger quality factor. To minimize the

Table 1

Material	ε	tan δ	Measured at Frequency (GHz)	Measured at Temperature	Non-linearity σ	Bias field (kV/cm)	Quality factor, Q_F (cm/kV)
$BaTiO_3$(11)	6140	0·01–0·11	10	130°C	1·69	10	0·046
PS68·5(9)	5475	0·065	3·1	room	1·4	17·7	0·025
$Pb_{0\cdot45}Sr_{0\cdot55}TiO_3$(15)	4180	0·006	0·218	115·8°C	1·28	20·5	0·17
$Ba_{0\cdot60}Sr_{0\cdot40}TiO_3$(24)	2600	0·15–0·09	3	26°C	1·47	28	0·014
$Ba_{0\cdot73}Sr_{0\cdot27}TiO_3$(33)	4100	0·15–0·09	3	20°C	1·5	8·4	0·048
$SrTiO_3$(13)	7890 ε_{100} (50 MHz)	0·0014	22	40 K	2·79(34) (50 MHz)	23	1·9 (3 GHz)
$KTaO_3$(29)	35000	0·03	1·5 MHz	10 K	4·19	7	1·1
TGSe(30)	17150			22·9°C	4·12	2·4	

v.s.w.r. variation, the non-linearity must be moderate. Large permittivity reduces the impedance of the device. For an efficient scanning element, it is necessary to have a small bias field produce a reasonable non-linearity for a material with a low loss and low dielectric permittivity to facilitate impedance matching requirements. Ferroelectrics[31] have Curie temperatures from several hundred degrees celsius above to below zero. Operation at lower temperatures is practical because of the efficient refrigeration systems.[32] Properties of several ferroelectrics and their Q_F are presented in Table 1. As the relaxation frequency of $SrTiO_3$ (ref. 13) is above 35 GHz, its low-frequency non-linearity[34] is assumed to be present at microwave frequencies. The loss tangent of $SrTiO_3$ (ref. 27) increases with the applied bias voltage and it is assumed to be 0·003 at 3 GHz at a bias field of 23 kV/cm. To the best knowledge of the author, $SrTiO_3$ is the superior ferroelectric material at the microwave frequencies.

5 Discussion

For application in microwave devices[15, 16, 25, 26, 35–39], the use of a ferroelectric material is confined below its relaxation frequency and over a frequency range without any anomalous behaviour. As a result, for TEM-mode propagation, equations (1)–(9) are independent of frequency and the size of the aperture. The scan angle that can be obtained is then determined by (i) the ratio of the dielectric constants that can be obtained and (ii) the wedge angle and is independent of the frequency of operation and the beamwidth of the element. Scanning ferroelectric apertures are particularly suitable for millimetre wavelengths where the sizes are small. It is hoped that this paper will provide an incentive for experimental work in scanning ferroelectric apertures and for the discovery of low-loss non-linear dielectric materials.

6 References

1. Angelakos, D. J. and Korman, M. M., 'Radiation from ferrite-filled apertures', *Proc. IRE*, **44**, pp. 1463–8, October 1956.
2. Palais, J. C., 'Radiation from a ferrite cylinder', *J. Appl. Phys.*, **35**, pp. 779–81, March 1964.
3. Wheeler, M. S., 'Nonmechanical beam steering by scattering from ferrites', *IRE Trans. on Microwave Theory and Techniques*, **MMT-6**, pp. 38–42, January 1958.
4. Engelbrecht, R. S., 'Antenna with electrical lobing', U.S. Patent 3,007,165, 31st October 1961.
5. Schiller, T. R., 'Electronically steerable array for space vehicle application', RADC–TDR–64–222, Contract No. AF 30 (602)–3041, August 1964, AD 607439.
6. Schiller, T. R., Johnson, R. E. and Weiss, P. F., 'Ferrimagnetic beam steering at millimeter wavelengths', *IEEE G-AP International Symposium Digest*, pp. 71–7, 1965.
7. Schiller, T. R. and Heath, W. S., 'An electronically scanned array at millimeter wavelengths employing ferrite apertures', *IEEE Trans. on Antennas and Propagation*, **AP-16**, pp. 180–7, March 1968.
8. Das, A., 'Multi-mode excitation of large aperture horns to produce electronic deflection of directional patterns', *The Radio and Electronic Engineer*, **38**, pp. 180–3, September 1969.
9. Das, R., 'Thin ferroelectric phase shifters', *Solid State Electronics*, **10**, pp. 857–63, August 1967.
10. Matthaei, G. L., Young, L. and Jones, E. M. T., 'Microwave Filters, Impedance Matching Networks and Coupling Structures', p. 165 (McGraw-Hill, New York, 1964).
11. Nekrasov, M. M., 'Investigation of ferroelectric materials at superhigh frequencies', *Bull. Acad. Sci. USSR Phys.*, **31**, pp. 1928–30, 1972.
12. Kaminow, I. P. and Harding, G. O., 'Complex dielectric constant of KH_2PO_4 at 9·2 Gc/s', *Phys. Rev.* **129**, pp. 1562–6, 15th February 1963.
13. Rupprecht, G. and Bell, R. O., 'Microwave losses in strontium titanate above the phase transition', *Phys. Rev.*, **125**, pp. 1915–20, 15th March 1962.
14. Cohn, S. B., 'Problems in strip transmission lines', *IRE Trans.*, **MTT-3**, p. 119, 1955.
15. Cohn, M. and Eikenberg, A. F., 'A large-power ferroelectric limiter', *IEEE Trans.*, **MTT-13**, pp. 47–54, January 1965.
16. Horton, J. B. and Donaldson, M. R., 'A one-GHz ferroelectric limiter', *IEEE Trans.*, **MTT-15**, pp. 517–23, September 1967.
17. DiDomenico, Jr., M., Johnson, D. A. and Pantell, R. H., 'Ferroelectric harmonic generator and the large-signal microwave characteristics of a ferroelectric ceramic', *J. Appl. Phys.*, **33**, pp. 1697–1706, May 1962.
18. Hyltin, T. M., 'Microwave integrated circuits in phased array radars', *IEEE International Convention Record*, Part 5, pp. 105–12, 1966.
19. Das, A., 'Microwave integrated circuits for phased arrays', Report No. 68–7340–TN–01, TRW Systems, Redondo Beach, Calif., U.S.A., July 1968.

20. Hansen, D. C. and Heinz, W. H., 'Integrated electrically tuned X-band power amplifier utilizing Gunn and IMPATT diodes', *IEEE J. Solid State Circuits*, **SC-8**, pp. 3–14, February 1973.
21. Upadhyayula, C. L. and Perlman, B. S., 'Design and performance of transferred electron amplifier using distributed equalizer networks', *IEEE J. Solid State Circuits*, **SC-8**, pp. 37–43, February 1973.
22. Okean, H. C., Allen, C. M., Sard, E. W. and Weingart, H., 'Integrated parametric amplifier module with self-contained solid state pump source', *IEEE Trans.*, **MTT-19**, pp. 491–3, 1971.
23. Baechtold, W., 'X- and Ku-band amplifiers with GaAs Schottky-barrier field-effect transistors', *IEEE J. Solid State Circuits*, **SC-8**, pp. 54–8, February 1973.
24. Okean, H. C. and Meier, P. J., 'Microwave integrated tunnel diode-amplifier for broadband high performance receivers', *IEEE Trans.*, **MTT-20**, pp. 165–72, February 1972.
25. Amos, J. W., Donaldson, M. R., Lavedan, L. J., Stanford, A. L. and Pippin, J. E., 'A ferroelectric microwave switch', *IEEE Trans.*, **MTT-13**, pp. 789–93, November 1965.
26. Johnson, K. M., 'Variation of dielectric constant with voltage in ferroelectrics and its application to parametric devices', *J. Appl. Phys.*, **33**, pp. 2826–31, September 1962.
27. Rupprecht, G., Silverman, B. D. and Bell, R. J., 'Investigation of the microwave properties of ferroelectrics', Final Report, Contract No. AF 19(604)–4085, 16th June–15th October 1960, AFCRL–TR–60–371, PB 154077.
28. Silverman, B. D., 'Microwave absorption in cubic strontium titanate', *Phys. Rev.*, **125**, pp. 1921–30, 15th March 1962.
29. Demurov, D. G. and Veenevtsev, Y. N., 'Character of phase transition of ferroelectric $KTaO_3$', *Sov. Phys. Solid State*, **13**, pp. 553–6, 1971.
30. Zarembovskaya, T. A. and Varikosh, V. M., 'Dielectric constant of triglycine selenate close to the transition point', *Sov. Phys. Solid State*, **13**, pp. 2989–92, 1972.
31. Jona, F. and Shirane, G., 'Ferroelectric Crystals' (Pergamon Press, London, 1962).
32. Crouthamel, M. S. and Shelpuk, B., 'A combustion heated, thermally actuated Vuilleumier refrigerator', International Cryogenic Conf., Boulder, Colorado, August 1972.
33. Davis, L. and Rubin, I. G., 'Some dielectric properties of barium-strontium titanate ceramic at 3000 megacycles', *J. Appl. Phys.*, **24**, pp. 1194–7, 1953.
34. Neville, R. C., Hoeneisen, B. and Mead, C. A., 'Permittivity of strontium titanate (optic modes)', *J. Appl. Phys.*, **43**, pp. 2124–31, May 1972.
35. Das, R., 'Ferroelectric phase shifters', *IEEE G-MTTT International Convention Digest*, pp. 185–7, 1967.
36. Das, S. N., 'Quality of a ferroelectric material', *IEEE Trans.*, **MTT-12**, pp. 440–5, July 1964.
37. Das, S. N., 'Application of barium titanate compositions to parametric amplification', *IEEE Trans.*, **MTT-13**, pp. 245–7, March 1965.
38. Das, S. N., 'Application of barium titanate to microwave parametric amplification', *The Radio and Electronic Engineer*, **32**, pp. 21–32, July 1966.
39. Das, S. N., 'Ferroelectrics for time delay steering of an array', *Ferroelectrics*, **5**, pp. 253–7, 1973.

Manuscript first received by the Institution on 27th April 1973 and in final form on 13th November 1973 (Paper No. 1584/Com. 89).

UDC 621.396.677.833.1

The effect of deviation of feed polarization characteristics from that of a Huygens source on cross-polarization in reflector antennas

MUNA M. A. EL FUTUH*

and

S. I. GHOBRIAL, B.Sc., M.Sc., Ph.D.*

SUMMARY

The requirements for feed characteristics to give zero cross-polarization in reflector antennas are discussed. It is shown that equal E and H amplitude patterns is not a sufficient condition for zero cross-polarization. Effects of phase error due to feed are also discussed briefly.

* Department of Electrical Engineering, University of Khartoum, Sudan; formerly at the University of Bradford, England.

1 Introduction

The problem of cross-polarization in parabolic reflectors has been treated recently by a number of workers.[1–4] This problem is of interest since cross-polarization can be responsible for high levels of cross-talk between orthogonal channels in frequency re-use systems. It is therefore important that every attempt should be made to reduce cross-polarization. One method for the reduction of cross-polarization is to use a Cassegrain arrangement. In this system the hyperboloidal sub-reflector corrects to a large extent the cross-polarization that is introduced by the main reflector.[1] Another method for reduction of cross-polarization is to use a primary feed with polarization characteristics which will compensate for the cross-polarization introduced by the reflecting system.

It can be shown that the condition for zero cross-polarization is that the field due to the feed (when operated in the transmitting mode) and the field due to the reflector in the receiving mode should be orthogonal everywhere in space.[5] This condition is satisfied by a Huygens source which can be, theoretically, represented as a combination of electric and magnetic dipoles.[6] A number of authors[2,4,7] claim that corrugated horns have polarization characteristics which come very close to that of a Huygens source. It is the purpose of this work to investigate the effect of deviation of such feeds from the Huygens source characteristics on the total cross-polarization of the antenna systems.

2 Analysis

2.1 Basic Concepts

The voltage at the terminals of a feed placed at the focus of a paraboloid is, in general, given by[5]

$$V = C\iint_S (\bar{E}_r . \bar{E}_f)\, e^{-j\delta}\, \bar{r} . d\bar{S} \qquad (1)$$

where

- C is a constant
- $\bar{E}_r$ is a vector describing the electric field reflected by the paraboloid
- $\bar{E}_f$ is a vector describing the electric field due to the feed when transmitting
- $\bar{r}$ is a unit vector along the ray associated with $\bar{E}_r$
- $d\bar{S}$ is a vector normal to the surface of the paraboloid at the point of reflexion with magnitude dS, being the differential element of area

From equation (1) the condition for zero cross-polarization mentioned in the previous Section is readily verified.

Now if the reflector is excited by a plane wave linearly polarized along the x-axis, then the reflected electric field will have components along the x, y and z axes given by

$$\bar{E}_r = \bar{i}[\sin^2\phi(1-\cos\psi)-1]+ \\ +\bar{j}\sin\phi\cos\phi(1-\cos\psi)-\bar{k}\sin\phi\sin\psi, \qquad (2)$$

or in spherical coordinates (Fig. 1),

$$\bar{E}_r = \bar{a}_\psi \sin\phi + \bar{a}_\phi \cos\phi. \qquad (3)$$

On the other hand, if the field due to the feed (which we

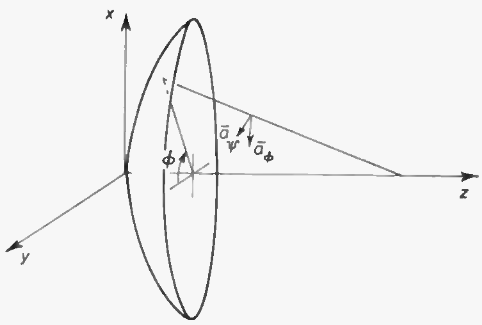

Fig. 1. Coordinates system.

will assume to be cross-polarized with respect to the incident wave) is written as

$$\bar{E}_f = E_\psi(\psi, \phi)\bar{a}_\psi + E_\phi(\psi, \phi)\bar{a}_\phi, \tag{4}$$

the scalar product $\bar{E}_r . \bar{E}_f$ which appears in equation (1) can be written as

$$\bar{E}_r . \bar{E}_f = E_\psi(\psi, \phi) \sin \phi + E_\phi(\psi, \phi) \cos \phi.$$

From this expression it is obvious that zero cross-polarization can be achieved if

$$\left.\begin{aligned} E_\psi(\psi, \phi) &= E(\psi, \phi) \cos \phi \\ E_\phi(\psi, \phi) &= -E(\psi, \phi) \sin \phi \end{aligned}\right\} \tag{5}$$

where $E(\psi, \phi)$ is some arbitrary function of ψ, ϕ.

Equation (5) suggests that the requirement for the feed to correct the cross-polarization of the reflector is that it should have far field components E_ϕ and E_ψ which are related by

$$\frac{E_\phi}{E_\psi} = -\tan \phi$$

It is important to note that it would be wrong to conclude from equation (5) that a necessary condition for zero cross-polarization is equality of the E and H patterns. That this condition is not necessary can be seen by considering the function $E(\psi, \phi)$. This function does not necessarily assume the same value for $\phi = 0$ and $\phi = \pi/2$. For example, $E(\psi, \phi)$ may assume the form

$$E(\psi, \phi) = \left[\frac{\sin(\alpha \sin \psi \sin \phi)}{\alpha \sin \psi \sin \phi}\right] \cdot \left[\frac{\cos(\beta \sin \psi \cos \phi)}{1 - \left(\frac{2\beta}{\pi} \sin \psi \cos \phi\right)^2}\right]$$

which is a typical expression that appears in the theory of radiation from rectangular apertures. From the above expression it is seen that

$$E_\psi(\psi, 0) = E(\psi, 0) = \frac{\cos(\beta \sin \psi)}{1 - \left(\frac{2\beta}{\pi} \sin \psi\right)^2} \qquad H \text{ plane}$$

$$E_\phi(\psi, \pi/2) = E(\psi, \pi/2) = \frac{\sin(\alpha \sin \psi)}{\alpha \sin \psi} \qquad E \text{ plane}$$

which need not be identical.

This point is of major importance since a number of workers have in the past assessed feeds on the basis of their E and H patterns only. In fact a comparison between the E and H patterns could be useful if it is known that the function $E(\psi, \phi)$ is independent of ϕ; in which case (5) becomes

$$\left.\begin{aligned} E_\psi(\psi, \phi) &= E(\psi) \cos \phi \\ E_\phi(\psi, \phi) &= -E(\psi) \sin \phi \end{aligned}\right\} \tag{5a}$$

From this it is seen that zero cross-polarization can be achieved with a feed that has identical amplitude patterns in all planes (i.e. an amplitude pattern with circular symmetry). Equal E and H amplitude patterns is only a special case.

2.2 Effect of the Deviation of Feed from Ideal Characteristic

Let us now consider a feed that does not satisfy the above condition for zero cross-polarization. The deviation from the ideal characteristic can be represented in terms of either, (i) the error in the angle ζ (which is included between the vectors $\bar{E}_f$ and $\bar{a}_\psi$); or (ii) unequal E and H patterns.

Since it is easier to measure patterns than the angle between the above vectors, the latter method will be chosen. Thus let

$$\left.\begin{aligned} E_\psi(\psi, \phi) &= A(\psi) \cos \phi \\ E_\phi(\psi, \phi) &= -B(\psi) \sin \phi \end{aligned}\right\} \tag{6}$$

where $A(\psi)$ and $B(\psi)$ are functions describing the radiation patterns in the E and H planes respectively. From equation (6) the error in the angle ζ can be readily seen to be

$$\Delta = \phi - \tan^{-1}\left[\frac{B(\psi)}{A(\psi)} \tan \phi\right] \tag{7}$$

Using (6) and (4) we have

$$\bar{E}_f = A(\psi) \cos \phi \; \bar{a}_\psi - B(\psi) \sin \phi \; \bar{a}_\phi \tag{8}$$

substituting (8) and (3) in (1) we get

$$V_{\text{cross-pol}} = C \iint [A(\psi) - B(\psi)] \sin \phi \cos \phi \; e^{-j\delta} \; \bar{r} . d\bar{S} \tag{9}$$

Equation (9) gives the voltage appearing at the terminals of the feed when cross-polarized with respect to the incident wave. On the other hand if the feed is oriented to match the incident wave, the voltage expression becomes

$$V_{\text{co-pol}} = C \iint [A(\psi) \sin^2 \phi + B(\psi) \cos^2 \phi] \; e^{-j\delta} \; \bar{r} . d\bar{S} \tag{10}$$

In order to evaluate (9) and (10) we need to know the form of the functions $A(\psi)$ and $B(\psi)$. These can be found from the E and H patterns of the particular feed under consideration. In general these are usually of the form

$$\frac{1}{\rho}\left[\frac{\sin(\alpha \sin \psi)}{\alpha \sin \psi}\right];$$

where ρ is the distance from the focus to any point on the reflector's surface.

3 Computations and Results

In order to obtain numerical figures for the cross-polar isolation that could arise due to imperfections of the primary feed, equations (9) and (10) were computed

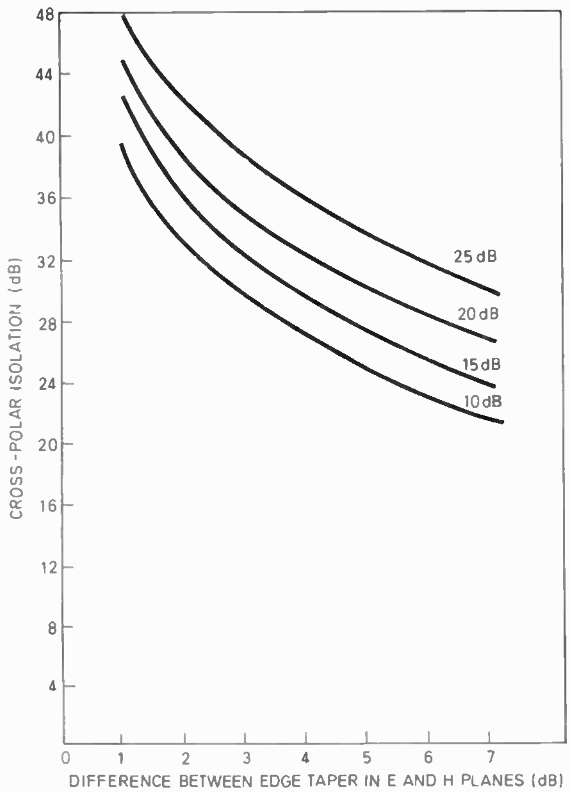

Fig. 2. Relationship between feed symmetry, edge taper and cross-polar isolation.

for a typical paraboloid with the following geometry:

$$f/D = 0{\cdot}332$$

$$D/\lambda = 75{\cdot}59$$

angular semi-aperture $= 74°$

The functions $A(\psi)$ and $B(\psi)$ were taken as

$$A(\psi) = \frac{1}{\rho}\frac{\sin(\alpha \sin \psi)}{\alpha \sin \psi}, \qquad B(\psi) = \frac{1}{\rho}\cdot\frac{\sin(\alpha' \sin \psi)}{\alpha' \sin \psi}$$

where the constants α and α' were chosen such that they result in some predetermined maximum deviation between the edge illumination in the E and H planes.

Figure 2 shows a set of curves for the cross-polar isolation as a function of the difference in edge illumination taper between the E and H planes (expressed in dB). It is seen from the curves that cross-polar isolation decreases with increasing difference between the taper of the E and H planes. This result is not unexpected. It is also observed that for a given difference cross-polar isolation increases as the edge taper decreases. This can be explained either in terms of the reflector's cross-polarization or in terms of the feed imperfection. Since the curvature of the paraboloid increases with angular semi-aperture, it is therefore expected that more depolarization should take place as we move from the vertex of the paraboloid towards the edge. Thus if illumination taper is increased then the total cross-polarized field at the focus decreases. However, some workers[2,3] prefer to think of the paraboloid as a perfect system. In their opinion cross-polarization should be attributed only to the feed departure from the Huygens source characteristics. In this case the decrease of cross-polar isolation level with increase in edge taper can be explained mathematically in terms of the behaviour of the integrands appearing in equation (9) and (10). Finally it can be concluded from Fig. 2 that the requirement for feed symmetry increases as the edge taper decreases. For a feed that produces 10 dB edge taper a difference of 2·7 dB between the E and H planes can be afforded (assuming a figure of 30 dB for the isolation as acceptable).

For edge taper less than 10 dB, 7 dB say, perhaps a difference of only 1 dB can be afforded.

Figure 3 shows a plot of the error in the angle ζ versus ϕ as given by equation (7) for both 3 dB and 1 dB difference between the edge taper of the E and H planes. It is seen from this Figure that the maximum error in ξ is less than 10°, from which it can be concluded that if the feed had identical E and H amplitude patterns but the $\bar{E}_f$ vector is misoriented through an angle as small as 10°, then high levels of cross-polarization could arise.

In fact equation (9) can be expressed in terms of the angular error Δ, as follows

$$\begin{aligned} V_{\text{cross-pol}} &= C\iint (\bar{E}_r \cdot \bar{E}_f)\, e^{-j\delta}\, \bar{r}.d\bar{S} \\ &= C\iint |E_f| \sin \Delta\, e^{-j\delta}\, \bar{r}.d\bar{S} \end{aligned} \tag{11}$$

It is shown in the Appendix that this expression is identical to that given by equation (9) for the case when equation (6) describes the primary feed far field. However, equation (11) is more general and holds true for any type of feed.

Finally, perhaps it is worth noting that in the above analysis no mention was made to the effect of phase errors due to the feed. Although this point is not dealt with in depth here, a brief discussion is given below.

Consider equation (1). If two vectors $\bar{E}_r$ and $\bar{E}_f$ are orthogonal, then the value of the integrand is zero and is independent of the form the phase function assumes.

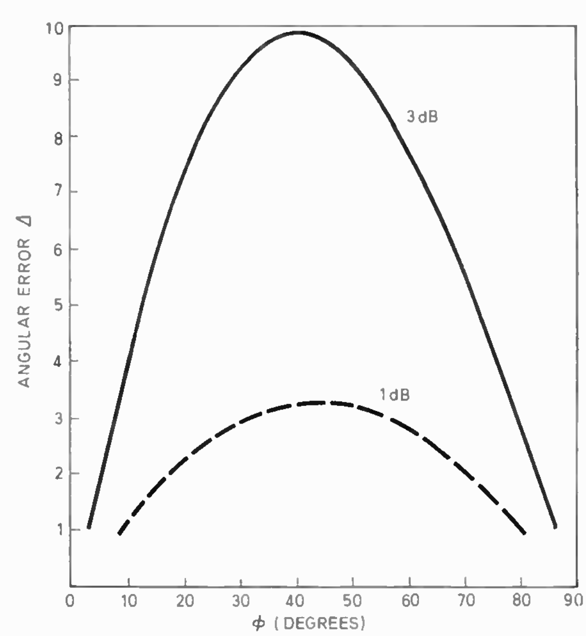

Fig. 3. Error in angle for differences in ϕ.

This suggests that phase errors can be completely ignored (as far as cross-polarization is concerned) if the condition of orthogonality of $\bar{E}_r$ and $\bar{E}_f$ is satisfied. (Of course phase errors degrade the antenna gain considerably and should therefore be considered from that point of view.) However, if the feed departs from the Huygens source characteristics, phase errors will affect cross-polarization. In fact if phase errors do not have circular symmetry then cross-polarization could arise even along boresight. It is not difficult to show that maximum on-axis cross-polarization takes place if phase errors are cyclic with two periods in the ϕ direction[8].

4 Conclusions

It has been shown that equal E and H primary feed amplitude patterns is neither a necessary nor sufficient condition for zero cross-polarization in paraboloidal reflectors. A necessary and sufficient condition for zero cross-polarization is that the feed and reflector E vectors should be orthogonal when the feed is cross-polarized with respect to the incident wave. For parabolic reflectors this leads to $E_\phi/E_\psi = -\tan\phi$.

It has been shown, too, that if the feed satisfies the orthogonality condition mentioned above, phase errors will not contribute to cross-polarization providing the feed is ideal. For a non-ideal feed, phase errors could be responsible for cross-polarization on axis.

5 Acknowledgments

The authors wish to thank Professor D. P. Howson, Chairman of the Postgraduate School of Electrical Engineering Studies, University of Bradford, for allowing them to conduct this research in his Department. Dr. Ghobrial is also indebted to Dr. P. A. Watson for many useful discussions.

6 References

1. Watson, P. A. and Ghobrial, S. I., 'Off-axis polarization characteristics of Cassegrainian and front fed antennas', *IEEE Trans. on Antennas & Propagation*, **AP-20**, No. 6, pp. 691–8, November 1972.
2. Ludwig, A. C., 'The definition of cross-polarization', *IEEE Trans.*, **AP-21**, No. 1, pp. 116–9, January 1973.
3. Wood, P. J., 'Depolarization with Cassegrainian and front fed reflectors', *Electronics Letters*, **9**, No. 8/9, pp. 181–3, 3rd May 1973.
4. Chu, T. and Turrin, R. H., 'Depolarization properties of offset reflector antennas', *IEEE Trans.*, **AP-21**, No. 3, pp. 339–45, May 1973.
5. Ghobrial, S. I., 'On the effect of the polarization characteristics of the receiving feed on receiving reflector antennas cross-polarization', University of Bradford Postgraduate Electrical and Electronic Engineering Department, Report 152, June 1973.
6. Jones, E. M. T., 'Paraboloidal reflector and hyperboloid lens antennas', *IRE Trans.*, **AP-2**, pp. 119–29, July 1954.
7. Difonzo, D. F. and Krentel, R. W., 'Communication satellite antennas for frequency reuse', International Symposium of IEEE Professional Group on Antennas and Propagation, September 1971.
8. Ghobrial, S. I. and Watson, P. A. 'A theoretical study of cross-polarization and antenna surface tolerance', University of Bradford Postgraduate Electrical and Electronic Engineering Department, Report 136, February 1973.

7 Appendix

To show that

$$\iint|\bar{E}|\ \sin\Delta\ e^{-j\delta}\bar{r}.d\bar{S} = \iint[A(\psi)-B(\psi)]\sin\phi\cos\phi\ e^{-j\delta}\bar{r}.d\bar{S}$$

This requires that

$$|\bar{E}_f|\sin\Delta = [A(\psi)-B(\psi)]\sin\phi\cos\phi \qquad (12)$$

Using equation (7) we have

$$\Delta = \phi-\xi = \phi-\tan^{-1}\left[\frac{B(\psi)}{A(\psi)}\tan\phi\right] \qquad (13)$$

Therefore $\sin\Delta = \sin\phi\cos\xi-\sin\xi\cos\phi$.

Fig. 4.

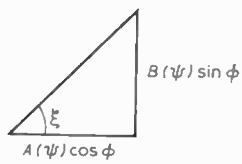

Using the geometrical representation of Fig. 4 we get

$$\sin\Delta = \frac{\sin\phi\cos\phi[A(\psi)-B(\psi)]}{\sqrt{A^2(\psi)\cos^2\phi+B^2(\psi)\sin^2\phi}} \qquad (14)$$

From equations (4) and (6) we have

$$|\bar{E}_f| = \sqrt{A^2(\psi)\cos^2\phi+B^2(\psi)\sin^2\phi} \qquad (15)$$

From equations (14) and (15), the required result is readily obtained.

Manuscript received by the Institution on 10th August 1973 (Paper No. 1585/Com. 90).

UDC 621.317.742

A novel standing-wave indicator in microstrip

P. H. LADBROOKE, B.Tech., Ph.D.*

SUMMARY

Although there have been numerous applications for a standing-wave detector in microstrip for many years, there has until now been no clear idea as to how a reliable indicator could be built. This paper presents the practising engineer with a fixed probe/sliding load test instrument that has proved successful where travelling probe methods have failed. The circuit (or load) is printed on a very thin dielectric leaf so that it can be moved along the surface of the substrate proper (e.g. alumina), passing over a probe of special design etched into the ground plane. Details for extending the basic method to elements mounted in shunt with the microstrip are given.

* *Formerly at the Royal Military College of Science, Shrivenham; now with Plessey Radar Research Centre, Southleigh Park House, Havant, Hampshire PO9 5DH*

1 Introduction

From time to time the need has arisen in this laboratory, and in others as well,[1] for a standing-wave indicator in microstrip. In an effort to satisfy this requirement, a series of tests has been carried out with travelling probes above and below the strip. They reveal what is arguably a fundamental problem with such an approach—that higher-order modes propagating along the dielectric surface or slot where the probe travels can mask the quasi-TEM fields one wishes to detect. Alternatively, the probe can be coupled to the circuit at a fixed point, and the load shifted in some way to achieve relative movement between the two. Experiments on these lines have led to the prototype indicator described in this paper, which demonstrates that standing-wave measurements in microstrip are feasible.

The conceivable uses for the device are at least as extensive as those that coaxial and waveguide slotted sections are put to, and fall broadly into two categories. First, to provide an alternative to these slotted sections for measurements on microwave integrated circuit components, by no longer having to measure through a transition. Secondly, as an aid to the physical understanding of microstrip dispersion, and how bends, corners, and other discontinuities affect the propagation. A few simple demonstrations from the second category are given in the paper, including an evaluation of the complex propagation coefficient for the microstrip.

Historically, the literature appears to contain only two previous accounts of similar work. Kostriza[2] some years ago produced a slotted-ground plane instrument, and reported peculiar effects due to radiation from the slot. Hasegawa *et al.*[3] used what they referred to as a 'measurement microstrip line' involving a probe travelling above a strip conductor supported on a Teflon tape of the same width. Their paper gave no indication of whether they had been troubled by extraneous fields. It can be said that neither device approximates modern microstrip quite as well as does the device described here.

2 Principle of Operation

A diagram of the component parts is given in Fig. 1. Apart from the probe, which constitutes a small and ideally insignificant discontinuity in the line, the most obvious additions to the basic microstrip are the two dielectrics above the strip. The first of these is a thin leaf ($\varepsilon \sim 5$), typically 0·05–0·1 times the thickness of the primary substrate ($\varepsilon \sim 10$), whose purpose is to support the circuit to be tested together with a straight length of measurement line so that the whole can be moved over the probe. The other is an expanded polystyrene pressure block ($\varepsilon = 1{\cdot}04$) which, like the dielectric leaf, resides in a region where the electric field is weak.

It is important to be clear about what actually constitutes the circuit. The circuit (or load) consists of the alumina substrate (or similar), its ground plane, and the conductor pattern. The dielectric leaf and the polystyrene are nothing more than perturbations of this basic integrated circuit, and represent the price that has to be paid for being able to move the pattern (which amounts to being able to move the load) in the manner desired.

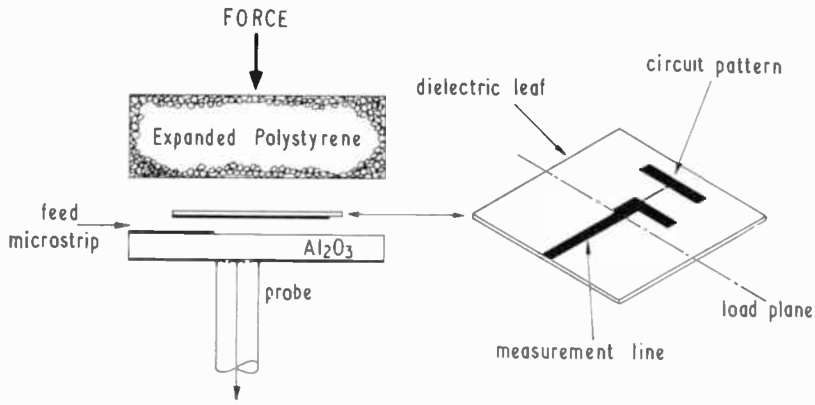

Fig. 1. Side view of indicator components.

The measurement of a standing-wave proceeds on a point-by-point basis by incrementing the longitudinal position of the leaf and then forcing it, metallized-surface down, into close contact with both the primary feed line and the rest of the substrate-free surface. It takes little practice to achieve a rate of about one point measured every twenty seconds. One should note:

(i) The substitution of a layered dielectric structure for the pure open microstrip. The validity of this has been judged by the practical results obtained, in the absence of a theoretical analysis.

(ii) The fact that the probe should not respond to the magnetic fields in the line, which dictates the shapes allowed for the probe (evaluated in Section 3.1).

(iii) Errors arising from probe susceptance and conductance.[4]

(iv) The existence of a small discontinuity caused by the leading edge of the dielectric leaf. This introduces no error, however, because it remains at a fixed distance from the load and to the generator side of the probe (covered in the Appendix).

(v) An amplitude error, varying from point to point in the standing wave, which comes about due to the launcher discontinuity between the generator and the primary microstrip. This discontinuity does not remain at a fixed distance from the load. It is shown in the Appendix that *the error in the v.s.w.r. is least when an 'almost matched' condition obtains at the load*—a particularly important result. A method for minimizing this discontinuity is given.

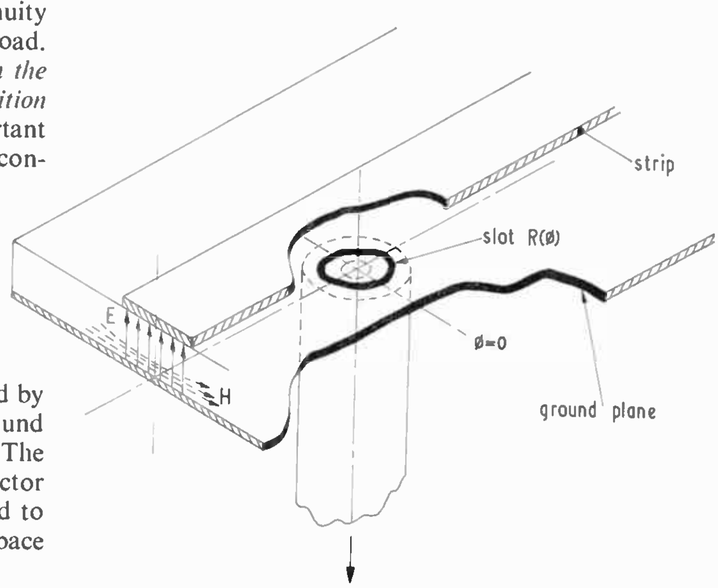

Fig. 2. Planar probe in microstrip.

3 Probe Response

3.1 Theoretical Evaluation of Admissible Shapes

The probe (shown in Fig. 2) is a planar type formed by etching a slot $R(\phi)$ in the otherwise continuous ground plane to separate out a small island of conductor. The inner of a miniature coaxial line which feeds a detector is connected to the island, and its outer is connected to the ground plane. The slot is confined to the space between the coaxial conductors.

Neglecting any possible penetration of **E** directly through the slot, it is easy to see that the coaxial line will be excited via charge induced on the island by the electric field immediately above it. The strength of this excitation is proportional to the island area, which must be fixed according to the generator power available, and the detector sensitivity. A fundamental requirement of the probe is that it should respond to only one or other of **E** or **H**, but not to both. Since with the arrangement of Fig. 2 magnetic field will loop through the slot, energy will be coupled to the output unless a special form for $R(\phi)$ can be found such that the nett excitation due to **H** reduces to zero. The following is an approximate treatment which yields useful engineering design data. Only the quasi-TEM mode fields are considered.

It is assumed that the detector can be driven by a probe small enough that changes in the phase of **H** over the slot can be neglected. The **H** field in the microstrip acting through the slot is equivalent to a current sheet $\mathbf{J}_1$, where $\mathbf{J}_1$ is given by:[5]

$$\mathbf{J}_1 = \mathbf{n} \times \mathbf{H}$$

and **n** is an outwardly directed normal to the microstrip ground plane.

The calculation of how such a current sheet excites the coaxial line proceeds through a standard application of the Lorentz Reciprocity Theorem,[6] resulting in the following integral for the radiated fields $\mathbf{E}_r$ and $\mathbf{H}_\phi$ with amplitude constant K;

$$-2K \int_{S'} (\mathbf{E}_r \times \mathbf{H}_\phi).\mathbf{a}_x \, \mathrm{d}S = \int_{S_0} (\mathbf{E}_r.\mathbf{J}_1) \, \mathrm{d}S$$

where: $\mathbf{a}_x$ is a unit vector along the coaxial line axis.

S_0 is the plane in which the current sheet $\mathbf{J}_1$ lies.

S' is a transverse surface similar to S_0, but located somewhere in the coaxial line to the detector side of S_0.

The surface integral over S_0 is a reduced volume integral taken in the coaxial line, and follows from the fact that $\mathbf{J}_1$ is the only source within V.

Hence

$$\int_{S_0} (\mathbf{E}_r.\mathbf{J}_1) \, \mathrm{d}S = 0$$

is the condition for the probe not to respond to H in the microstrip. This is an integral equation which can be solved for the $R(\phi)$ term implicit in $\mathbf{J}_1$. We have:

$$\mathbf{E}_r = \mathbf{a}_r(k/r)$$

$$(k = \text{constant})$$

$$\mathbf{a}_r.\mathbf{J}_1 = \mathbf{J}_{1r} = -|\mathbf{J}_1| \sin \phi$$

so the integral can be written:

$$I = -|J_1| k \int_{S_0} \frac{1}{r} \sin \phi \, \mathrm{d}S$$

If the slot is of small uniform width δ,

$$I \simeq -|J_1| k \delta \oint_C \frac{1}{r} \sin \phi \, \mathrm{d}l$$

where $\mathrm{d}l$ is an element of length along the contour C (Fig. 3);

$$\mathrm{d}l = \sqrt{R^2 \, \mathrm{d}\phi^2 + \mathrm{d}R^2}$$

and $r = R(\phi)$ along the contour. Thus we require the following integral (call it I') to be zero:

$$I' = \int \sin \phi \sqrt{\mathrm{d}\phi^2 + (\mathrm{d}R/R)^2}$$

or, since $\mathrm{d}R = (\mathrm{d}R/\mathrm{d}\phi) \, \mathrm{d}\phi$,

$$I' = \int_0^{2\pi} \sin \phi \, (1 + (1/R^2)(\mathrm{d}R/\mathrm{d}\phi)^2)^{\frac{1}{2}} \, \mathrm{d}\phi$$

For this integral to vanish, the bracketed term must be orthogonal to $\sin \phi$ over the interval $0 < \phi < 2\pi$. In general there will be a set of such functions, say $f_n(\phi)$, each definining a shape $R_n(\phi)$ for the slot through the equation,

$$R_n^2 + (\mathrm{d}R_n/\mathrm{d}\phi)^2 = f_n^2 R_n^2$$

From this relationship we may deduce by simple reasoning the solutions for $R_n(\phi)$ that are practically significant (requiring $R_n > 0$ for all ϕ).

We start by assuming that there exists a set $R_n(\phi)$ where the functions themselves, their derivatives and their squares, are all orthogonal to $\sin \phi$ over the interval $0 \leqslant \phi \leqslant 2\pi$. Then it follows from multiplying the preceding equation by $\sin \phi$ and integrating over $0 \leqslant \phi \leqslant 2\pi$, that the equation will be satisfied provided ${}_n(\phi)$ is one of a set of functions having the same orthogonality properties as the assumed $R_n(\phi)$. That is to say,

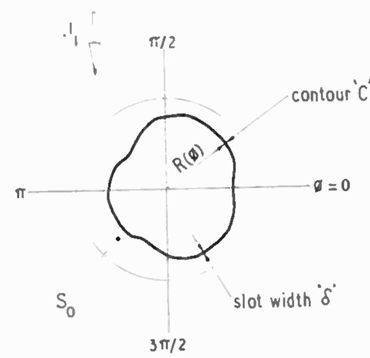

Fig. 3. Probe slot in the plane S_0.

the assumption of a set $R_n(\phi)$, with the properties as defined, is wholly valid and consistent.

It is useful to sketch trial functions having these properties on cartesian co-ordinates, and then transfer them to polar co-ordinates. For example, one may draw a smooth continuous curve (everywhere greater than zero) that has one form in the first and third quadrants, and a different form in the second and fourth quadrants. On polar co-ordinates a closed contour is generated which has no axis of symmetry—the function R_0 in Fig. 4. Classes of solutions having one, two or more axes of symmetry may be sketched similarly (Fig. 4).

In the next subsection a case will be made for using the circular shape, and it is an easy matter to derive this rigorously. Set $f_n = 1$. Then

$$I' = \int_0^{2\pi} \sin \phi \, \mathrm{d}\phi = 0$$

which verifies $f_n = 1$ as a valid choice. The equation for R_n now reduces to:

$$\mathrm{d}R_n/\mathrm{d}\phi = 0$$

with the solution

$$R_n = \text{constant}$$

which is the polar representation of a circle.

3.2 Practical Considerations

Case R_0 seems to offer little or no practical advantage. Triangles are a special case of R_1, while ellipses,

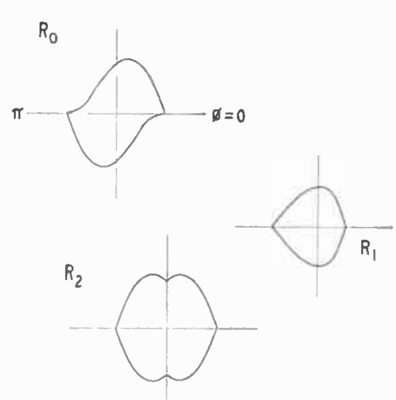

Fig. 4. Family of probe shapes.

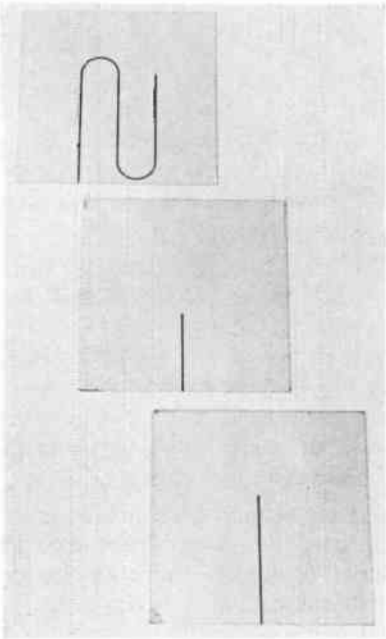

Fig. 5. Mica leaf slides.

rectangles, squares and circles are special cases of R_2, and are the shapes most likely to find useful application. A significant point to emerge from the analysis is that a probe having twofold symmetry which is laterally misplaced over the coaxial conductor becomes an effective shape having only one axis of symmetry: that is to say, precise lateral alignment is not essential. For similar reasons, slight lateral misplacement of the entire probe assembly under the strip is of no consequence either.

Notwithstanding the opening remarks in Section 3.1, the island area should be kept as small as possible both to avoid overcoupling, which effectively distorts the standing-wave,[4] and to maximize the probe resolution. A probe of longitudinal extent d senses an apparent reflexion coefficient of;

$$|\rho| = \frac{(2\lambda/\pi d)-1}{(2\lambda/\pi d)+1}$$

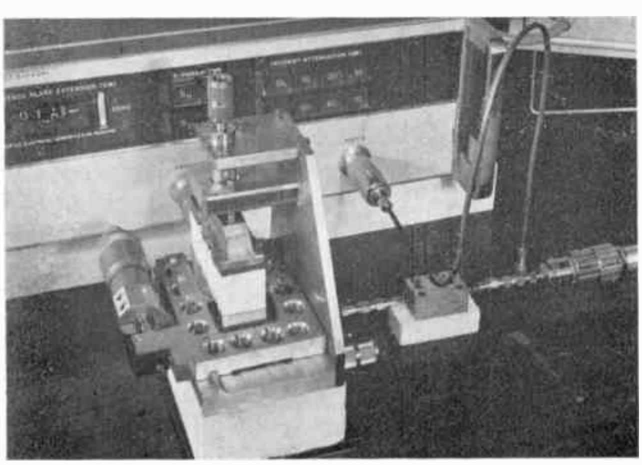

Fig. 6. Complete standing-wave indicator.

when the correct value is unity. Hence (d/λ) should be 1% or less for the error to remain within 2%: $d = 0{\cdot}1$ mm is satisfactory up to about 12 GHz.

The foregoing considerations suggest the circular shape is as good as any, and probably simplifies the alignment task during manufacture anyway. Thus the results of this paper were obtained exclusively with a probe of diameter $d = 0{\cdot}1$ mm—henceforth referred to as a 'disk probe'.

4 Experiments

A substrate of 99·5% alumina is cut to 75 mm × 25 mm × 0·5 mm so that, with a 50 mm × 50 mm dielectric slider (or leaf) there is an area 25 mm × 25 mm for the circuit, and a length of 25 mm for the measurement stripline. Good quality ruby mica ($\varepsilon \simeq 5{\cdot}4$) is used for the slider dielectric, and in the work described here is

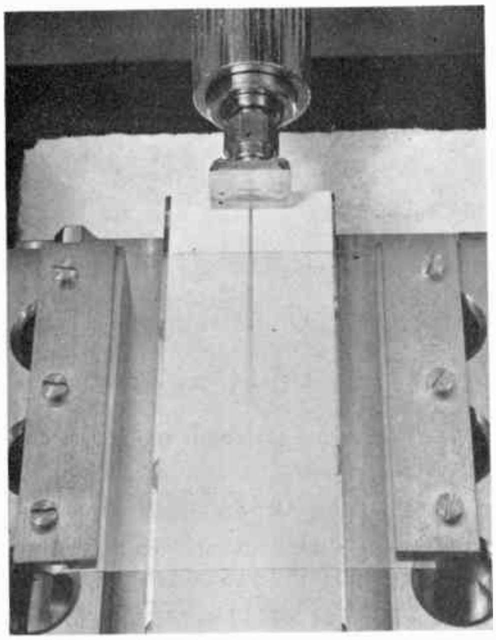

Fig. 7. Standing-wave indicator with foam pressure block removed. The two lines are identical in width, but the upper one is casting a shadow.

0·05 mm thick (it can be thinner). Several examples, the lower two with 'open-circuit' loads, are shown in Fig. 5. The conductors are 3–5 μm copper, resistivity $\sim 1{\cdot}8 \times 10^{-8}$ [Ω-m], formed by electroplating over evaporated films of copper and chromium. A strip width of 0·5 mm is used, so $w/h = 1$. These parts, together with a 75 mm × 25 mm × 25 mm foam polystyrene block, are held in the correct relative positions by a special jig (Fig. 6), that has a micrometer-driven saddle to which the dielectric slide is clamped. It also carries the input launcher (Americon 0·5 mm tab type), coaxial output (2·1 mm) and so forth, as illustrated in Fig. 7. The separate striplines, one on the mica and one on the alumina, can be distinguished in this second picture. The probe disk has a diameter of 0·1 mm as stated, with a clearance slot width of about 12 μm. A 0·075 mm copper wire is soft-soldered to the disk using a hot-gas bonder, and the free end is pushed into a fine hole drilled in the coaxial inner to contact the output circuit. There is a two-screw tuner and a GR 900–D20 stub for tuning the probe, also visible in Fig. 6.

In view of the fact that a point-by-point standing-wave measurement may take thirty minutes or more, amplitude drift in the power source has to be compensated. Although it is possible to do this manually in the simple generator/heterodyne detector system, a better technique is to use the Hewlett Packard network analyser which provides a degree of compensation automatically (Fig. 8).

The attenuator added between the S parameter set and the converter is an artifice to improve the detector sensitivity by reducing the ratio of powers in the reference and test channels respectively. The relative amplitude at any point in the standing wave is measured with this equipment by inserting gain into the test channel on the HP 8410A mainframe until the meter on the phase/gain indicator is within 1 dB of the zero mark; tenths of a dB are then read off the meter.

5 Examples of Use

These illustrations are confined to open-ended strips.

5.1 Verification of the TEM-like Mode

Up to moderate frequencies at least (lower X band), the indicator shows the fields in the bulk dielectric underneath the strip to be TEM-like; the standing waves (Fig. 9) have the $|\sin \beta z|$ dependence characteristic of that single mode of propagation.

The curves shown in Fig. 9 are plotted directly by a Hewlett-Packard calculator, which rounds the experimental readings to the nearest 0·1 dB. All readings are repeatable to better than 0·1 dB.

The calculator normalizes the points to the standing-wave maxima, which are therefore plotted without error. Thus the normalization process contributes (at most) 0·1 dB rounding error at any point, and the measurement precision contributes another 0·1 dB, giving 0·2 dB (2%) in all. The length of the vertical bars on the plotted crosses is intended to indicate this error. As a final step, the calculator plots a pre-programmed unity standing-wave ratio curve through the data by adjusting the wavelength for the best fit.

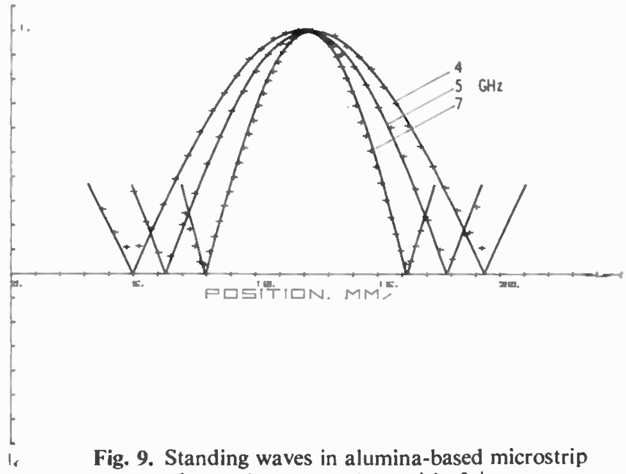

Fig. 9. Standing waves in alumina-based microstrip + data points; —— theory $|\sin \beta z|$.

Upon close examination, Fig. 9 reveals that the minima are not sharp—an observation which cannot be explained either in terms of the foregoing errors on the probe resolution. It implies that an open-ended microstripline is not lossless—a fact which has now been given a satisfactory physical interpretation elsewhere.[13] (See also Section 5.4.)

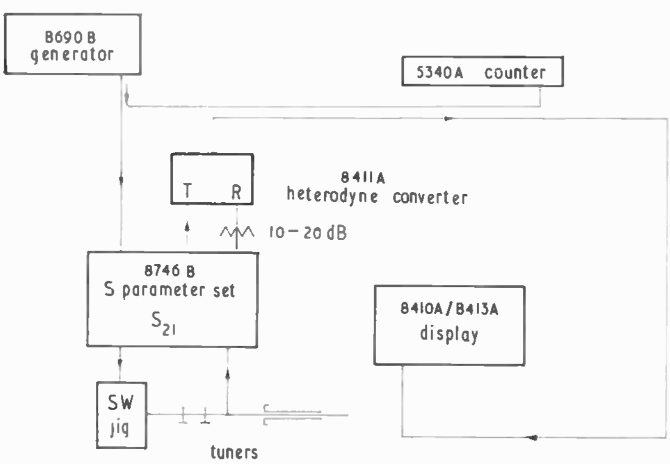

Fig. 8. Network analyser used as a source/detector system.

5.2 Effective Dielectric Constant as a Function of Frequency

The effective dielectric constant is;

$$\varepsilon_{\text{eff}} = \left(\frac{\lambda \text{ free space}}{\lambda}\right)^2$$

where λ is obtained from the measured separation of adjacent minima in the standing wave. Figure 10 shows the variation for the materials quoted in Section 4. There is dispersion that reconciles best with the lower values in the range reported,[7–9] while the extrapolated value for ε_{eff} at low frequencies is about 3% higher than calculated for pure microstrip.†[10]

Note that an equivalent way of expressing the same measured data is to specify the imaginary part of the propagation coefficient, $\beta = 2\pi/\lambda$.

5.3 Loss Measurements

If the standing-wave amplitudes at adjacent minima are a_1 and a_2 respectively, and if the attenuation constant α is small, then α can be found from;

$$\alpha \simeq 8{\cdot}686\, a_1 \left\{\frac{a_2}{a_1} - 1\right\} \frac{1}{z_2 - z_1} \text{ dB cm}^{-1}$$

where z_1 and z_2 are the minima positions. Typically, $a_2/a_1 \simeq 0{\cdot}2 - 0{\cdot}4$ dB, which is too small to measure with any great accuracy with the existing apparatus because the signal/noise ratio is no better than about unity. The

† A value of $\varepsilon = 9{\cdot}8$ was assumed for the substrate material: the manufacturers (Materials Research Corporation) quote 9·6—10·0 over our frequency range. At the time of writing, we have not yet had the opportunity to measure ε accurately for our particular substrates.

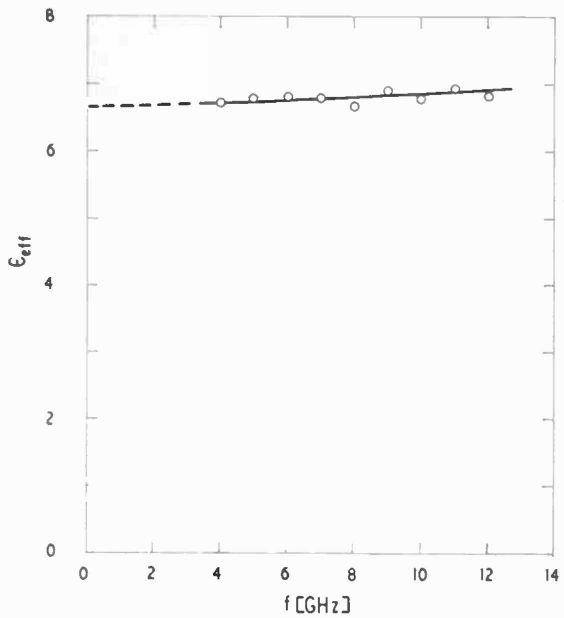

Fig. 10. Effective dielectric constant measured for alumina-based microstrip.

absolute magnitude measured for α nonetheless reconciles well with earlier reports;[9,11] by measurement, $\alpha \simeq 0{\cdot}04$ dB cm^{-1} at 10 GHz, rising as the frequency increases.

5.4 Conditions at the End of an Open Microstrip Line

In Fig. 11 is shown what is detected when the probe is moved beyond the line end. One finds that, at 8 GHz and above, the rate of change of phase across the end is comparable with that in the standing wave itself. Hence at these frequencies one would not expect a 'lumped' equivalent circuit for an open-ended microstrip to be valid. Furthermore, a travelling wave is launched into the dielectric whose amplitude is not insignificant, and which is in addition to the radiated component evaluated by Sobol.[12] There is evidence to suggest that this wave can be influenced by conductors and other perturbing objects as far as several centimetres away, which implies the equivalent circuit for open-ended microstrip should

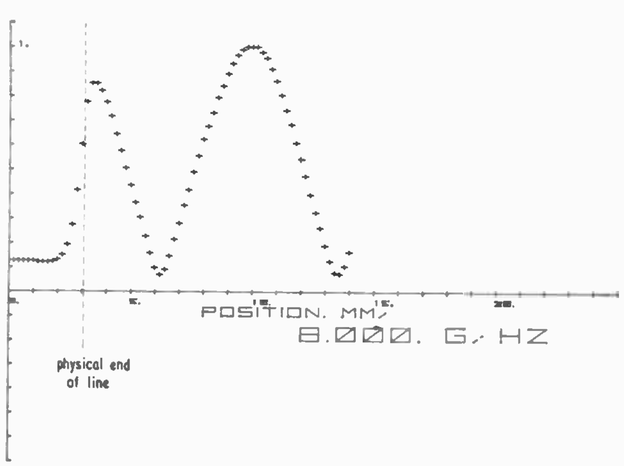

Fig. 11. Wave launched off open-ended microstrip.

be similarly dependent on these remote objects. It must be stressed that, without a detailed knowledge of what the launched fields are, the probe's response to them can be considered qualitative only; the quantitative data the probe is able to provide is the effect of these waves on the line conditions in shifting the standing-wave minima. An approximate treatment of the launched fields has been given elsewhere;[13] it gives a reasonable physical account of the energy that is lost to these 'surface waves'.

The error in the standing-wave amplitudes is the same as in Fig. 9, i.e. 2%. The accuracy with which the physical end of the line can be drawn on Fig. 11 is dictated by the precision with which the slider can be positioned over the probe in the first place. With opaque substrates this operation has to be carried out 'blind', leading to a probable error of about $\pm 0{\cdot}1$ mm.

6 Extension to Shunt Elements

A number of applications require elements mounted in shunt with the microstrip: an encapsulated solid-state device (Gunn, Schottky, etc.) is one example, and there are others. We outline here the principle of how the indicator can be modified to accommodate such measurements.

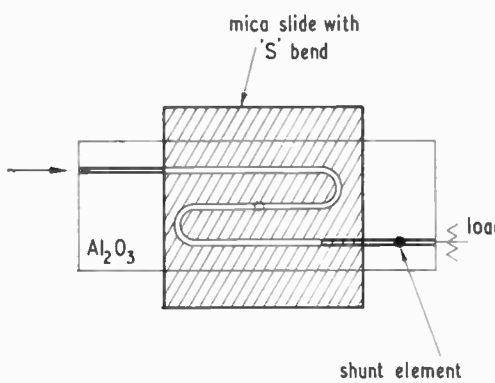

Fig. 12. Modification for shunt-mounted elements.

The Al_2O_3 substrate is drilled ultrasonically to receive this element (Fig. 12) which now remains stationary in a fixed output line, and is connected to the primary feed strip by an 'S'-shaped slider whose central limb passes over the probe (see also Fig. 5). The method has the disadvantage of a bend between the probe and load—requiring prior accurate calibration—but simultaneously the advantage of a fixed distance between the launch discontinuity and the load, which therefore does not distort the measured standing-wave (see Appendix).

7 Conclusions

This paper has described a standing-wave indicator intended for the practising microstrip engineer. The working principle can best be summarized by contrasting it with the commonplace coaxial and waveguide slotted sections: the circuit (or load) is made to move, *not* the probe, and a thin dielectric leaf with the circuit pattern printed on it is *added* to the basic structure, instead of a section being removed (cf. a slot). One substrate only is required, and any number of circuit designs can be tested

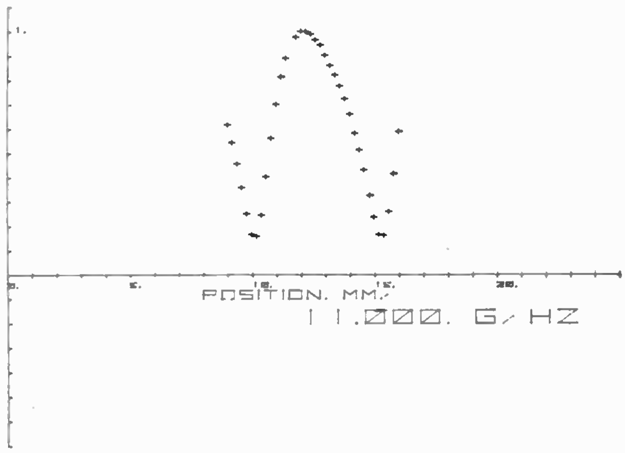

Fig. 13. Typical distortion due to launcher mismatch.

by printing them on individual mica leaves—a process that is both cheap and quick.

8 Acknowledgment

This work was done as part of an m.i.c. research programme supervised by Professor M. H. N. Potok, who first pointed out the significance of the launcher discontinuity. The jigs were constructed by H. Wall and H. Whetham, and much of the photo-lithographic processing was done by Mrs. C. Garrett. Acknowledgment is made to E. H. England for general collaboration, and especially for the calculator programs described in Section 5.1.

9 References

1. L. Lewin and G. H. B. Thompson, 'Measurements in microstrip', *Proc. Instn Elect Engrs*, **109**, pt. B, Suppl. No. 23, pp. 760–5, 1962.
2. J. A. Kostriza, 'Microstrip components', *Electrical Commun*, **30**, pp. 46–54, March 1953.
3. Hideki Hasegawa, Mieko Furukawa and Hisayoshi Yanai, 'Measurements on high-frequency transmission characteristics of metallization patterns in monolithic i.c.s', *Electronics and Communications in Japan*, **54**-B, pp. 52–60, March 1971.
4. C. G. Montgomery (Ed.), 'Technique of Microwave Measurements', chap. 8 (McGraw-Hill, New York, 1947).
5. R. E. Collin, 'Field Theory of Guided Waves', chap. 1 (McGraw-Hill, New York, 1960).
6. R. E. Collin, 'Foundations for Microwave Engineering', chap. 2 (McGraw-Hill, New York, 1966).
7. W. J. Getsinger, 'Microstrip dispersion model', *IEEE Trans. on Microwave Theory and Techniques*, **MTT-21**, pp. 34–9, January, 1973.
8. K. Mehmet, M. K. McPhun and D. F. Michie, 'Simple resonator method for measuring dispersion of microstrip', *Electronics Letters* **8**, pp. 165–6, 23rd March 1972.
9. J. Deutsch and H. J. Jung, 'Measurement of the attenuation and effective dielectric constant of microstrip lines in the frequency range between 2 and 12 GHz' in Proc. 1971 European Microwave Conf (Stockholm, Sweden), pp. C3/4:1–4.
10. H. A. Wheeler, 'Transmission-line properties of parallel strips separated by a dielectric sheet', *IEEE Trans.*, **MTT-13**, pp. 172–85, March 1965.
11. R. A. Pucel, D. J. Masse and C. P. Hartwig, 'Losses in microstrip', *IEEE Trans*, **MTT-16**, pp. 342-50, June 1968.
12. H. Sobol, 'Radiation conductance of open-circuit microstrip' *IEEE Trans.*, **MTT-19**, pp. 885–7, November 1971 (Letters).
13. J. R. James and P. H. Ladbrooke, 'Surface-wave phenomena associated with open-circuited stripline terminations', *Electronics Letters*, **9**, pp. 570–1, 29th November 1973.

10 Appendix: Effect of the launcher discontinuity upon the standing wave

If the distance between the launcher and the load varies, there is a non-constant division of energy in the forward wave between the launcher susceptance and the changing susceptance that appears in parallel with it due to the transformed load. That is to say, the excitation of the microstrip is not constant, but varies with the load position. As the load is moved, therefore, the probe samples points in a standing wave whose amplitude undergoes continually a systematic change. Hence the pattern detected has the appearance of being distorted, in analogous manner to the distortion caused by excess probe coupling.[4] An example is shown in Fig. 13.

It can be proved that this apparent standing wave, as sensed by a probe at a distance x_P from the launcher, is of the form

$$E'(x_P, x_L) = a(b_S, \rho_L, x_L) \times E(x_P, x_L)$$

where $E(x_P, x_L)$ is the correct law, and the amplitude factor under discussion is;

$$a = \left(1 + \frac{b_s^2}{4}(1 + |\rho_L|^2) + b_S|\rho_L| \sin 2\beta x_L + \frac{b_s^2}{2}|\rho_L| \cos 2\beta x_L\right)^{-\frac{1}{2}}$$

where b_S is the normalized susceptance of the launcher, $|\rho_L|$ is the magnitude of the load reflexion coefficient, βx_L is the electrical length from load to launcher and includes the phase of ρ_L.

There are several important observations to be made from this equation. First, if x_L is constant, the amplitude multiplier is invariant and leads to no distortion (as in the 'S' slide indicator). Secondly, there is no error if $b_S = 0$, as would be expected. Thirdly, when $|\rho_L| = 1$ the minima appear in the right place regardless, since the field there is zero anyway. Fourthly, exactly how the amplitude error affects the probing results depends upon the relationship between x_L and x_P, i.e. whereabouts the probe is sited in the standing wave. From the general form of a (Fig. 14) the worst case occurs if $\beta x_L \simeq \pi/4$ and the probe is simultaneously located at a

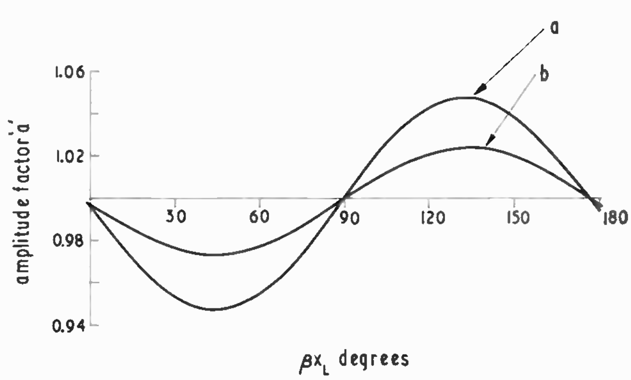

Fig. 14. Amplitude error due to launcher mismatch. Curve (a): $|\rho_L| = 1$, $b_S = 0{\cdot}1$; Curve (b): $|\rho_L| = 0{\cdot}5$, $b_S = 0{\cdot}1$.

standing-wave minimum. Observe that the fractional error in the minimum detected will then be $(a(\pi/4)-1)$. On moving the carriage to $\beta x_L \simeq 3\pi/4$ a standing wave maximum will appear at the probe, and will be detected with a fractional error of $(a(3\pi/4)-1)$. Therefore the error in the v.s.w.r. will be

$$\varepsilon = a(3\pi/4) - a(\pi/4)$$

$$\varepsilon \simeq \frac{|\rho_L| b_s}{1+\frac{b_s^2}{4}(1+|\rho_L|^2)}$$

for small $|\rho_L| b_S$

i.e. $\varepsilon < |\rho_L| b_S$

Apart from giving a practical guide to the error limits for any load/launcher combination, this relation states the very important physical fact that *the error is least when the load is almost matched, which is the exact converse of what happens when a coaxial slotted line is used to measure through the transition.* In that case, it is difficult to retrieve with any accuracy the reflexion coefficient of an 'almost matched' load from the total reflexion coefficient, which is dominated by reflexions from the launcher.

A few simple tests have been carried out with coaxial-microstrip transitions to see what physically is responsible for the mismatch, and to examine ways of reducing it. The tentative finding is a lowering of characteristic impedance just to the microstrip side of the junction, because there is an excess electric flux above the strip there. In 'lumped' terms the transition has a capacitive susceptance located just inside the microstrip. It can be all but eliminated by etching into the ground plane, immediately underneath, a hole of diameter comparable to the strip width to introduce a compensating inductance. A workable strategy is to over-compensate, and have a trimming screw which at maximum travel shorts the hole out again. (A system of this kind is employed in the Hewlett-Packard 11608A transistor test fixture.)

These tests were made after the results in the text had been taken, which therefore relates to the uncompensated launcher only.

Manuscript first received by the Institution on 26th November 1973 and in final form on 7th February 1974 (Paper No. 1586/CC 199).

STANDARD FREQUENCY TRANSMISSIONS—March 1974

(Communication from the National Physical Laboratory)

March 1974	Deviation from nominal frequency in parts in 10^{10} (24-hour mean centred on 0300 UT)			Relative phase readings in microseconds NPL—Station (Readings at 1500 UT)		March 1974	Deviation from nominal frequency in parts in 10^{10} (24-hour mean centred on 0300 UT)			Relative phase readings in microseconds NPL—Station (Readings at 1500 UT)	
	GBR 16 kHz	MSF 60 kHz	Droitwich 200 kHz	*GBR 16 kHz	†MSF 60 kHz		GBR 16 kHz	MSF 60 kHz	Droitwich 200 kHz	*GBR 16 kHz	†MSF 60 kHz
1	−0·1	0	−0·1	697	593·0	17	0	0	−0·1	697	594·6
2	0	0	−0·1	697	593·2	18	0	−0·1	−0·1	697	595·2
3	0	0	−0·1	697	593·2	19	0	0	−0·1	697	597·9
4	+0·1	0	−0·1	696	592·8	20	0	−0·1	−0·1	697	596·1
5	0	+0·1	−0·1	696	591·8	21	0	0	−0·1	697	596·2
6	0	+0·1	−0·1	696	591·3	22	0	0	−0·1	697	596·4
7	+0·1	0	−0·1	695	591·0	23	−0·1	−0·1	−0·1	698	596·7
8	0	0	−0·1	695	591·2	24	+0·1	−0·1	−0·1	697	597·2
9	0	0	−0·1	695	591·4	25	0	−0.1	0	697	597·9
10	−0·1	−0·1	−0·1	696	592·1	26	0	0	−0·1	697	598·3
11	0	0	−0·1	696	592·3	27	0	0	−0·1	697	598·5
12	0	0	−0·1	696	592·7	28	0	0	−0·1	697	598·6
13	0	0	−0·1	696	593·1	29	−0·1	0	−0·1	698	599·0
14	0	0	0	696	593.5	30	−0·1	0	0	699	599·2
15	0	−0·1	0	696	593·8	31	−0·1	0	0	700	599·4
16	−0·1	−0·1	0	697	594·3						

All measurements in terms of H-P Caesium Standard No. 334, which agrees with the NPL Caesium Standard to 1 part in 10^{11}.

* Relative to UTC Scale; $(UTC_{NPL} - \text{Station}) = +500$ at 1500 UT 31st December 1968.

† Relative to AT Scale; $(AT_{NPL} - \text{Station}) = +468{\cdot}6$ at 1500 UT 31st December 1968.

UDC 621.395.625.3

A simplified model of the writing process in saturation magnetic recording

V. A. J. MALLER,
M.A., M.Inst.P., C.Eng., F.I.E.R.E.*

and

B. K. MIDDLETON,
B.Sc., Ph.D., M.Inst.P.†

Based on a paper presented at the IERE Conference on Video and Data Recording held in Birmingham from 10th to 12th July 1973.

SUMMARY

The writing process in saturation magnetic recording is analysed and a model is proposed which is sufficiently simple to enable the functional relationship of the various parameters to be identified. The predictions of the model are compared with experiment and good agreement is obtained.

* *Research and Advanced Development Centre, International Computers Ltd., Stevenage, Hertfordshire.*

† *Department of Electrical & Electronic Engineering, Manchester Polytechnic, Manchester.*

1 Introduction

For many years most analyses of saturation recording disregarded the losses imposed by the writing process due mainly to the apparently formidable problems involved. However the advent of high coercivity materials, in particular thin films, stimulated much work into experimentally investigating the relationship between overall recording performance and medium properties. In an attempt to produce a theoretical model several authors used self-consistent field techniques[1–3] which, being essentially numerical, were analytically unmanageable although good agreement with experiment was obtained. Recently an analytical model has been proposed and shown to make some progress towards giving a simple description of many of the processes involved,[4] although it is restricted to thin film media. In the present paper a similar model with greater analytical flexibility is discussed which enables the quantitative effects of any change in the parameters to be determined relatively easily. In addition it is applicable to thick media although with less accuracy than for thin films.

2 Theory

To be able to predict the recording and replay performance of a given medium it is necessary to know the lengths of the magnetization transitions that may be written into it and how these are affected by the properties of the medium itself and the geometry of the recording system. In the analysis which follows recording alone is considered and particular attention is paid to the crucial influence of demagnetizing fields.

In the recording process demagnetizing fields and record head fields are both present at the moment of writing and hence a transition is written whose length depends on the nature and properties of both fields. As this transition moves away from the record head and the influence of the latter's field declines, the medium will be left with only its own demagnetizing field, whereupon there will be a 'relaxation' of the magnetization to form a new longer transition. Finally, during replay there will be a reorganization of the magnetization distribution under the influence of the high permeability replay head which will tend to shorten the transition. With this picture in mind the magnetization process can be followed through from recording to replay in a rather simple way as a three-stage process.

A further simplification may arise if the 'relaxation' on removal of the head field is drastic and leads to a transition of much greater length than the written one. This situation, which will be distinguished by calling it 'self-demagnetization', is most likely to occur in media of high remanence where a short transition would result in very high demagnetizing fields. Moreover, calculating transition lengths in this case is relatively easy and consequently such lengths are frequently employed in analyses of recording performance, often in circumstances where they are quite inapplicable.

In the following sections these two cases will be considered in detail. Section 2.1 deals with 'self-demagnetization' alone and in Section 2.2 the influence of demagnetizing fields in both the writing and 'relaxation'

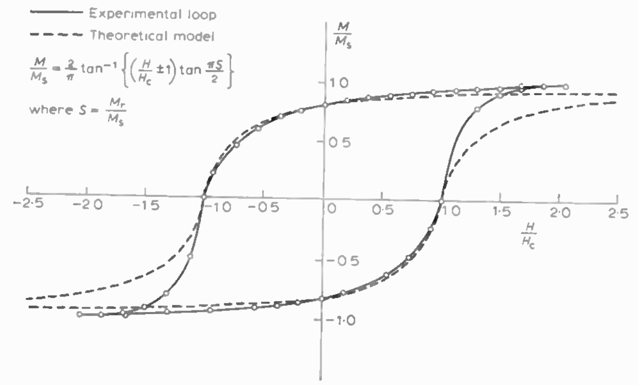

Fig. 1. Comparison of an experimental hysteresis loop with the theoretical model.

processes is discussed. The effect of remagnetization under the replay head is considered in both sections.

2.1 Transition after Self-demagnetization

Many of the simple theories of self-demagnetization have assumed that the stray field alone will impose a limit on the narrowest transition that can be recorded and observed. In these analyses the minimum transition length is determined by equating the peak demagnetizing field and the coercivity.[5] At best this can be interpreted as giving the narrowest transition that can be observed in a rectangular hysteresis loop material. For a more general hysteresis loop some modification is necessary to this simple approach.

Consider the magnetization distribution in the x-direction along the direction of motion to be given by

$$M(x) = \frac{2}{\pi} M_r \tan^{-1} \frac{x}{a} \qquad (1)$$

where M_r is the remanent magnetization and a is a measure of the transition length. The corresponding self-demagnetizing field $H_d(x)$ can be shown to be

$$H_d(x) = -4M_r D\left(\frac{x}{a^2+x^2}\right) \qquad (2)$$

for $a \gg D$ where D is the medium thickness.

Let the hysteresis loop of the same material be given by the following relationship between magnetization M(H) and field H:

$$M(H) = \frac{2M_s}{\pi} \tan^{-1}\left\{\frac{H \pm H_c}{H_c} \tan\left(\frac{\pi s}{2}\right)\right\} \qquad (3)$$

where M_s is the saturation magnetization, H_c the coercivity and $s = M_r/M_s$ the squareness. This is plotted in Fig. 1 where it is compared with an experimental loop from which it can be seen that there is very good agreement in the second quadrant.

In Fig. 2 the second quadrants of a number of hysteresis loops are plotted for various values of squareness.

If the postulated values of magnetization given by equation (1) are to be stable then they cannot give rise to stray fields, equation (2), which are greater than those given by the hysteresis loop. Therefore the actual graph of magnetization against stray field must lie within the latter and the narrowest transition occurs when the two curves touch. This happens at a point which is common to both and where the gradients must also be the same as shown in Fig. 2. Application of these two conditions to equations (1), (2) and (3) leads to the following:

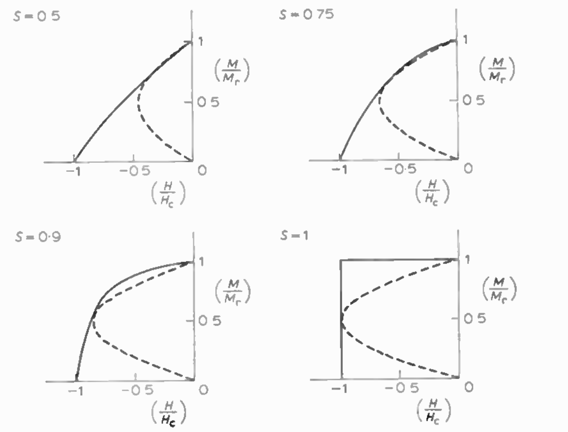

Fig. 2. Second quadrants of a number of hysteresis loops plotted for different values of squareness.

$$a_d = \frac{2M_r D}{H_c} \cdot \frac{\sin\left(\frac{\pi M}{M_r}\right)\tan\left(\frac{\pi s}{2}\right)}{\tan\left(\frac{\pi s}{2}\right) - \tan\left(\frac{\pi s}{2}\frac{M}{M_r}\right)}$$

and

$$a_d = \frac{-4M_r D}{sH_c} \cdot \tan\left(\frac{\pi s}{2}\right)\cos\left(\frac{\pi M}{M_r}\right)\cos^2\left(\frac{\pi s}{2}\frac{M}{M_r}\right)$$

These combine to form a transcendental equation for (M/M_r) which can be solved numerically. The values of (M/M_r) can then be substituted back to give values of 'a_d':

$$\frac{a_d}{a_0} = \frac{\sin\left(\frac{\pi M}{M_r}\right)\tan\left(\frac{\pi s}{2}\right)}{\tan\left(\frac{\pi s}{2}\right) - \tan\left(\frac{\pi s}{2}\frac{M}{M_r}\right)}$$

where

$$a_0 = \frac{2M_r D}{H_c}$$

Values of a_d/a_0 have been computed and these are plotted in Fig. 3 as a function of s.

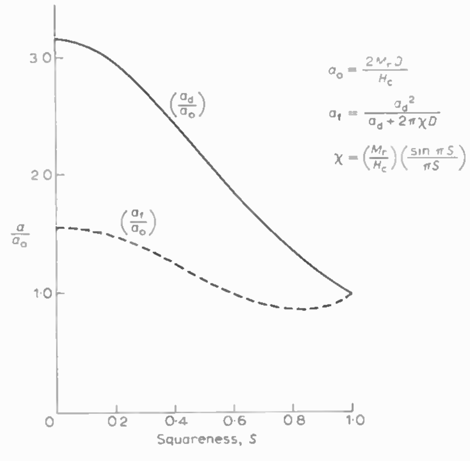

Fig. 3. Plot of computed values for a_d/a_0 as a function of s.

When the medium passes under the replay head there will be some shunting of the stray fields due to the head's high permeability. The minor loop along which the remagnetization takes place is assumed to be linear and is shown in Fig. 4. This has the form

$$M_f - M_i = \chi(H_f - H_i) \quad (4)$$

where χ is the remagnetization susceptibility and M_f (H_f) and M_i (H_i) are final and initial values of magnetization (field) respectively. If there is total flux-closure maximum remagnetization is achieved. Equation (4) then becomes:

$$M_f - M_i = -\chi H_i$$

Differentiating with respect to x gives

$$\frac{dM_f}{dx} - \frac{dM_i}{dx} = -\chi \frac{dH_i}{dx}$$

If values for these differentials at $x = 0$ are obtained from equations (1) and (2) and substituted it is then possible to relate the initial and final values of the transition length in a very simple manner.

$$\frac{2M_r}{\pi a_f} - \frac{2M_r}{\pi a_d} = \chi \frac{4M_r D}{a_d^2}$$

Therefore,

$$a_f = \frac{a_d^2}{a_d + 2\pi\chi D} \quad (5)$$

An approximate and reasonable value for χ may be obtained from the gradient of the major hysteresis loop at $H = 0$.

$$\text{i.e. } \chi = \left(\frac{dM}{dH}\right)_{H=0} = \frac{M_r}{H_c}\frac{\sin \pi s}{\pi s} \quad (6)$$

The modified values of transition width may now be calculated and the effect is shown in Fig. 3 on the values obtained by self-demagnetization. From this graph it is clear that the significant differences between a_d and a_0 attributable to non-unity squareness may be completely compensated by remagnetization in the range $0{\cdot}5 < s \leqslant 1$ where $a_f \simeq a_0$. If there were significant head to medium separation then there would be incomplete flux-closure with a corresponding reduction in the compensation.

2.2 Transition after Writing with Demagnetizing Fields

Since demagnetizing fields are in fact present during the writing process they must be taken into account in order to obtain the correct result. Nevertheless in certain conditions the results should be similar to those obtained by considering self-demagnetization alone. The treatment of this situation in this paper is similar to that of Williams and Comstock[4] but with some convenient and revealing modifications as well as the addition of the effect of remagnetization under the replay head.

The magnetization gradient at the centre of the transition recorded in the medium is given by

$$\frac{dM}{dx} = \frac{dM}{dH}\left(\frac{dH_h}{dx} + \frac{dH_d}{dx}\right) \quad (7)$$

where H_h is the head field and H_d the demagnetizing field of equation (2). Each of the terms now has to be determined.

The position H_1 on the hysteresis loop at which recording is assumed to take place is such that after the recording head field is removed this becomes the centre of the transition. It can easily be shown using equations (3), (4) and (6) and referring to Fig. 4 that

$$H_1 = -H_c \operatorname{cosec}^2 \frac{\pi s}{2} \quad (8)$$

provided that the hysteresis loop gradient at H_1 is taken as being the same as at H_c, that is,

$$\left(\frac{dM}{dH}\right) = \frac{2M_s}{\pi H_c} \tan\left(\frac{\pi s}{2}\right) \quad (9)$$

To calculate dH_h/dx, the head field distribution of Karlquist will be used:

$$H_h(x) = \left(\frac{H_g}{\pi}\right)\left\{\tan^{-1}\left(\frac{x}{y}\right) - \tan^{-1}\left(\frac{2g+x}{y}\right)\right\}$$

where H_g is the field at the gap centre. In what follows y will be taken as the head-to-medium separation plus $D/2$.

If it is assumed that $2g \gg y$ then it can be shown that the maximum head field gradient occurs under the gap edge and is given by

$$\left(\frac{dH_h}{dx}\right)_{max} \simeq \frac{H_g}{\pi y} \quad (10)$$

Furthermore if it is assumed that the transition is written under the gap edge ($x = 0$) in the maximum field gradient then

$$H_1 = -\frac{H_g}{\pi} \tan^{-1}\left(\frac{2g}{y}\right)$$

and for

$$\tan^{-1}\left(\frac{2g}{y}\right) \to \frac{\pi}{2},$$

$$H_1 \simeq -\tfrac{1}{2}H_g \quad (11)$$

Substituting from equations (8) and (11) into (10) gives:

$$\left(\frac{dH_h}{dx}\right)_{max} \simeq \frac{2H_c}{\pi y} \operatorname{cosec}^2\left(\frac{\pi s}{2}\right). \quad (12)$$

Finally, substituting from equations (1), (2), (9) and (12) into equation (7) for $x = 0$ enables the written transition

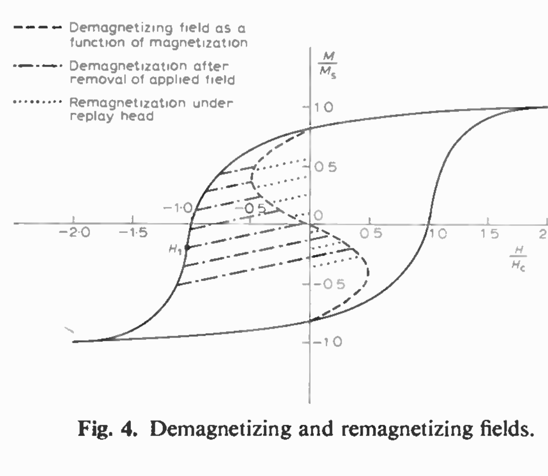

Fig. 4. Demagnetizing and remagnetizing fields.

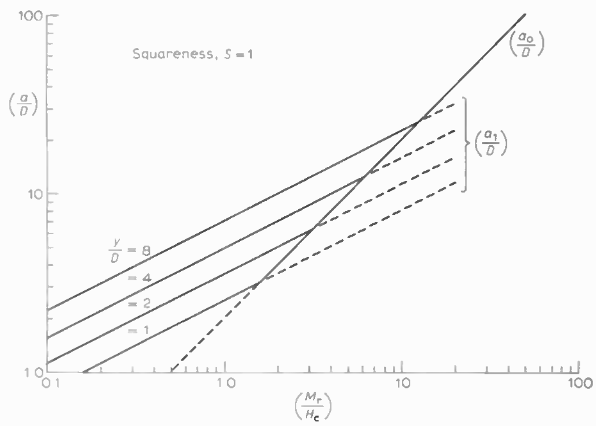

Fig. 5. Limiting case of high squareness, $s = 1$.

in the presence of the writing field to be determined as

$$a_1 = \left(\frac{\pi s y}{8}\right)\sin \pi s + \left(\frac{\pi s y}{8}\right)\sin \pi s \times \left\{1+\frac{16\sec^2(\pi s/2)}{\pi y s^2}\left(\frac{2M_r D}{H_c}\right)\right\}^{\frac{1}{2}}.$$

For $y/D \simeq 1$ to 10 and typical values of M_r/H_c the second term in the brackets dominates and this equation becomes

$$a_1 = \left(\frac{\pi s y}{8}\right)\sin \pi s + \sqrt{\pi y}\left(\frac{2M_r D}{H_c}\right)^{\frac{1}{2}}\sin\left(\frac{\pi s}{2}\right) \qquad (13)$$

Moreover if $M_r/H_c > 1$ or $y/D \simeq 1$ the last term dominates and

$$a_1 \simeq \sqrt{\pi y}\left(\frac{2M_r D}{H_c}\right)^{\frac{1}{2}}\sin\left(\frac{\pi s}{2}\right) \qquad (14)$$

When the applied field is removed, i.e. when the transition moves away from the recording head, there will be further demagnetization and the resulting change in magnetization at any point will be given by equation (4). Hence using equations (1), (2), (4), (6), (7) and (9) and methods similar to those used for calculating remagnetization under the read-head enables the following relationship to be obtained between a_1 and the demagnetized transition a_2:

$$a_2 = \left(\frac{a_1}{2K}\right) + \left\{\left(\frac{a_1}{2K}\right)^2 + \frac{2\pi\chi D a_1}{K}\right\}^{\frac{1}{2}} \qquad (15)$$

where

$$K = \sin^2\left(\frac{\pi s}{2}\right)$$

Finally using equation (5) the remagnetized transition a_3, as seen by the replay head may be calculated:

$$a_3 = \frac{a_2^2}{a_2 + 2\pi\chi D}$$

Now equation (15) may be rewritten in the form

$$a_2^2 = \frac{a_1}{K}(a_2 + 2\pi\chi D)$$

which enables a result of great simplicity to be obtained as follows:

$$a_3 = \frac{a_1}{K} = a_1 \operatorname{cosec}^2\left(\frac{\pi s}{2}\right) \qquad (16)$$

Therefore, equations (13) and (16) give:

$$a_3 = y\left(\frac{\pi s}{4}\right)\cot\left(\frac{\pi s}{2}\right) + \sqrt{\pi y}\left(\frac{2M_r D}{H_c}\right)^{\frac{1}{2}}\operatorname{cosec}\left(\frac{\pi s}{2}\right) \qquad (17)$$

and for $M_r/H_c > 1$ or $y/D \simeq 1$

$$a_3 \simeq \sqrt{\pi y}\left(\frac{2M_r D}{H_c}\right)^{\frac{1}{2}}\operatorname{cosec}\left(\frac{\pi s}{2}\right) \qquad (18)$$

3 Discussion and Experimental Results

From the theoretical analysis it would appear that two regimes exist, namely one in which

$$\left(\frac{a}{D}\right) \propto \left(\frac{M_r}{H_c}\right)^{\frac{1}{2}}\left(\frac{y}{D}\right)^{\frac{1}{2}}$$

and the other in which

$$\left(\frac{a}{D}\right) \propto \left(\frac{M_r}{H_c}\right).$$

Moreover it is clear that these two results do not correspond in the limit of high M_r/H_c where demagnetization might be expected to predominate. This is shown in Fig. 5 for the limiting case of unity squareness where the susceptibility $\chi = 0$ and therefore that $a_1 = a_2 = a_3$ and $a_f = a_d$. The reason for this apparent anomaly lies in the approximations made in the analysis. In the case where the effect of demagnetizing fields during and after writing was investigated only the centre of the transition was considered. This did not allow for the possibility that part of the resultant curve of stray field as a function of magnetization might still lie outside the hysteresis loop, and that therefore further demagnetization was energetically necessary. Nevertheless a plausible and reasonable approximation may be made by taking the greater of the two transition lengths. Obviously a more detailed analysis would probably show a smooth progression from one regime to the other without a discontinuity in gradient.

The three stages of the process with the corresponding values for the transition length are shown in Fig. 6 for

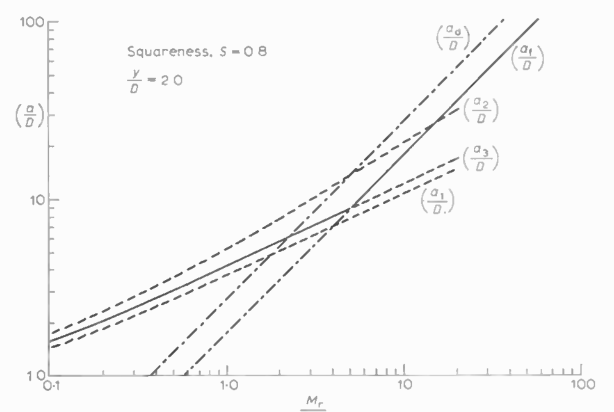

Fig. 6. Three stages of demagnetization process with corresponding values for the transition length.

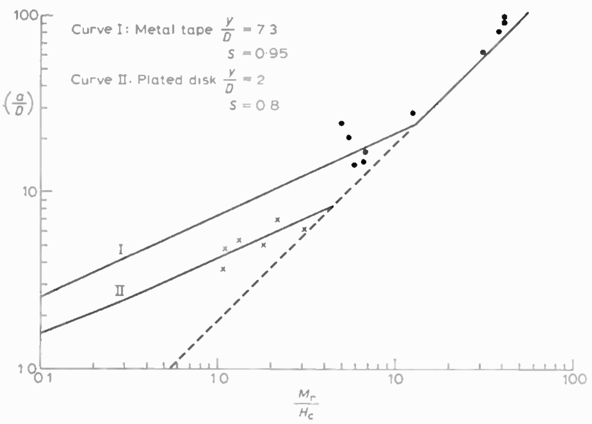

Fig. 7. Experimental results for a cobalt-coated tape and for a cobalt-plated disk.

$s = 0{\cdot}8$ and $y/D = 2$. These latter parameters are typical for contact recording on metallic media.

Some experimental results are shown in Fig. 7 for a cobalt-coated tape and a cobalt-plated disk. The experimental points are marked with either dots or crosses and the solid lines are calculated from the theory for the appropriate conditions. Despite the limited range of experimental values agreement is very reasonable and the two regimes are clearly identifiable. The values of transition length were, of course, not measured directly, but were determined from the width of isolated replay pulses obtained under known geometrical conditions, using the following equation for the half-pulse width.[5]

$$P_{50} = \sqrt{(a+d)(a+d+D)+g^2}$$

where d is the head-to-medium separation.

4 Conclusions

The theory presented in this paper is comprehensive in that it takes into consideration the recording geometry, the writing field distribution, demagnetization effects whilst writing and after writing, and remagnetization on reading. The results are analytically simple thereby enabling the quantitative effects of any change in the parameters to be determined relatively easily. Finally the agreement with experiment is very reasonable for thin recording media.

5 References

1. Iwasaki, S. I. and Suzuki, T., 'Dynamical interpretation of magnetic recording process', *IEEE Trans on Magnetics*, MAG-4, pp. 269–72, September 1968.
2. Curland, N. and Speliotis, D. E., 'A theoretical study of an isolated transition using an iterative hysteretic model', *IEEE Trans.*, MAG-6, pp. 640–6, September 1970.
3. Lee, J. E., 'Calculation of the output pulse shape for the digital recording process', *IEEE Trans.*, MAG-6, pp. 652–3, September 1970.
4. Williams, M. L. and Comstock, R. L., 'An analytical model of the white process in digital magnetic recording', Proc. A.I.P. Conference on Magnetism and Magnetic Materials, 1971.
5. Middleton, B. K., 'The dependence of recording characteristics of thin metal tapes on their magnetic properties and on the replay head', *IEEE Trans.*, MAG-2, pp. 225–9, September 1966.

Manuscript received by the Institution on 30th April 1973 (Paper No. 1587/CC200)

The Authors

Dr. B. K. Middleton has been a Senior Lecturer in the Department of Electrical and Electronic Engineering at Manchester Polytechnic since September 1972. He graduated from Sheffield University in 1962 with an honours degree in physics and then worked for four years for International Computers Limited on computer storage and logic devices. In 1966 he became Research Fellow in the Department of Pure and Applied Physics at Salford University where he studied the properties of magnetic materials and thin films and their application to information storage devices. In 1970 a thesis on magnetic thin films and their magnetic recording properties, was accepted by Salford University for the degree of Doctor of Philosophy. In his present post he is establishing research in digital magnetic tape recording and is currently supervising a postgraduate research student in this area. His other research interests are in a.c. bias recording, computer storage devices, bubble domains, and the properties of magnetic materials.

Mr. V. A. J. Maller graduated in 1959 and for the next three years worked for the Admiralty on theoretical aspects of guided missile control systems. Since 1962 he has been employed by International Computers Limited where he has been a member of the research staff. During this period he has worked on superconducting computer devices, integrated circuit packaging, design automation, digital magnetic recording and magneto-optic recording. Recently he has changed his field of interest to the 'software' aspects of data processing in technology, and he is currently concerned with new techniques for data base management.

IERE News and Commentary

Canadian Engineers' Salaries Increase

According to the latest membership salary survey by the Canadian Council of Professional Engineers, the increase in median salaries of Canadian engineers in 1973 over 1972 was 8·4%. The median salaries for all Canada ranged from $23,484 for 1946 graduates with a top high decile of $55,000 recorded by graduates of 1940 working in Alberta, and the lowest decile reported by graduates of 1973 working in the prairie and Atlantic provinces at $8,400.

A membership salary and employment status survey is conducted on behalf of the constituent associations of CCPE in December of each year. In considering the results of the latest survey the Canadian Engineering Manpower Council noted that the percentage of engineers unemployed and seeking employment on a full-time basis and engineers employed in a temporary position with a fixed termination date and actively seeking other employment did not vary substantially from the data obtained through a similar survey carried out one year earlier; the Council concluded that in view of the evident difficulty employers are meeting in recruiting engineers at this time, the majority of engineers reported in the above two categories would be either between jobs, temporarily unemployable or permanently unemployable. The survey indicates that 90·7% of all Canadian engineers are currently employed in secure positions, while, on the other hand, 0·8% are unemployed and seeking full-time employment.

Based on all available information at this time including the expected number of new graduates from Canadian engineering schools this year, it appears evident that the demand for engineers during the rest of 1974 will exceed the supply and that a critical shortage may develop in some branches of engineering and some geographic areas.

The Canadian Engineering Manpower Council has also completed a nationwide survey of employment among 1973 Ph.D. graduates in engineering and found no significant unemployment. Out of 290 graduates from 20 Canadian universities, three were reported unemployed.

The majority of the graduates were in electrical, civil, chemical and mechanical engineering. The total number of graduates was larger than expected and 61% were from the province of Ontario. Approximately 16% have left Canada, which is about the same as for previous years and is probably due to the return of foreign students to their home countries. A notable increase in employment in industry has occurred; approximately 36% were employed in industry, 26% went to university staffs and 9% to government departments and agencies.

New Presidents of the Institutions

Sir St. John Elstub, C.B.E., B.Sc., F.I.Mech.E., F.Inst.P., Hon.D.Sc.(Aston) is the new President of the Institution of Mechanical Engineers, having taken over from the retiring President, Mr. J. W. Atwell, C.B.E., LL.D., C.Eng., F.I.Mech.E., F.R.S.E. Sir St. John, who was knighted in 1970, is a strong advocate of unification of the engineering profession as a means of better serving the nation's scientific and industrial needs. He has occupied or continues to occupy directorships in nationally important companies such as ICI (Metals Division) Limited, Imperial Metal Industries Limited, Rolls Royce (1971) Limited, the Royal Insurance Company, the British Engine Insurance Company and Tube Investments Limited.

Sir St. John has served on many important committees of I.Mech.E., and has maintained a continuous interest in technical education. He was a member of the Engineering Industry Training Board from 1964 to 1972.

Mr. Barry Pemberton Laight, O.B.E., C.Eng., M.Sc., M.I.Mech.E., F.R.Ae.S., Director and Chief Projects Engineer, Military, of Hawker Siddeley Aviation Limited, has been installed as President of The Royal Aeronautical Society. The retiring President was Dr. George Steedman Hislop, B.Sc.(Eng.), A.R.C.S.T., C.Eng., F.I.Mech.E., F.R.Ae.S., Executive Vice-Chairman of Westland Aircraft Limited.

Mr. Laight joined the Bristol Aeroplane Company in 1937 as an apprentice and later went to Bristol University where he eventually obtained his M.Sc. degree for structural work on the *Brabazon*. Leaving the Bristol Company in 1952, Mr. Laight became Chief Designer of Blackburn Aircraft Ltd., and eleven years later he moved to Hawker Siddeley Aviation's headquarters at Kingston-upon-Thames, as Head of the Advanced Projects Group. As Chief Engineer of the Hawker-Blackburn Division he was responsible for the *HS 1154* and later he took charge of the design and development of the *Harrier*. In 1968 he became a Director of Hawker Siddeley Aviation Limited and Chief Projects Engineer, Military, with responsibilities for the introduction of new military aircraft.

Mr. Laight has served on many committees of the Society and has served on Research and Technology Committees of the CBI, on the Education Committee and Technical Board of the SBAC and on Transport Committees of the SRC. He was for a time a Governor of Kingston Technical College.

Grants for Research Instrument Construction

Among grants totalling over £60,000 made by the Paul Instrument Fund Committee, are the following which are for electronic instruments:

£1839 to Professor A. L. Cullen, O.B.E., Pender Professor of Electrical Engineering, University College London, as a supplement to the grant of £10,717 made in 1970, for the construction of a wide-band microwave impedance bridge of high accuracy, using a new and very precise absolute impedance standard.

£600 to Dr. V. I. Little, Reader in Experimental Physics, Royal Holloway College, Englefield Green, as a supplement to the grant of £7050 made in 1971, for the construction of an optical klystron in which novel types of buncher and catcher are formed by the deposition of metallic films in the presence of optical standing waves.

Up to £1200 to Dr. R. C. Smith, Reader in the Department of Electronics, University of Southampton, for the construction of an infrared spectrometer operating from 2 μm to beyond 25 μm using a tunable coherent infrared source obtained by frequency mixing of dye laser radiation in non-linear media.

The Paul Instrument Fund Committee, composed of representatives of the Royal Society, the Institute of Physics and the Institution of Electrical Engineers, was set up in 1945 to receive applications from research workers in Great Britain for grants for 'the design, construction and maintenance of novel, unusual or much improved types of physical instruments and apparatus needed for an investigation in pure or applied physical science'.

Committee of Enquiry into the Future of Broadcasting

Replying to a written question in the House of Commons on 10th April, the Secretary of State for the Home Department, Mr. Roy Jenkins, stated that the Government had decided to set up a Committee of Enquiry into the future of broadcasting. In response to a question from Mr. Phillip Whitehead asking whether he was now in a position to make a statement about the Government's policy on the future of broadcasting the Home Secretary said:

'The Government has decided to set up a Committee of Enquiry into the future of broadcasting with the following terms of reference:

> To consider the future of the broadcasting services in the United Kingdom, including the dissemination by wire of broadcast and other programmes and of television for public showing; to consider the implications for present or any recommended additional services of new techniques; and to propose what constitutional, organizational and financial arrangements and what conditions should apply to the conduct of all these services.

Lord Annan has agreed to serve as Chairman of the Committee. I will announce the names of the other members as soon as possible.'

Mr. Jenkins added that, to allow time for the Committee to complete its task and for consideration of its proposals, the Government proposed to bring forward legislation to extend the Independent Broadcasting Authority Act 1973, which expires in July 1976, to July 1979 and extend the Charter of the B.B.C. for a similar period.

Co-operation Agreement with USSR

A 10-year Co-operation Agreement between the United Kingdom and the USSR has recently been signed in London, which will provide a framework for all forms of economic, scientific, technological and industrial co-operation between firms and organizations in the two countries. It provides that both Governments will work for the development of all these forms of co-operation with the aim of strengthening the economic relations of the two countries. The two Governments undertake to support and encourage the conclusion of agreements and contracts on economic, scientific, technological and industrial co-operation between firms and organizations of the two countries: but the Agreement makes it clear that the conditions governing particular co-operation projects must be agreed between the organizations, enterprises and firms directly involved. In addition, the two Governments undertake, where this is in their mutual interest, to support and encourage their firms and enterprises in projects of economic, scientific, technological and industrial co-operation in the third markets.

In an important article of the Agreement the two Governments have included an initial list of specific sectors which have been identified as of particular interest. These include: computers, scientific instruments, medical equipment and instruments, machine tools, electric power, copying machines, environmental engineering, automation, packaging technology and materials handling. Other fields of mutual interest may be agreed from time to time.

It is the aim of both Governments to formulate within the next few months a concrete programme of economic collaboration based on this Agreement There will be preliminary discussions about this at an early meeting of the Anglo Soviet Joint Commission. British exports to the USSR have continued to stagnate, whereas, in value terms, Soviet exports to the United Kingdom are growing significantly.

This co-operation Agreement with the USSR is broadly similar to the 10-year Co-operation Agreements with Poland, Bulgaria and the GDR. Similar Co operation Agreements have been concluded with CMEA countries by most other Member States of the EEC in recent years.

British Machine Tools and Scientific Instruments to be shown in China

The Chinese authorities have agreed to a proposal by the British Overseas Trade Board that a British Machine Tools and Scientific Instruments Exhibition should be staged in China in March–April, 1975. The exhibition, which is being jointly sponsored by the Machine Tool Trades Association, the Scientific Instrument Manufacturers Association and the Gauge and Tool Makers Association in conjunction with the Sino-British Trade Council, is a follow-up to the highly successful British Industrial Technology Exhibition held in Peking in the Spring of 1973.

In preparation for this exhibition a team headed by Mr. W. T. Pearce, Director of Fairs and Promotions Branch of the BOTB, recently visited Peking for discussions with the China Council for the Promotion of International Trade. It is expected that some 70 British companies will participate in the exhibition next spring, which will run for up to 12 days and is expected to occupy some 6,000 square metres of exhibition space in Shanghai.

Nearly 350 British companies exhibited £2·5M worth of industrial goods at the Peking Exhibition. The Exhibition, which was the largest of its kind ever held in the People's Republic of China, attracted over 200,000 visitors.

Noise and Vibration Control Conference

Complete sets of papers issued at the above conference, held at the University of Bath in April, are available at a cost of £2·50 each, plus postage. Please apply to The Courses Office, South Building Annexe, University of Bath, Claverton Down, Bath BA2 7AY. (Telephone: Bath 6941, Ext. 622).

Details of this conference, of which the South Wales Section of the IERE was a co-sponsor, were published in the February 1974 Journal.

U.K. exports to China rose from £31·6M in 1972 to £84·7M in 1973, only £14M below those to the USSR, and this trend appears to be continuing in 1974.

Binding Members' Journals

Members are reminded that they may have their journals bound by the Institution at a charge of £3·00 plus postage and packing (50p British Isles, 60p Overseas). The twelve issues for binding should be sent to the Publications Department, IERE, 9 Bedford Square, London WC1B 3RG. It will minimize book keeping and other overheads if payment for binding is included with the issues.

The charge to members for supplying and inserting any missing issue of the *Journal* is 50p. An Index will be incorporated free of charge (see March Journal, p. 173).

Members' Appointments

CORPORATE MEMBERS

Mr. K. G. Nichols (Fellow 1967, Member 1960), has been appointed to a personal Chair in Electronics at the University of Southampton. Professor Nichols, who joined the Department of Electronics in 1961 as a Lecturer, was appointed to a Readership four years ago. He is at present on periodic and special leave from the University as an IBM Fellow at the Hursley Park Laboratories of IBM United Kingdom Ltd, near Winchester; in the course of this Fellowship, which runs from October 1973 to September 1974, he has

been working with a group concerned with computer-assisted design of large micro-electronic systems. As well as being a contributor to the Institution's Journal, Professor Nichols is currently on the Education and Training Committee, and has served on the Examinations Committee, the Southern Section Committee, BSI Technical Committees and on CEI working parties. He was appointed a member of the Council last October.

Mr. A. S. Pudner, M.B.E. (Fellow 1961, Member 1943) has retired from Cable and Wireless Ltd., where he has been Engineer in Chief since 1965; in 1969 he became the first C & W engineer to be appointed to the Court of Directors. Mr. Pudner joined the Company in 1934 and has served at many overseas stations as well as on cable ships. During the Korean War he was Manager of the Cable and Wireless field telegraph unit and he was appointed M.B.E. in December 1952 for his services to the unit. He has represented the Company at various international conferences.

Mr. Pudner served on the Institution's Membership Committee from 1963 to 1965 and since 1969 he has been a member of the Finance Committee. He was elected to Council in 1968 and was a Vice-President from 1969–1972.

Vice-Admiral P. A. Watson, M.V.O. (Fellow 1967) has been appointed Chief Naval Engineer Officer and Senior Naval Representative, Bath. Rear-Admiral Watson held the appointment of Director General Weapons (Naval) from 1970 and his previous appointments include command of HMS *Collingwood* (the Naval Weapons and Engineering School) from 1967–1969 and Deputy Director of Engineering (Electrical) in the Ship Department, Ministry of Defence from 1969–1970. He was promoted Rear-Admiral in 1971 and Vice-Admiral on 13th May, 1974.

Sqn. Ldr. D. R. Ainge, RAF (Member 1973, Graduate 1967) who has just completed the Advanced Engineering Course at the RAF College, Cranwell, has been posted to RAF Rheindahlen, Electrical Engineering 3C, Headquarters, RAF West Germany.

Mr. R. A. Allman (Member 1961) is now Eastern Regional Manager of Lambda Electronics Corporation, New York. He joined the Company in 1973 as Field Marketing Manager shortly after going to the United States from Great Britain where he was for some ten years a Sales Manager with Standard Telephones and Cables Ltd.

Major M. S. Body, REME (Member 1967, Graduate 1958) has been appointed Officer in-charge of Radar Production at 35 Central Workshop REME, Old Dalby, Leics. He was previously Officer-in-charge of Management Services at 12 Field Workshop REME.

Mr. P. Broomer (Member 1964, Graduate 1962) who is with Rank Xerox, has been appointed Senior Production Control Resident for the Company in Webster, New York.

Flt. Lt. J. F. Cogswell, RAF (Member 1973, Graduate 1969) is now Officer Commanding Electrical Engineering Flight, RAF Locking. He previously commanded the Electrical Engineering Support Flight.

Mr. M. W. Farley (Member 1953, Associate 1946) has been appointed Technical Director of Visionline Ltd., New Malden, Surrey. He was previously General Manager of the Company.

Mr. I. M. Findlay (Member 1970, Graduate 1969) is now with the British Aircraft Corporation, Bristol, as an Electronics Design Engineer. (In the November 1973 Journal it was incorrectly stated that Mr. Findlay had joined McMichael Ltd., whereas in fact this was his previous appointment).

Mr. B. C. Gray (Member 1956, Graduate 1954) has been appointed Assistant Director, Ordnance Factories/Quality in the Procurement Executive of the Ministry of Defence.

Mr. D. Haley (Member 1966) has moved from East Ham College of Technology where he was Lecturer of Electrical Principles and Electronics to the West Kent College of Further Education, Tonbridge as Lecturer in charge of Telecommunications in the Department of Engineering.

Flt. Lt. G. P. Hallam, RAF (Member 1973, Graduate 1970) is now Officer Commanding Technical Flight, Ground Radio Installation Squadron, Radio Engineering Unit at RAF Henlow.

Mr. M. E. Jones (Member 1972, Graduate 1919) who is with Hunting Engineering Ltd., has been promoted to Senior Project Engineer.

Mr. R. Lawton (Member 1973, Graduate 1970) is now with National Semi-Conductor (U.K.) Ltd., as a Senior Design Engineer on linear integrated circuits. He was previously Design Engineer with Plessey Semiconductors, Swindon.

Lt. Col. N. R. F. MacKinnon (Ret.) (Member 1970, Associate 1964) has been appointed Marketing Manager for Racal-Mobilcal Ltd. Lt. Col. MacKinnon who was in the Royal Signals held the post of Commander Force Communications in the Qatar Security Forces from 1972 to 1973.

Sqn. Ldr. D. McLean, RAF (Ret.) (Member 1965, Graduate 1961) has taken up the appointment of Lecturer in Control Engineering in the Department of Transport Technology at the University of Loughborough. His last Service appointment before retirement was RAF Exchange Professor at the Air Force Institute of Technology, Wright-Patterson Air Force Base, Dayton, Ohio.

Sqn. Ldr. D. F. Macleod, RAF (Member 1973, Graduate 1968) has been posted to RAF Wattisham as Officer Commanding Engineering Support Squadron. From 1971 to 1973 he was Deputy Unit Commander and Radar Signature Analyst with 1020 Signals Unit RAF.

Flt. Lt. K. M. Moore, RAF (Ret.) (Member 1973, Graduate 1970) has joined Kode Limited as an Electronics Engineer responsible for setting-up a systems test and commissioning facilities for micro-processing equipment. His last Service appointment was Officer in Command Electrical Engineering Flight at RAF Colerne.

Mr. J. L. G. Newman (Member 1963, Graduate 1967) has moved from Data Recording Instrument Co. Ltd., where he was Senior Design Engineer to the Plessey Company at Poole to work on point of sales terminals as a Senior Engineer.

Mr. S. C. Newman, B.Sc. (Member 1969) has been appointed Production Manager with Weatherford Oil Tool (U.K.) Ltd., Great Yarmouth. He was previously for nearly twenty years with Erie Electronics Ltd., latterly as Chief Resistor Design Engineer.

Lt. Cdr. B. R. O'Carroll, RN (Member 1971, Associate 1968) has been posted to HMS *Collingwood*, as Communications Group Officer. He was previously

Weapons Electrical Engineer Officer in HMS *Falmouth*.

Inst. Cdr. R. H. Parsons, M.A., RN (Member 1969) has been appointed Director Naval Training Support at the Ministry of Defence (Navy).

Mr. B. A. Spencer (Member 1971, Graduate 1967) who joined English Numbering Machines Ltd., as a Project Engineer in 1971, is now Engineering Consultant with Logica Ltd.

Mr. R. Spencer (Member 1967, Graduate 1966) has been appointed Technical Director of Simon-Barron Ltd., Gloucester; he was previously Manager of the Design and Development Division of the Company.

Mr. J. A. Surtees (Member 1973, Graduate 1969) has been appointed to Telecommunications Branch, Ministry of Defence at REME Christchurch, Hants. as a Professional & Technology Officer II.

Flt. Lt. R. M. Webster, RAF (Member 1973, Graduate 1969) has been posted to RAF Manston as Officer Commanding Engineering Squadron. He was previously Officer Commanding Air Radio and Navigation Instrument Flight at RAF Kinloss.

Lt. Col. W. L. Wood, R Sigs (Member 1971) is now Trials Director at the School of Signals at Blandford Camp.

NON-CORPORATE MEMBERS

Mr. A. C. Bentley (Companion 1968) who is Director of the Radio and Electronic Component Manufacturers' Federation has been appointed a Honorary Life Member of the Committee of European Associations of Electronic Components (CEMEC) following his retirement from the CEMEC Board. This honour, the first of its kind, marks the culmination of Mr. Bentley's personal connection with CEMEC and its predecessor in the passive components sector, CEPEC, extending over the past ten years. Mr. Bentley played a significant part in the activities of CEPEC as a founder-member in 1965, becoming Vice-President in 1967–1968, and President in 1969–1970.

Mr. E. J. Boswell (Graduate 1971) has been appointed Assistant Executive Engineer at the Post Office Research Department, Ipswich. He was previously a Scientific Officer at the RAF College, Cranwell.

Mr. K. D. M. Bowman (Graduate 1971) who is with Post Office Telecommunications, has been promoted to Executive Engineer and is with the Transmission and Power Planning Department of the General Manager's Office in Oxford. He was previously with the North West Telecommunications Board.

Mr. D. A. George (Graduate 1971) has been appointed Electrical Department Manager with Benson and Hedges Ltd., Brampton, Ontario. After graduating from the University of Wales Institute of Science and Technology he went to Canada in 1967 and was until February of this year with Johnson Controls Ltd., Toronto, as a Project Designer.

Flt. Lt. M. R. Hubbard, B.Sc., RAF (Graduate 1972) has been posted to RAF Medmenham as Project Officer.

Mr. F. B. Norman (Graduate 1969) who joined Stromberg-Carlson Corporation, Rochester, New York in June 1973 has moved to GTE Lenkurt Electric (Canada) Ltd., Burnaby, British Columbia as an Equipment Engineer.

Mr. P. Dunne (Graduate 1970) has joined Robert Bosch Fernsehanlagen, as a Systems Planning Engineer. He was previously with Radio Telefis Eireann, Dublin.

Mr. G. T. Elsmere (Graduate 1970) formerly at Rothamsted Experimental Station, has now joined Rank Xerox as a Laboratory Supervisor.

Mr. S. S. Rayat (Graduate 1970) is now a Senior Test Engineer with Data Recording Instrument Co. Ltd.

Mr. D. M. Svensson (Graduate 1971) has moved from Teleng Ltd., to Marconi-Elliott Avionics Ltd., Rochester, where he is an Electronics Development Engineer.

Mr. A. C. F. Leadbitter (Associate 1962) who was a Divisional Manager with Belling and Lee Ltd., has been appointed Managing Director of Wolsey Electronics, Porth, Glamorgan.

Mr. B. R. Robertson (Associate 1973) has retired from the RAF in the rank of Chief Technician after 13 years' service and joined Rank Xerox Ltd., as Training Officer at their Newport Pagnell Training Centre.

Mr. B. F. Webb (Associate 1972) who has been with Bell Northern Research since 1969, has been appointed Manager Quality Engineering with the Northern Electric Company at London, Ontario.

Mr. D. W. Hall, B.A. (Associate 1970) has joined the British Aircraft Corporation, GW Division, Bristol, as a Systems Engineer, following his retirement from the RAF.

Obituary

The Council has learned with regret of the deaths of the following members.

Arthur Frederick Bulgin, O.B.E. (Fellow 1943) died on 29th March, aged 74; he leaves a widow and one son and one daughter.

Born in Barry, South Wales, Mr. Bulgin served in the first World War as a Wireless Operator in the Royal Flying Corps. On demobilization he joined an electrical engineering company and during this period studied at Northampton Engineering College. In 1923 he formed his own Company A. F. Bulgin and Co., of which he continued to be Chairman and Managing Director, and which celebrated its Golden Jubilee last year. As a leading manufacturer of electronic components Mr. Bulgin was active in the industry's trade associations and in 1932 he was one of the six founders of the Radio Component Manufacturers Federation (now RECMF). After that date he held numerous offices in the Federation and he was President from 1961–1966. In his capacity of Chairman of the RECMF Exhibition Committee he led the organization of the Components Exhibitions held initially at Grosvenor House and in recent years at Olympia. From 1934–1943 Mr. Bulgin was a member of the Radio Manufacturers Association Council, predecessor of the present British Radio Equipment Manufacturers Association.

During the Second World War Mr. Bulgin took a leading part in the development of the Air Training Corps in Essex and he eventually became Commanding Officer of the West Essex Wing with the rank of Wing Commander in the RAFVR. In recognition of his services was appointed M.B.E. in 1947 and on his retirement from the RAFVR in 1956 after 15 years' service he was granted the honorary rank of Wing Commander. For his contribution to the development of the Electronic Components industry, particularly through overseas exhibitions, Mr. Bulgin was promoted to O.B.E. in 1967.

In 1962 he was appointed to the Institution's Membership Committee and shortly afterwards became a member of the Finance Committee, on both of which he continued for some years. His professional interests were evidenced by the establishment in 1952 by the A. F. Bulgin Premium which is now awarded annually for the outstanding paper published in the Journal on the theory and practice of electronic components and circuits.

Alexander Bernard Avery (Fellow 1966, Member 1965) died on 3rd December, 1973, at Kota Kinabalu, Sabah, Malaysia, aged 59.

Born in London and educated at the Regent Street Polytechnic, Mr. Avery worked with several radio manufacturing companies in the middle 'thirties before going to the Far East as Manager of the radio and electrical import department of a company in Rangoon, Burma; and subsequently he was apponted Engineer to Radio Supplies Ltd. of Rangoon. On the outbreak of the Second World War he joined the RAF and served initially in Malaysia and later in Karachi as a Station Signals

Officer. From 1943 to 1944 he was on the Staff Air Command South East Asia, and later he took charge of a Research and Development Section at a Base Signals Depot in Calcutta. During the next ten years he held senior signals appointments with the RAF in the United Kingdom and the Far East and immediately prior to retirement was Chief Signals Officer with the rank of Squadron Leader in Singapore.

In 1955 Mr. Avery joined H. A. O'Connor & Company of Singapore, initially as Engineer and latterly as General Manager in East Malaysia. In this capacity he was concerned with the design and planning of police and other communications networks links, in Sabah, Sarawak, Brunei and Singapore.

From 1962 until his death Mr. Avery was a Representative of the Institution in Malaysia and Singapore and he was responsible for convening meetings of members in the area both separately and in collaboration with other professional institutions.

Keith Pannell (Graduate 1964) died on 29th March, 1974 after a short illness aged 31. He leaves a widow and two young children.

On leaving school in Hammersmith, London, in 1958, Mr. Pannell joined the Admiralty Research Laboratory at Teddington as a Scientific Assistant. During the next five years he studied at Kingston Technical College and obtained a Higher National Certificate in Applied Physics. In 1965 he was promoted to Assistant Experiment Officer and three years ago became a Higher Scientific Officer. Mr. Pannell was latterly concerned with the development and commissioning of advanced computerized signal processing systems and similar equipment. In December 1973, his transfer to Corporate Membership was recommended by the Membership Committee but its approval by the Council was cut short by his untimely death.

Michael John Albert Carrington (Graduate 1970) died suddenly on 28th February, 1974, while at work at the Rutherford Laboratory. He was 43 years of age and leaves a widow.

Mr. Carrington went into the Royal Navy in 1946 as an Electrical Artificer and he later converted to Radio Electrical Artificer; on his retirement from the Navy in 1961 he was Chief Radio Electrical Artificer in charge of a Fleet Repairs Workshop. He then joined the Rutherford Laboratories of the Science Research Council as Technical Officer and for the next eight years was a Shift Leader on a 50 MeV Proton Linear Accelerator. Since the completion of the accelerator programme he had been engaged on the design and commissioning of equipment for large electrical and electronic projects including a novel display system for spark chamber experiments.

Thomas Havana Cooper (Graduate 1970) died suddenly in Madrid on 1st April, 1974, aged 55.

Born in Cuba and educated in Rugby, Mr. Cooper was apprenticed to the British Thomson-Houston Company from 1936 to 1939. During the War he served as a Sergeant in the Royal Signals and on demobilization studied for a degree in electrical engineering at Northampton Engineering College. In 1950 he joined Marconi's Wireless Telegraph Company as a Junior Development Engineer with whom he remained until 1971, by which time he was a Senior Engineer in the Transmitter Design Department. For the past three years he was Chief of the Television Design Department of Nortron S.A., of Madrid.

CEI News

CEI Seeking Energy Experts List for Government

CEI has asked constituent members to supply it with the names of individuals within their respective organizations whose expertise could be made available to the Government in the context of the energy crisis. This follows an approach by CEI's Chairman to the previous Government in which he forwarded a copy of the CESE letter published in *The Times* to Lord Carrington and offered the co-operation of the engineering profession in dealing with the energy problems facing the country. (See Journal for March 1974, page 117.) The response of the previous Government was favourable and the matter is now being pursued with the new Government.

With its memorandum to constituent members CEI has attached a schedule of energy sources and users as a lead to the area in which they might identify individuals who may be able to help. This includes provision both for those working full-time in the areas listed and for those able to offer useful advice.

The names have been forwarded by the Chairman to the Government advising it on those put forward in any particular field. Any follow-up action will be directed through the institutions concerned.

A Reminder on the Use of the Designatory Letters C.Eng.

In July 1972, CEI's Board adopted the Report and Recommendations of its Working Party on Nomenclature which had been asked to consider the related problems of the proliferation of titles and designatory letters, and the diversity of the nomenclature in the membership structure of CEI member institutions.

The Chairman of CEI has particularly requested that members should be reminded of these recommendations. All those who registered as Chartered Engineers are encouraged to use the designation 'C.Eng.' either alone or in combination with the letters describing their corporate membership of their Institution.

CEI 1973 Annual Report

Copies of CEI's Annual Report for 1973, which was discussed in the April Journal, are now obtainable from the Council at 2 Little Smith Street, London, SW1P 3DL at a cost of 15p each.

Tin in Electronics Production

*The second largest use for tin is in solders and today the bulk of these are used in the electronics industry. In this industry, reliability is essential, and methods of ensuring the quality of soldered joints are being pursued. Progress in research at the Tin Research Institute into improving solders and solderability is therefore discussed in some detail in the latest annual report of the International Tin Research Council.**

Impurities. An extensive programme of research into the ways in which certain impurities and additions affect the wetting properties of 60% tin-40% lead solder has been completed during 1973. A detailed report on this research programme has been compiled, covering the effects of copper, antimony, cadmium, bismuth, arsenic, aluminium, zinc, sulphur and phosphorus impurities. This work will be published in the near future, and the results have already proved valuable when T.R.I. were called upon to advise on the revision of British Standard 219 for soft solders.

During this programme of solderability testing, it has been observed that, with 60% tin-40% lead solder, trace amounts of aluminium or zinc influence oxidation behaviour. Work is now in hand to extend the study on impurities by investigating in more detail the oxidation behaviour of molten solder alloys and the effects of certain impurities on oxidation rate.

The Institute receives many enquiries relating to the performance of solder joints under severe service conditions, and it has become apparent that industry is demanding that soldered joints should withstand increasingly searching environmental and stress conditions. At the present time relevant data on mechanical properties are sparse; hence the need for studies in this field. At elevated temperatures, the strength of a joint is largely determined by the creep strength of the bulk solder and data are being accumulated from a continuing programme on the stress/time-to-rupture testing of bulk solders. Complete data are now available for 60% tin-40% lead solder at room temperature, 80°C and 100°C. The test programme on 40% tin-60% lead solder at 100°C is at an advanced stage and testing of a 62% tin-36% lead-2% silver solder is commencing. Other alloys designed to have higher creep strength, such as 95% tin-5% antimony, and 96·5% tin-3·5% silver will be included as test rigs become available.

Solderability testing. The Institute has had many years of experience in solderability testing and has done much to encourage its application in industry. Recently, new techniques for measuring solderability have become available and an investigation to compare different techniques for measuring solderability has been continued. This work has included the development of standard, reproducible techniques for preparing clean copper test pieces and lightly oxidized copper test pieces using a benzotriazole treatment.

A surface tension balance solderability testing instrument was used to study various wetting parameters, and the usefulness of this type of equipment as a commercial solderability test assessed. A technique was devised whereby the surface tension balance could also be used for measuring the height of rise of a solder meniscus in contact with a test surface, whilst, at the same time, recording the wetting time, the wetting force, and the rate of wetting. Tests correlating these various parameters have been completed for a range of rosin fluxes.

These new techniques of assessing solderability are being compared with the well-established rotary-dip, area-of-spread and globule solderability tests.

Solders for gold plated components. In the electronics industry a substantial number of components have termination leads or other surfaces which are gold plated and to which soldered joints have to be made. When the normal tin-lead solders are used to solder gold coated surfaces, the gold dissolves very quickly into the solder and reacts rapidly to form a thick layer of intermetallic compound at the interface. This produces long needles of tin-gold intermetallic compound in the solder in the joint, which can cause a reduction in the mechanical strength.

To study whether the presence in the solder of elements other than tin and lead might influence the rate of formation of the intermetallic phase, several solder alloys of differing composition have been used to make overlap-type joints between strips of gold-plated copper sheet. Joints were subjected to metallographic examination and to Chadwick-type peel tests. The elements which have been added to tin were silver; silver together with lead; antimony; antimony plus lead; bismuth; cadmium; nickel; copper; zinc; indium, and cobalt.

Of all the compositions investigated, the binary alloys of tin with cadmium were the only ones which reduced the rate of the gold dissolving into the solder. However, the presence of cadmium caused increasing problems of oxidation. Four tin-cadmium alloys were finally selected for detailed examination, with 5, 10, 18 and 30% Cd. Of these the 10% Cd alloy was found the most suitable, combining maximum suppression of the dissolution of the gold with a reasonably low oxidation rate. However, the joint strength values determined to date have been somewhat inconsistent and further quantitative experiments are in progress.

Oxide on tin surfaces. The oxidation of solid tin has important practical implications since it may cause discoloration and may interfere with lacquer adhesion on tinplate and with solderability. Oxide formed on differing tin surfaces in various environments has been examined by galvanostatic and potentiodynamic cathodic reduction and by electron diffraction. The rate of oxidation and the nature of the oxide formed depend on the conditions of oxidation and on the purity of the tin. Identification of oxide composition by the cathodic reduction method is not reliable because it is affected by the type of tin surface, apparently depending on the crystal faces exposed. The method is, however, capable of giving a useful measure of the total amount of oxide except for some special conditions of oxide formation which result in loss by undermining during reduction. Coupled with this research is another concerned with the development of artificial ageing tests intended to help assessment of loss of solderability of surfaces during storage. The most promising method is exposure to steam, which certainly produces a considerable growth of stannic oxide on tin surfaces. However, the effect both of steam treatment and of natural ageing depends on the

* Annual Report of the International Tin Research Council, 1973. T.R.I. Publication No. 480, Tin Research Institute, Fraser Road, Perivale, Greenford, Middlesex UB6 7AQ.

thickness and continuity of tin coatings and on the nature of the substrate and it seems that the surface contamination which interferes with soldering is more often a corrosion product of the substrate rather than oxides of tin.

Compound growth in plated coatings. The operating temperature of modern electronic equipment is often sufficiently high to promote diffusion of atoms and the growth of intermetallic compounds in soldered joints. For example, the tin in a tin-lead solder, or in a plated coating reacts with the base material, and this in extreme circumstances may lead to poor solderability and to brittleness of solder joints. An extensive investigation has therefore been carried out to obtain quantitative data on the growth rate of these compound layers as a function of both temperature and solder composition.

The results which have been obtained for coatings of pure tin and of tin-lead, containing 30% and 60% tin, on copper, silver, or brass, have now been published and have proved to be of considerable value to the industry.

Further studies on tin coatings over electroplated nickel showed that the scatter in the initial results was partly due to some uncertainty in determination of the actual position of the intermetallic phase boundaries. The interface between the layers of nickel and compound, and that between the compound and the tin, were difficult to define when any normal etching technique was employed. However, it has been found that the evaporation under vacuum of a semiconducting layer of TiO_2 on to the surface (the Pfefferhof technique) delineated the interfaces clearly, and far more consistent results for the rate of compound growth have been obtained.

In addition, the rate of reaction of tin-lead coatings containing 10% tin and 90% lead has been studied and initial indications are that the tin-copper compound grows substantially more slowly than with the higher tin contents. Tests have also been carried out on pure tin coatings produced by hot-dipping, which have some intermetallic compound present at the start as a result of the coating process. It appears, however, that the subsequent rate of growth in thickness of the layer conforms with the results previously obtained for electro-deposited tin coatings.

Advisory Services for Industry

Temporary Protectives against Corrosion

On the advice of its Committee on Corrosion and Protection, the Department of Industry is supporting a technical survey into the application and efficiency of anti-corrosion protective systems. The survey will be carried out by the Fulmer Research Institute Ltd.

Corrosion can spoil a product, in storage, in transit and even at inter-stage processing, before it ever reaches the user. The 1971 Report of the Committee on Corrosion and Protection estimated that the annual cost of corrosion in the UK, including costs incurred in taking preventive measures (both temporary and permanent) was at least £1300M, and that potential savings which could arise from the better use of existing knowledge and techniques would be of the order of £310M.

The remedy often lies in use of temporary protectives and these are particularly desirable for overseas exports. For manufacturers the survey will independently monitor the efficiency of established products and assist in the launching of new systems. For the user, the survey will show which anti-corrosive treatments are likely to provide the best combination of properties to meet specific requirements. Tests included in the programme will cover the effects of relative humidity, fluctuating temperature, salt spray and sulphur dioxide atmospheres, wear resistance and outdoor exposure, besides the determination of other physical properties required by BS 1133, Section 6.

The subscription fees for manufacturers and suppliers of temporary protective treatments range form £180 upwards according to the number of treatments nominated for testing. The fee for users, who want an assurance that a product or system meets their requirements and specification, will range from £80. Further information may be obtained from Dr. G. Sanderson, Fulmer Research Institute Limited, Stoke Poges, Slough, Bucks. (Telephone: Fulmer 2181).

Equipment for Hazardous Atmospheres

The Electrical Research Association Limited is to introduce a service to provide industry with up-to-the-minute reports and assessments of developments in the field of national and international standardization related to electrical equipment for use in hazardous atmospheres.

The service is designed to provide:

(a) for managerial purposes, regularly up-dated reviews of developments, and their implications, which may face industry as a consequence of changes in national and international standards, paying particular attention to developments in Europe;

(b) detailed accounts, also at regular intervals, of the work of the various committees concerned, in most of which ERA staff actively participate;

(c) frequent meetings with companies' representatives to discuss developments, progress and future policies;

(d) additional information dissemination services tailored to the needs of individual companies, as required.

The need for such a service arises from the growing economic pressures and the greater volume and complexity of national and international activities, which make it increasingly difficult for senior engineers to keep abreast of developments and to participate in the preparation of specifications and codes of practice to the extent they have in the past. This is particularly so in the field of electrical equipment for hazardous atmospheres where, for techno/political reasons, the rapid changes now in progress emphasize the need for reliable and effective machinery to assess new developments and their implications.

Further information about the service may be obtained from Electrical Research Association Ltd., Cleeve Road, Leatherhead, Surrey KT22 7SA. (Telephone Leatherhead 74151, ext. 274 or 269.)

Letters to the Editor

The Institution's Council does not necessarily agree with views expressed by correspondents.

Correspondence of a technical nature, or on any matter of interest to electronic and radio engineers, is welcomed.

From: **S. J. MacSweeney,** C.Eng., M.I.E.E.;
A. Towning (Graduate).
R. M. Hodgson, B.Sc.,
F. W. Stephenson, B.Sc., Ph.D.,
and **D. G. Whitehead,** B.Sc.

Electronic Tuning of Musical Instruments

With reference to Mr. Towning's letter on the above subject (February 1974, p. 109) may I suggest that he refers to the pages on 'meters and their uses' in a suitable text book (there are several) on the subject of ergonomics. This should prove to him the efficiency of using an analogue meter for tuning and the advantage of a digital type meter for checking final or absolute values.

Regarding a relatively cheap oscillator capable of producing a stable 12-note (or at least 4-note) output, I would like to suggest to him the following ideas as possible food for thought.

Has he considered designing and constructing a multivibrator, frequency corrected by the application of 'limited' mains (50 Hz) pulses? Such an oscillator might prove to be relatively inexpensive and be coincident in frequency with at least four piano notes, i.e. middle C and the three C notes in succeeding octaves, and yielding an accuracy of 2·4% (taking middle C as 256 Hz (at standard temperature).

Mr. Towning's reference to 12-note equal or even temperament does not make clear whether he means per octave, e.g. tonic solfa notes d, de, r, re, m, etc., and their corresponding frequency ratios 1, $2^{1/12}$, $2^{2/12}$, $2^{3/12}$, $2^{4/12}$, etc., or even-temperament notes at random over the entire frequency range of the piano. If the reference is to an octave then there would seem to be no easy or inexpensive solution to his problem. On the other hand if he means 'random' even-temperament notes then my suggestion of a frequency corrected multivibrator might be of value. Should the latter prove to be the case then other notes closely coincident with multiples of 50 Hz can easily be worked out by correcting the frequency ratios (1, $2^{1/12}$, $2^{2/12}$, etc.) of each octave to their actual frequency values and comparing them with multiples of 50 Hz.

SEAMUS J. MACSWEENEY

17 Beech Lawn,
Meadowbrook,
Dundrum, Dublin 14.
4th April, 1974.

I would like to thank Mr. MacSweeney for his suggested texts and look forward to reading scientific and mathematical proofs of what I was attempting to express in words about analogue *v.* digital indication.

Surely, however, there is no need for digital indication of the 'final or absolute value' of a tuned string since the ear is the best arbiter of zero beat (or one of Mr. L. H. Bedford's electronic aids).

The question I really postulated in my letter is: given 12 stable oscillators (or more if needed), how does one tune them to accurate equal temperament? The answer to this problem is not given in Mr. Bedford's excellent and interesting article. My solution to the problem is a trial-and-error one and, very briefly, it is to set two RC oscillators an interval apart (this interval to be a semitone and it is capable of being varied) and, going up the scale tune 12 other oscillators, after which a test is made for the octave and this, if not perfect, means that the interval was not a true semitone, so it is reset and the whole process repeated till the octave is perfect. Assuming stable oscillators the end-product is 12 equally-tempered notes, preferably in a centre octave for convenience. I have obtained sufficient stability from a long-tail pair oscillator (using discrete or i.c. components).

Now in my letter I was maintaining that given such a 12-note standard, I was content to tune a piano by ear, while from the same starting position, Mr. Bedford needs his aids. Probably the easiest solution to the question lies in the now commercially available 'top note generators' which produce 12 equally-tempered notes from a single c.m.o.s. i.c. using frequency division techniques.

ARTHUR TOWNING

9 Middlesex Drive,
Bletchley MK3 7JE
9th April, 1974.

Computer Scientists are not Engineers

In recent years there has been a rapid growth in Computer Science studies. These much-heralded courses have attracted hoards of semi-numerate, non-scientific entrants. We are concerned that the proliferation of such courses may mask separate and continuing need for engineering courses which deal with computer hardware as a major topic. Whilst not wishing to minimize the importance of Computer Science, there is a danger that the separate roles of the 'Computer Scientist' and 'Computer Engineer' may become confused. This would be to the detriment of both student and industry. This danger is identified in a recent report[1] of the Cosine Committee. It is our contention that a clear distinction does exist. To take advantage of the technological advances in digital computers, in particular the increasing importance of the minicomputer, industry requires an engineer with a firm grounding in the fundamentals of both electronic engineering and digital systems, with sound working knowledge of computing systems. The skills of the computer scientist whose technological training may in many cases consist of a single 'Computer Hardware' course are inappropriate to meet this need.

At Hull the Department of Electronic Engineering offers a 4-year degree course in Computer Engineering. The early years of our course concentrate on subjects basic to electronic engineering. The specialist courses are introduced in subsequent years. We aim to produce a graduate who is an educated engineer, his knowledge and skill equipping him for a career in a subject which finds increasing application in communications, signal processing and control systems.

A student of Computer Engineering must be familiar with all aspects of hardware, software, and system design. The necessary experience in all these areas can be derived from the use of a minicomputer as an educational tool.[2] It is essential that the student be given free access to such a machine—the 'hands-on' approach. It is not adequate to provide a mere simulation on a large machine whose organization is well beyond the average student's comprehension. It is vital that the student be exposed to the limitations and capabilities of the minicomputer, whose structure and organization can be readily understood, and for which interface instrumentation equipment can be designed and built.

Our experience has shown that it is possible to achieve these aims within the framework of a balanced undergraduate course.[3] By use of the project as the unifying activity of the final year, involving students in the design and construction of digital systems, basic engineering insights are acquired. The effectiveness of project work can be enhanced by the involvement of industry.[4]

It is during the final year that subjects such as computer architecture and language programming can best be introduced, building on the switching theory and logic design covered in earlier years. It is also important that the student should become proficient in at least one high level language. A student who has studied fundamental circuit theory, electronics, and electromagnetism, is well able in his final year to assimilate subjects such as computer hardware theory and digital system design. Indeed, adequate understanding cannot be achieved without expertise in basic electrical theory.

The success and relevance of a course can only be judged by its end product. Is the graduate of such a course both suitably equipped for his chosen career and educated in the wider sense? We believe that he is.

R. M. Hodgson
F. W. Stephenson
D. G. Whitehead

Department of Electronic Engineering,
The University of Hull.

References

1. Sloan, M. E., Coates, C. L., and McCluskey, E. J., 'Cosine survey of electrical engineering departments', *Computer*, **6**, No. 6, pp. 30–9, June 1973.
2. 'Minicomputers in the digital laboratory program. Task force on minicomputers VII.' *Computer*, 6, No. 1, pp. 28–42, January 1973.
3. Hodgson, R. M., Stephenson, F. W., and Whitehead, D. G. 'An Undergraduate Course in Computer Engineering.' Proceedings of the Conference on the Teaching of Electronic Engineering—Degree Courses, University of Hull, April 1973.
4. 'The Hull Project Scheme—an annotated project listing'. Department of Electronic Engineering, University of Hull, Autumn 1973.

The Duke of Kent visits Plessey Research Centre

Left to right: Mr. Michael Clark, Dr. F. A. Myers (Head of Microwave Applications Laboratory), The Duke of Kent, Dr. J. C. Bass (General Manager of the Allen Clark Research Centre) and Dr. Ieuan Maddock, discussing a new microwave solid state development.

HRH The Duke of Kent (Fellow), who is Deputy Chairman of the National Electronics Council, and a member of the Council of the Institution, recently visited the Plessey Company's Allen Clark Research Centre at Caswell, Northants. The Duke was welcomed and conducted around the laboratories by Mr. Michael Clark, Managing Director of Plessey and a Member of the NEC, and saw many of the Company's highly advanced research and development activities, including work on the design and production of integrated circuits which has this year won the Company a Queen's Award to Industry for outstanding achievement in technological innovation. Also present during the visit were Dr. Ieuan Maddock, Chief Scientist, Department of Industry, and President of the IERE, and Mr. D. Dibsdall, Secretary of the NEC.

His Royal Highness has during recent months visited a number of important industry and government establishments concerned with electronics. On several of these occasions he was accompanied by the President or by the Director of the Institution, Mr. G. D. Clifford. These have included Mullard Southampton, Hirst Research Centre, Wembley, GEC-Marconi at Stanmore, Formica, Tynemouth, de La Rue, Gateshead and the Royal Radar Establishment as well as several industry exhibitions. Further similar visits are planned during the coming months.

INSTITUTION OF ELECTRONIC AND RADIO ENGINEERS

Applicants for Election and Transfer

THE MEMBERSHIP COMMITTEE at its meetings on 28th December 1973, 2nd and 23rd April 1974 recommended to the Council the election and transfer of 202 candidates to Corporate Membership of the Institution and the election and transfer of 25 candidates to Graduateship and Associateship. In accordance with Bye-law 23, the Council has directed that the names of the following candidates shall be published under the grade of membership to which election or transfer is proposed by the Council. Any communications from Corporate Members concerning these proposed elections must be addressed by letter to the Secretary within twenty-eight days after the publication of these details.

Meeting: 28th December 1973 (Membership Approval List No. 180)

GREAT BRITAIN AND IRELAND

CORPORATE MEMBERS

Transfer from Graduate to Fellow

AHERN, Brian Henry Walter. *Portsmouth, Hampshire.*

Direct Election to Fellow

HILL, Frederick Norman. *Llangristiolus, Anglesey.*

Transfer from Associate to Member

ELLIS-JONES, Frank. *Seaford, Sussex.*

Transfer from Graduate to Member

ADDO, John Motey. *Glasgow.*
ANDERSON, Richard Cameron, B.Eng., Flight Lieutenant. *Marlow, Buckinghamshire.*
APPLEYARD, Stephen Frank. *Maldon, Essex.*
ARNOLD, James, B.Sc. *Purbrook, Hampshire.*
AYRES, Allan John. *Dalton-in-Furness, Lancashire.*
BAILEY, Raymond James. *Glasgow, G14.*
BAKER, Derrick William. *Maldon, Essex.*
BAKER, Keith Alan. *Westcliffe-on-Sea, Essex.*
BARFIELD, Edward George. *Malvern, Worcestershire.*
BARTON, Roy George. *Poole, Dorset.*
BATEMAN, Anthony John. *Largs, Ayrshire.*
BECKETT, David. *Arlesey, Bedfordshire.*
BERRY, Leonard John. *Tadley, Hampshire.*
BILLINGHURST, Peter John Harold, Major. *London, W2.*
BISHOP, Graham Paul. *Maidstone, Kent.*
BLAND, Bernard Douglas. *Stevenage, Hertfordshire.*
BLYTH, Walter. *Harrow, Middlesex.*
BOTHERWAY, Geoffrey. *South Croydon, Surrey.*
BOTTOMLEY, Edward Annan. *Southway, Edinburgh.*
BOUND, Edward Charles. *Emsworth, Hampshire.*
BOWEN, John Henry. *Chelmsford, Essex.*
BOWKER, Roger Anthony. *Ilford, Essex.*
BOYLAN, James Andrew. *London, N.W10*
BRANAGAN, Peter Francis. *Ballinteer, Dublin, 14.*
BRAY, William Lister. *Brighton, Sussex.*
BRIAN, David Robert. *Andover, Hampshire.*
BRIDGEMAN, James Neville, *Ventor, Isle of Wight.*
BRIGHT, Paul William. *Boreham Wood, Hertfordshire.*
BROWN, Anthony Roger. *Stevenage, Hertfordshire.*
BRUCE, George Henry. *Glasgow, G12*
BUTLER, Alan Francis Oscar. *Stratford-upon-Avon, Warwickshire.*
BUTLER, Michael William. *Bracknell, Berkshire.*
CATLING, Gerald Carden. *London, N8*
CARROLL, Jeremy Antony. *Horsham, Sussex.*
CAVANAGH, Stephen. *Glossop, Derbyshire.*
CAWSON, Douglas Michael Gustave Henry. *Emsworth, Hampshire.*
CHIPPINGTON, Geoffrey Richard. *Aston-on-Trent, Derby.*
CLAYTON, David Harry. *Eastleigh, Hampshire.*
CLEWS, Malcolm. *Harrow, Middlesex.*
CLOUGHER, John Michael. *Perry Barr, Birmingham.*
COOK, Christopher John. *Greenford, Middlesex.*
COOK, Terence Bernard. *Sale, Cheshire.*
COOKE, Tony Alfred. *Epping, Essex.*
COOPER, Derek William. *Rochester, Kent.*
CORK, John Michael. *East Molesey, Surrey.*
CORRIE, William Jackson. *Broadbottom, Hyde, Cheshire.*
COX, Robert Ernest. *Gotham, Nottinghamshire.*
CROWLEY, Gerald Patrick. *Chigwell, Essex.*
CUTLER, Kelvin John. *Templecombe, Somerset.*
DAVIDSON, Peter Donald. *Stanway, Essex.*
DAVIES, Victor John. *Reigate, Surrey.*
DAWES, Ronald Granville. *Tamworth, Staffordshire.*
DEVONALD, Raymond. *Gt. Urswick, Ulverston Lancashire.*
DODGE, John Arthur. *Leicester.*
DOMONE, Anton Stewart. *Southampton, Hampshire.*
DONOGHUE, Peter Thomas. *Radcliffe-on-Trent, Nottingham.*
DUNNE, Peter. *Dun Laoghaire, County Dublin.*
EASTWOOD, Peter Michael. *Epsom, Surrey.*
EDEN, Ronald. *Leeds.*
ELLISON, Michael. *Upton-by-Chester, Chester.*
EMERY, John. *Brentwood, Essex.*
EPPS, John. *Newbury, Berkshire.*
EVANS, David Haydn. *Harrow, Middlesex.*
EVERITT, Michael Anthony. *Byfleet, Surrey.*
EVERITT, Richard Martin. *Corsham, Wiltshire.*
FERRINGTON, Leslie Joseph. *Ratby, Leicestershire.*
FLEMING, David Findlay, M.Sc. *Harlow, Essex.*
FORDRED, Derek Peter. *Dartford, Kent.*
GALPIN, Paul Christopher Leroi. *Carlisle, Cumberland.*
GILPIN, Allan Ray. *Luton, Bedfordshire.*
GOOSTRAY, John. *Wigginton, York.*
GRAVES, Gerald Ernest George. *Buntingford, Hertfordshire.*
GREENLAND, Elwyn. *Fawley, Hampshire.*
GUZZETTI, Mario, M.Sc. *St. Albans, Hertfordshire.*
HAINES, James Edward. *Stevenage, Hertfordshire.*
HALL, John Keeble. *Seaford, Sussex.*
HALLWORTH, Robert. *Poynton, Cheshire.*
HANNAFORD, Colin William. *Ringwood, Hampshire.*
HARRIS, Robert Michael. *Somerton, Somerset.*
HARRIS, William Charles Henry. *Plympton, Plymouth, Devon.*
HICKIN, Philip. *Sheffield*
HILL, Alan James. *Cheshunt, Hertfordshire.*
HADDOCK, Lawrence. *Chatham, Kent.*
HADLEY, Alan Thomas. *Shenstone, Lichfield, Staffordshire.*
HORN, Donald Talbot. *Camberley, Surrey.*
HUDGELL, Ernest John. *Farnham, Surrey.*
JACKSON, Peter. *Ulceby, Lincolnshire.*
JONES, Cyril Edwin. *Downham Market, Norfolk.*
IRVINE, Neil John. *South Croydon, Surrey.*
JONES, David Dudgeon. *Feltham, Middlesex.*
KELLY, Francis John. *Newtownabbey, County Antrim.*
KERR, John Campbell. *East Hagbourne, Berkshire.*
LIDSTONE, Denis. *Barrow-in-Furness, Lancashire.*
LOWSLEY, John. *Warrington, Lancashire.*
LUSH, Stephen Francis. *Worcester Park, Surrey.*
McGRATH, John. *Dundrum, Dublin 14.*
McINTOSH, Gareth Peter. *Healing, Grimsby, Lincolnshire.*
MAIDENS, Michael Joseph. *Burgess Hill, Sussex.*
MAILE, Raymond John. *Broadstone, Dorset.*
MARTIN, John Christopher. *Worthing, Sussex.*
MAYNARD, Brian Roderick. *Moulton, Northwich, Cheshire.*
MAYO, Sean Alfred. *Brockworth, Gloucester.*
MUMFORD, Richard John. *Hatfield, Hertfordshire.*
O'CONNOR, Brian Stuart. *Rustington, Sussex.*
PORTMAN, Lawrence Howard. *Swindon, Wiltshire.*
PITT, Alan David. *Bristol 2.*
PLENTY, Adrian Colin. *Winterbourne, Bristol.*
PRATT, Roger Tyrell, Lieutenant, R.N. *Portsmouth, Hampshire.*
PRATT, David Michael. B.Tech. *Bingley Yorkshire.*
RICHARDS, Ian. *Congleton, Cheshire.*
RILEY, Richard James. *Epsom Downs, Surrey.*
RIXON, Anthony Victor. *Leighton Buzzard, Bedfordshire.*
ROBERTS, Frederick John. *Malvern, Worcestershire.*
ROBERTS, Gordon Joseph. *London, NW6*
ROBINSON, Richard Ian. *Hindhead, Surrey.*
RODDAM, Alexander. *Ipswich, Suffolk.*
ROSE, Joseph Radi. *New Malden, Surrey.*
ROSS, Raymond. *Bishops Stortford, Hertfordshire.*
SCOTT, Norman Calland, Lieutenant R.N. *Littlehampton Sussex.*
SHEPHERD, Peter James, M.Sc. *Seaton, Devon.*
SMITHERS, Peter Alan. *Haywards Heath, Sussex.*
SNOW, Anthony Cyril. *Cheltenham, Gloucestershire.*
STOCKFORD, Philip Michael. *Worthing, Sussex.*
SWANN, Nigel Ronald William. *Weybridge, Surrey.*
UL HAQ, Muhammad Ikram, B.Sc. *West Croydon, Surrey.*
TURNER, George Peter. *Staines, Middlesex.*
WARE, James Brian. *Emsworth, Hampshire.*
WHITAKER, Douglas Michael Hamilton. *Sutton, Surrey.*
WHITBOURN, Edward Albert. *Burgess Hill, Sussex.*
WILLCOX, Norman Morley. *Basingstoke, Hampshire.*
WILLIAMS, Francis Raymond. *Plymouth, Devon.*
WILLIAMSON, James Ronald. *Sandy, Bedfordshire.*
WORTON, Ian Gordon. *Congleton, Cheshire.*

Direct Election to Member

ARTHUR, Hugh MacDonald, M.Sc. *High Wycombe, Buckinghamshire.*
BARBER, Richard Devereux. *Bournemouth, Hampshire.*
CARMAN, Richard, Squadron Leader, M.B.E. *Andover, Hampshire.*
CLOUGH, Charles, B.Sc. *London, SE22.*
COLES, David Eric Alfred. *Hassocks, Sussex.*
ELLIOT, James. *Wells, Somerset.*
ELLIS, Brian James. *Camberley, Surrey.*
FERMOR, Geoffrey John. *London, N13*
FRIEDMAN, David. *Ilford, Essex.*
GAMBLE, Peter Dennis. *Mickleover, Derby*
GAYLER, James Robert. *Hertford, Hertfordshire.*
HADLEY, Michael Frederick. *Surbiton, Surrey.*
HAWES, Ivon Frederick Benjamin. *New Malden, Surrey.*
HUGHES, Michael John, M.A. *Westerham, Kent.*
LAWRENCE, Jeffrey Kenneth, *Cowplain, Hampshire.*
LUTHRA, Ashok Kumar. *Harrow, Middlesex.*
McCANDLESS, Robert Ian. *Belfast.*
McKEE, William. *Bathgate, West Lothian.*
McKENZIE, Roderick Alexander. *Balerno, Midlothian.*
NIGHTINGALE, Reginald Hugh. *Camberley, Surrey.*
STARLING, Peter Donald. *Boncath, Pembrokeshire.*
STEWART, Rodney Alan. *Histon, Cambridge.*
TAIT, Norman. *Warwick.*
TARBROOKE, Allen, Captain. *Arborfield, Berkshire.*
WARREN, Keith Edward. *London, N19*
WARREN, Nigel Henry. *Bushey, Hertfordshire.*
WHITTEN, Edward William. *Farnborough, Hampshire.*
WILSON, John Michael, B.Sc. *Cheadle, Cheshire.*
WRIGHT, Douglas James. *Orpington, Kent.*

OVERSEAS

CORPORATE MEMBERS

Direct Election to Fellow

OLDROYD, Derek Lee, B.Sc., Ph.D. *Warmond, Holland.*

Transfer from Graduate to Member

AWOSIKA, Christopher Olabamijo. *Port Harcourt, Nigeria.*
BHAT, Balemale Krishna. *Duliajan, India.*
BIUWOVWI, Julius. *Warri, Nigeria.*

BRETHERICK, Peter Fairbank. *Edenvale, Transvaal, South Africa.*
CARRINGTON-SMITH, Robert Ian. *Raleigh, North Carolina, U.S.A.*
CHAI, Chiap Fam. *Singapore, 13.*
CHAPLIN, Richard. *Cape Town, South Africa.*
CHONG, Randolph Townsend, Captain. *Singapore, 20.*
CUTLER, William Alan. *Wellington, New Zealand.*
DAY, John Colin, Captain. *B.F.P.O. 28.*
FADULU, Michael Mobolaji, B.Sc. *Ibadan, Nigeria.*
JAGGI, Tejbir Singh. *New Delhi 16, India.*
KING, Raymond John. *Natal, South Africa.*
LIDSTONE, Ivan Roy, Captain. *B.F.P.O. 45.*
MacCALLUM, William Anthony. *North Adelaide, Australia.*
MEENS, Philip Henry. *New South Wales, Australia.*
STARK, Robert Watson, Captain R. Sigs. B.Sc. (Eng)., *B.F.P.O. 53.*
WICKRAMASINGHE, Yapa Appuhamillage Buddhinanda Dayakumara. *Gampaha, Sri Lanka.*

Direct Election to Member

DUTTA, Bijay Bhushan. *Dhanbad, Bihar, India.*
STROMBERG, Lars O. *Helsinki, Finland.*
VRAHIMI, Georgios. *Nicosia, Cyprus.*

Meeting: 2nd April 1974 (Membership Approval List No. 181)

GREAT BRITAIN AND IRELAND

CORPORATE MEMBERS

Transfer from Member to Fellow

BOICE, Cyril John. *Woking, Surrey.*
CHICKEN, Edwin. B.Sc. *Morpeth, Northumberland.*
DAVIES, David Evan Naunton, M.Sc., Ph.D., D.Sc *London, WC1*
GARGINI, Eric John. *West Drayton, Middlesex.*
JOWITT, John Edward, B.Sc. *Halton, Lancaster.*
NIELD, Philip Newton, B.Sc., Ph.D. *Wythall, Birmingham.*
SANSOM, John Stuart. *London, SW19.*

Direct Election to Fellow

MACARIO, Raymond Charles Vincent, B.Sc. Pb.D. *Swansea, Glamorgan.*

OVERSEAS

CORPORATE MEMBERS

Transfer from Member to Fellow

MARTIN, Albert V.J., *Oegstgeest, Holland.*

NON-CORPORATE MEMBERS

Transfer from Student to Graduate

HAWORTH, Peter Lyndon, B.Sc. *Rochester, Kent.*

Direct Election to Graduate

MASCARENHAS, Neville Joseph. *Thornton Heath, Surrey.*
SHAKESHAFT, Andrew Duncan. *Reading, Berkshire.*

Direct Election to Associate

JONES, Peter John. *Beaconsfield, Buckinghamshire.*
SHELTON, Cecil Charles William. *Chelmsford, Essex.*

Direct Election to Associate Member

FOSTER, Peter. *Lichfield, Staffordshire.*
PINNEY, David Ralph. *Soham, Cambridgeshire.*

STUDENTS REGISTERED

CHOWN, David Philip Martin. *Wembley, Middlesex.*
HERBERT, Ian. *Hexborough, Yorkshire.*
MANN, Peter Duncan. *Kidderminster, Worcestershire.*
MORLAND, Robert John. *London, NW3*
NAYYAR, Vijai Kumar. *Newcastle upon Tyne.*
O'HEARN, Patrick Arthur. *Newcastle upon Tyne.*
THORPE, Christopher Robert. *Plymouth, Devon.*
WALTERS, Philip William. *London, N2*
WEST, Paul Jonathan. *Winchester, Hampshire.*

OVERSEAS

NON-CORPORATE MEMBERS

Transfer from Student to Graduate

WAN, Tong Weng. *Singapore 21.*

Direct Election to Graduate

DIETRICH, Clinton Cosmo. *Jamaica, West Indies.*

Transfer from Student to Associate

KULKARNI, Vilas Mahadeo. *Bombay 22, India.*

Transfer from Student to Associate Member

LOUIE, Kwok Sin. *Kowloon, Hong Kong.*

Direct Election to Associate Member

KOK, Kee Cheow. *Kuala Lumpur, Malaysia.*
MAGEE, James Michael. *Riyadh, Saudi Arabia.*

STUDENTS REGISTERED

AWONIYI, Timothy Ayanwola. *Jamnager, Gujarat State, India.*
DESHMUKH, Ajitkumar Shriniwas. *Baroda 4, India.*
KOTWANI, Ashok. *Assam, India.*
YAP, Eng Khong. *Singapore 15*

Meeting: 23rd April 1974 (Membership Approval List No. 182)

GREAT BRITAIN AND IRELAND

CORPORATE MEMBERS

Transfer from Member to Fellow

GREEN, Donald Charles. *New Barnet, Hertfordshire.*
LAWTON, Derek Elvidge. *Plymouth, Devon*
PICKERING, Eric Lancelot. *New Malden, Surrey.*

Transfer from Member to Fellow

SINHA, Kailash Nath, Wing Commander. *New Delhi, India.*

OVERSEAS

CORPORATE MEMBERS

Direct Election to Fellow

SETTY, Gopala Krishna. *Bangalore, India.*

Notice is hereby given that the elections and transfers shown on Lists 177, 178 and 179 have now been confirmed by the Council.